Section I

THE UNIVERSE, GALAXIES AND STARS

Edited by G. E. Kocharov and V. A. Dergachev

ISOTROPIZATION OF INHOMOGENEOUS CENTRALLY SYMMETRIC COSMOLOGICAL MODELS

V. A. Ruban and A. D. Chernin

The observational results of extragalactic astronomy /1, 2/ indicate that large-scale distribution of matter in regions greater than 100 Mpc, which contain numerous clusters of galaxies, is on the average homogeneous, nonstationary, and is characterized by Hubble's expansion law. It therefore seems that Fridman's cosmological models /3, 4/ on the whole provide an adequate description of the "smoothed" structure and the dynamics of the Metagalaxy in the present epoch and in the near past.

The maximum symmetry of the homogeneous isotropic distribution of gravitating matter in general relativity indicates that a priori Fridman's model, because of its exceptional features, may be expected to describe even the earlier stages of evolution of the expanding Universe. However, the assumption of maximum symmetry of the Universe constitutes a far-reaching idealization even for the observable part — the Metagalaxy — and at its best it is satisfied only approximately. Moreover, unlimited interpolation of the homogeneity and isotropy of the Universe into the past all the way to the singular state constitutes an arbitrary hypothesis, and there is definitely room for a diametrically opposite point of view, according to which the observed high symmetry of the Metagalaxy is not an "inborn" feature but rather has been acquired as a result of evolution from an essentially inhomogeneous and anisotropic state of lower symmetry. This idea is supported by the absolute instability of Fridman's contracting models under small perturbations changing their homogeneity and isotropy /5/. Moreover, qualitative analysis of the dynamics of relativistic cosmological models with arbitrary distribution and motion of matter also shows that overall expansion in the co-moving frame of reference should be accompanied by inevitable reduction of anisotropy (or at least of some of the anisotropic features) /6/, so that the absence of marked anisotropy and inhomogeneity in the Metagalaxy does not justify our ignoring the possibility of pronounced and significant anisotropy and inhomogeneity in the early stages of expansion of the Universe. A vivid illustration and direct confirmation of this alternative description of the initial low-symmetry singular state are provided by special cases of cosmological solutions of Einstein's equations /4, 7 — 10/ which constitute a wider family of homogeneous anisotropic models significantly deviating from Fridman's models in the early stages of evolution, near the singular state, when the various directions in space are nonequivalent, and then gradually approaching Fridman's models in the course of expansion and eventually acquiring the appropriate isotropy characteristic of the Metagalaxy.

In this paper, we intend to analyze a simple and well-known case of centrally symmetric cosmological models /3, 4, 11, 12/ in order to illustrate the fundamental feasibility of an isotropic and homogeneous Metagalaxy evolving from a globally inhomogeneous and anisotropic singular state with infinite density and velocity gradients of matter. The spherically symmetric case is of particular interest in cosmology, since all Fridman's isotropic models are spherically symmetric and the hypothesis of centrally symmetric distribution and motion of the gravitating matter in the past constitutes a natural generalization, especially if the Metagalaxy is considered as a bounded finite giant system with a strong relativistic gravitation field. We will only analyze the idealized version of the cosmological models of a dust sphere with zero pressure, for which an exact analytical solution of the gravitation equations can be obtained /3, 4/ and the conditions of isotropization in the course of expansion, when the sphere evolves toward Fridman's models, can be elucidated.

The high isotropy of the cosmic radiation background ($\frac{\Delta T}{T} \approx 0.5\%$, $T \approx$ $\approx 3°K$) /13/, if considered within the framework of the "hot" model, indicates that the expansion of the Metagalaxy did not display pronounced anisotropy and inhomogeneity in the past, all the way to red shifts of $z = \frac{\lambda - \lambda_0}{\lambda_0} = 10$ /4/. Since the effect of radiation becomes negligible and the nonrelativistic matter assumes the dominant role in field sources at earlier times with $z \approx 1000 - 100$, inhomogeneous models in principle may isotropize in the later stages of expansion, when matter is in a state of free motion in its own gravitation field and the effect of pressure and pressure gradients on the dynamics is ignorable (which is true for such a massive object as the Metagalaxy). Our group of isotropizing inhomogeneous dust sphere models with anisotropy and inhomogeneity rapidly diminishing with expansion therefore does not clash with the observed data and may be used as a point of departure for the analysis of more realistic inhomogeneous models of the early stages of Metagalactic evolution.

NEWTONIAN COSMOLOGY

Consider centrally symmetric models of distribution and homologous motion of a gravitating dust-like medium with zero pressure. We will first analyze the dynamics within the framework of Newtonian cosmology /6, 7/. The Metagalaxy is a priori known to be a relativistic object with a strong gravitation field ($\varphi / c^2 \sim 1$, $v \approx HR \sim C$), and if it is a bounded finite system, its present-day boundary should lie inside Schwartzschild's sphere in the "expanding" T region /4/. However, because of far-reaching similarity in the local properties of relativistic and classical models, which is attributable to the characteristic features of spherical symmetry /11, 14/, the main results for the density and radial velocity distribution of the "dust" in a general-relativistic sphere (as in Fridman's homogeneous and isotropic models) /4, 15/ can be obtained in a simple way by combining Newtonian gravitation with the equations of classical hydrodynamics in Lagrange's form:

$$\frac{\partial^2 R}{\partial t^2} = -\frac{GM}{R^2}, \quad M = 4\pi \int_0^R \rho R^2 dR, \tag{1}$$

where $M(\chi)$ is the current total rest mass of the "dust" contained inside a "fluid" sphere of Euler radius $R(t, \chi)$, ρ is the density of the "dust," t is the absolute time, G is Newtonian gravitational constant. If mixing of different layers and departure from continuity conditions are ignored, the gravitating mass $M(\chi)$ impelling the dust particles of a given spherical layer χ will remain constant in this case of homologous motion of "dust" and it may be used as a convenient radial Lagrangian coordinate.

The first integral of the equation of motion (1) is the conserved total energy per unit "dust" mass:

$$E(M) = \frac{1}{2}\left(\frac{\partial R}{\partial t}\right)^2_{\chi} - \frac{GM}{R} \tag{2}$$

and its sign differentiates between hyperbolic ($E>0$) and elliptical ($E<0$) types of motion of the layer. The law of motion of the "dust" in an arbitrary gravitating sphere may be derived in closed form by integrating (2). For the special case of parabolic motion ($E=0$), the integration can be carried out in explicit form:

$$R(t,M) = \left\{\frac{3}{2}\sqrt{2GM}\left[t - t_0(M)\right]\right\}^{\frac{2}{3}}, \tag{3}$$

whereas for $E(M) \neq 0$ it is expressed by implicit relations of the form

$$\begin{gathered} R(t,M) = |E(M)|^{\frac{1}{2}}\, a(t,M), \quad \frac{1}{2}\left(\frac{\partial a}{\partial t}\right)^2 = \frac{a_0(M)}{a} + \epsilon, \quad \epsilon = \pm 1, \\ \sqrt{2}\left[t - t_0(M)\right] = \int_0^a \left(\frac{a_0}{u} + \epsilon\right)^{-\frac{1}{2}} du, \quad a_0(M) = \frac{GM}{|E|^2}, \end{gathered} \tag{4}$$

or parametrically using a convenient dimensionless time $\eta = \int_0^t \frac{dt}{a(t,M)}$

Ideal spherical symmetry of "dust" motion produces focusing and accumulation of particles at a point. Therefore, a singular state is assumed to exist at the center of the sphere $R(t_0, M) = 0$, which is characterized by infinite density and infinite radial velocity of matter. It can be treated as an idealization of the superdense initial state, the Metagalactic "protonucleus," and the integration constant $t_0(M)$ then can be interpreted as the time at which a particle of a given layer left this central nucleus.

In the hyperbolic case, when $E(M)>0$,

$$a = \frac{a_0}{2}(ch\,\eta - 1), \quad \sqrt{2}\,(t - t_0) = \frac{a_0}{2}(sh\,\eta - \eta), \tag{5}$$

the only type of particle motion is unbounded recession from the central singularity ($0<\eta<\infty$).

In the elliptical case, when $E(M)<0$,

$$a = \frac{a_0}{2}(1 - \cos\eta), \quad \sqrt{2}\,(t - t_0) = \frac{a_0}{2}(\eta - \sin\eta), \tag{6}$$

the phase of outward motion ($0<\eta<\pi$) also originates in the singularity, but at a finite distance $R_{max}=\frac{GM}{|E|}$ from the center the direction of motion is reversed and the particles fall back to the center. The lifetime of the center is thus limited by the pulsation period $\Delta=\frac{\pi a_0}{\sqrt{2}}$. The corresponding distribution of the "dust" density and radial velocity in a nonstationary sphere is expressed by the relations

$$V(t,M)=|E|^{\frac{1}{2}}\left(\frac{a_0}{a}+\epsilon\right)^{\frac{1}{2}},\quad \rho(t,M)=\frac{1}{4\pi R^2}\cdot\frac{\partial R}{\partial M},$$

where for $E(M)\neq 0$

$$\frac{1}{|E|^{\frac{1}{2}}}\frac{\partial R}{\partial M}=\frac{d\ln|E|^{\frac{1}{2}}}{dM}a+\left(\frac{a_0}{a}+\epsilon\right)^{\frac{1}{2}}\left(\frac{da_0}{dM}I_0-\sqrt{2}\frac{dt_0}{dM}\right)-\frac{da_0}{dM}; \tag{7}$$

$$I_0=\begin{cases}\operatorname{Arcsh}\sqrt{\frac{a}{a_0}}\\ \arcsin\sqrt{\frac{a}{a_0}}\end{cases};\quad \epsilon=\begin{cases}+1\\ -1\end{cases}.$$

The parabolic case $E=0$ is obtained directly from (3) by taking the limit $a\to 0$:

$$\rho=\frac{1}{6\pi G(t-t_0)^2}\left[1-\frac{2M}{t-t_0}\frac{dt_0}{dM}\right]^{-1}. \tag{8}$$

The general solution of the Newtonian problem of centrally symmetric motion of "dust" in its own gravitation field depends on two essentially arbitrary functions of the radial Lagrangian coordinate: the distribution of the specific energy E(M) or, more precisely, of a combination of the form $a_0(M)=GM/|E|^{3/2}$, and the time of collapse of particles of a given layer $t_0(M)$. These functions account for all the possible initial distributions of the "dust" density and radial velocity in an arbitrary inhomogeneous sphere; they are restricted only by the most general requirements ensuring homologous motion. For the particular cases

$$a_0=\frac{GM}{|E|^{3/2}}=\text{const},\ t_0=\text{const};\quad E=0,\ t_0=\text{const} \tag{9}$$

the above solution reduces to analogs of Fridman's cosmological models, which represent homogeneous spheres with isotropic Hubble velocity field of "dust" $\vec{V}=H(t)\vec{R}$. *In this exceptional case, there is no particular point* of the medium which may be regarded as the center $R=0$ and this coordinate can be assigned to any element of the medium /4, 15/. The condition of isotropy of the radial velocity field $V=H(t)R$ or the equivalent requirement of homogeneous "dust" distribution $\rho(t)=\frac{3M}{4\pi R^3}$ (these two conditions are interrelated in a sphere) unambiguously isolate these special Milne-MacCrea solutions with separable variables, $R(t,M)=\varphi(M)a(t)$.

The law of total energy conservation of a homogeneous gravitating sphere for the case of parabolic "dust" motion ($E=0$) leads to the definition of

critical density $\rho_k = \frac{3H^2}{8\pi G}$, a well-known condition of quasi-Euclidean geometry of the Fridman universe, and the cases of elliptical ($E<0$) and hyperbolic ($E>0$) isotropic expansion of a homogeneous dust sphere correspond to a closed ($\rho > \rho_k$) and an open ($\rho < \rho_k$) Fridman models, and moreover present a complete classical analog of their local properties. Near the central singularity ($R(t_0, M)=0$ for $t \to t_0(M)$), the energy integral $E(M)$ does not affect the dynamics and in fact drops out from the leading term of the expansion of the general solution (4) for $R \ll \frac{GM}{|E|}$, so that it coincides with the degenerate parabolic case (3) with $E=0$. The distribution and the motion of "dust" in an arbitrary sphere at the early stages of expansion is essentially determined by one arbitrary function $t_0(M)$. Therefore the simultaneous collapse of the entire sphere to the center ($t_0=\text{const}$) in accordance with (9) constitutes a case of quasi-isotropic motion with an asymptotic velocity field $V=H(t)R$, $H=2/3(t-t_0)$, and in the limit $\rho \to \infty$ it leads to a homogeneous distribution of "dust", whose density goes to infinity as $\rho \approx 1/6\pi G(t-t_0)^2$, just like in the Milne—MacCrea model.

If different layers do not collapse simultaneously ($t_0(M) \neq \text{const}$), the motion of "dust" near the center is essentially anisotropic, and its density goes to infinity according to a different law:

$$\rho \approx \frac{1}{12\pi G} \frac{dt_0}{dM} (t-t_0)^{-1} \tag{10}$$

In accordance with this picture of successive collapse of the individual spherical layers, their longitudinal dimension in the direction of the radius is stretched because of the increase in the relative acceleration of the particles in the gravitation field (a characteristic "tidal effect") and the amplitude of the inhomogeneity, expressed in terms of the density gradient, increases indefinitely. In particular, its behavior in the parabolic case ($E=0$)

$$\frac{\partial \ln \rho}{2\partial M} = \frac{2\frac{dt_0}{dM} + M\frac{d^2t_0}{dM^2}}{\left(t-t_0-2M\frac{dt_0}{dM}\right)} - \frac{M\left(\frac{dt_0}{dM}\right)^2}{(t-t_0)\left(t-t_0-2M\frac{dt_0}{dM}\right)} \tag{11}$$

shows that in general the inhomogeneity near the center $R(t_0, M)=0$ varies as

$$\frac{\partial \ln \rho}{\partial M} \sim \frac{dt_0/dM}{t-t_0} \sim R^{-\frac{3}{2}} \to \infty.$$

The expansion of the sphere may be treated as a simple reversal in time of its collapse, and the density and velocity distribution in the explosive phase repeats in reverse order the variation of these parameters during collapse.

In case of simultaneous ejection of all the particles from the center ($t_0=\text{const}$, a "single explosion" of the protonucleus), the expansion begins with a homogeneous singular state and should involve a gradual growth of deviations from isotropy if $a_0(M) = \text{const}$:

$$R \approx \tilde{R}\left(1+\frac{\tilde{R}}{5R_0}\right), \quad \tilde{R} = \left\{\frac{3}{2}\sqrt{2GM}(t-t_0)\right\}^{\frac{2}{3}}.$$

The correction term in the expansion may be interpreted as spontaneous creation and growth of inhomogeneity, together with the associated anisotropy of "dust" motion, as a result of the gravitational instability of the homogeneous isotropically expanding sphere under spherically symmetric fragmentation in the parabolic stage of expansion with $R \ll R_0 = GM/|E|$:

$$\frac{\delta\rho}{\rho} = \frac{\tilde{R}}{5R_0}\left(1 + \frac{d\ln E^3}{d\ln M}\right) \sim \tilde{a} \sim t^{\frac{2}{3}}; \quad \frac{\delta V}{V} \approx \frac{2}{5}\frac{\tilde{R}}{R_0} \sim \tilde{a}. \tag{12}$$

The behavior of the general solution (4)—(7) in the late stages of expansion, when $t \gg t_0(M)$, is determined primarily by the total energy $E(M)$ of the "dust" and is relatively insensitive to the form of the function $t_0(M)$. Differences in ejection times of the successive envelopes from the "protonucleus" thus become insignificant at large distances from the center and do not affect the asymptotic behavior of hyperbolic motion. We thus conclude that the special class of solutions corresponding to the initial values

$$a_0 = \frac{GM}{|E|^{\frac{3}{2}}} = const, \; t_0(M) \neq const; \quad E = 0, \; t_0(M) \neq const, \tag{13}$$

represents all the possible isotropizing models of a dust sphere, which evolve into homogeneous isotropic models in the course of expansion from an essentially inhomogeneous singular state. In the parabolic case ($E = 0$, $t_0(M) \neq$ const), the inhomogeneity amplitude (11) decreases as $a^{-3/2}$ during expansion, and if $t \gg t_0(M)$, the motion is isotropized and solution (3), (8) reduces to a homogeneous plane model with damped small perturbations of the form

$$\rho = \frac{1}{6\pi G t^2}, \quad \frac{\delta\rho}{\rho} = \frac{2}{t}\frac{dt_0}{d\ln M} \ll 1. \tag{14}$$

For hyperbolic expansion of the sphere with $E > 0$, $a_0 = $ const, the "dust" distribution is also homogenized, and small deviations from the homogeneous isotropic background decay first according to (14) as $a^{-3/2}$ and then, for $a \gg a_0$, as $a^{-1} \sim 1/t$, although the two time dependences are identical:

$$\rho = \rho_0\left(\frac{a_0}{a}\right)^3, \; \rho_0 = \frac{3}{4\pi G a_0^2}, \quad \frac{\delta\rho}{\rho} \approx \frac{2}{a}\frac{dt_0}{d\ln E} \ll 1. \tag{15}$$

In the asymptotic limit $a \sim t \to \infty$, for vanishingly low density and constant inertial outward motion of the "dust" with $E > 0$, these initially inhomogeneous models of a sphere reduce to Milne's open kinematic model /4/. In the case of negative total energy $E(M) < 0$, the phase of overall expansion is of finite duration, of the order of $a_0(M)$, and perfect isotropization is unattainable, although inhomogeneous models with $t_0(M) \ll a_0 = $ const in the late stages of expansion ($t \gg t_0(M)$) may approach arbitrarily close to a "closed" homogeneous isotropic model.

For special classes of inhomogeneous spherical models, which contain a single arbitrary functions $a_0(M)$, or $t_0(M)$, and correspondingly isotropize during the collapse around a singular point or during the infinite expansion state, the dynamics may be treated as the case of nonlinear evolution of the

ascending and the declining branch of arbitrary spherically symmetric perturbations of "dust" distribution due to gravitational instability in the homogeneous isotropically expanding medium. We can thus readily investigate the behavior of any density and radial velocity perturbations in a sphere and, in particular, derive the classical results of the growth of Jeans instability in isotropic models /4, 5, 16/ from the exact solution, provided the variations in the initial values $\delta a_0(M)$ and $\delta t_0(M)$ are such that the deviations in density and velocity over a finite length of time from the original Fridman state are small, i.e., $\delta\rho/\rho \ll 1$, $\delta V/V \ll 1$, where

$$\frac{\delta\rho}{\rho} \approx A\alpha + B\alpha^{-\frac{3}{2}}, \quad \frac{\delta V}{V} \approx A'\alpha + B'\alpha^{-\frac{3}{2}} \tag{16}$$

In the linear approximation, the inhomogeneity amplitude contains a growing ($a_0(M) \neq$ const) and a decreasing ($t_0(M) \neq$ const) term; it increases only during the parabolic stage of expansion and goes to a constant limit for hyperbolic inertial outward motion of the "dust", when its gravitational interaction is negligible. Unlimited expansion of the sphere has a stabilizing effect on the growth of perturbations, whereas its collapse introduces substantial instability in the model and leads to a faster infinite growth of inhomogeneity and small velocity perturbations (including nonradial perturbations). The nonradial perturbations may become comparable with radial perturbations, thus increasing the nonsphericity and the instability of the ellipsoid figure under eccentricity-increasing forces and transforming it into a disk /17, 4/.

In the general case of hyperbolic expansion of a sphere with arbitrary initial "dust" distribution ($a_0(M) \neq$ const, $t_0(M) =$ const), the strong "inborn" inhomogeneity rapidly decays and the expansion reveals a tendency to isotropization, although the slowly growing Jeans branch (which is "frozen" in the inertial stage) prevents complete homogenization of the distribution of matter. In the asymptotic region ($a \sim t \to \infty$), where the "dust" particles move by inertia, hyperbolic expansion of any sphere becomes isotropic, and a slight residual density inhomogeneity is retained:

$$R \approx E^{\frac{1}{2}}(M)t, \quad \rho \approx \frac{1}{2\pi E^{\frac{1}{2}}} \frac{dE}{dM} t^{-3}. \tag{17}$$

Because of the relationship between isotropization and dynamic instability in collapsing spherical models, the results of linear analysis /17/ similarly indicate that the hypothesis of spherical symmetry of density and velocity distribution in the early stages of expansion is not unavoidable and there may be a more general initial inhomogeneous state, in particular a disk-shaped distribution /4/, which is also isotropized both in the Newtonian and in the relativistic theory.

RELATIVISTIC THEORY

The local similarity of relativistic and Newtonian spherical models does not extend to the global structure of these models; the classical concepts of absolute time and Euclidean space are clearly inapplicable to the

Metagalaxy, and we therefore have to repeat our analysis within the framework of the general relativity theory, additionally taking into consideration the possible existence of a nonzero cosmological constant $\Lambda \neq 0$ /18/.

Spherically symmetrical inhomogeneous models of dust matter constituted the subject of numerous studies and were analyzed from different points of view both in astrophysics (a bounded sphere) and in cosmology (an infinite medium) /11, 12, 19—23/ in connection with the problems of collapse, singularities, and formation of galaxies in the expanding Universe. As we know /3, 4, 11, 12/, Einstein's field equations in the co-moving (and synchronous) frame of reference of the "dust" with the metric

$$ds^2 = d\tau^2 - e^{\omega(\chi,\tau)}d\chi^2 - R^2(\chi,\tau)[d\vartheta^2 + \sin^2\vartheta d\varphi^2], \tag{18}$$

where τ is the intrinsic time,* χ is the radial Lagrangian coordinate of the particles in the spherical layer, have an exact solution which was derived by Tolman /21/:

$$e^{\omega} = \frac{R'^2}{1+f}, \quad \dot{R}^2 = f + \frac{2m}{R} + \frac{\Lambda R^2}{3}, \quad \rho = \frac{m'}{4\pi R^2 R'}. \tag{19}$$

The first integrals are $-1 < f(\chi) < \infty$, $m(\chi) \geq 0$ are arbitrary functions which define the distribution of the relativistic specific energy of the "dust" $W(\chi) = \sqrt{1+f}$ and the active gravitational mass of the sphere—the equivalent of its total energy; prime and dot denote partial differentiation with respect to χ and t.

The law of "dust" motion $R(\tau, \chi)$ is defined as the integral of the dynamic equation in (19):

$$\tau - \tau_0(\chi) = \int_{R_0(\chi)}^{R} \left(f + \frac{2m}{u} + \frac{\Lambda u^2}{3}\right)^{-\frac{1}{2}} du; \tag{20}$$

in the general case $\Lambda \neq 0$ it is expressed in terms of elliptical functions /12, 19/, and for $\Lambda = 0$ it is expressed by well known formulas in explicit or parametric form /3/ similar to (3)—(6) if we take $R = |f(\chi)|^{1/2} a(\tau, \chi)$ and set $R_0(\chi) = 0$, assuming $\tau_0(\chi)$ to be the time of collapse of the particles of a given spherical layer at the singular "center" $R(\chi, \tau_0) = 0$. The Tolman—Bondi—Lemaitre solution (19)—(20) actually depends only on two physically significant functions $a_0(\chi) = 2M/|f|^{3/2}$ and $\tau_0(\chi)$, since in view of the arbitrary choice of the radial Lagrangian coordinate, the function $f(\chi)$ may be expressed in a canonical form, which only depends on its sign

$$f(\chi) = \epsilon S^2(\chi), \quad S(\chi) = \begin{cases} \sin\chi, & \epsilon = -1 \\ \operatorname{sh}\chi, & \epsilon = +1 \end{cases}, \quad m(\chi) = \frac{a_0(\chi)}{2} S^3(\chi), \tag{21}$$

thus expressing the metric and the distribution of matter in the TBL models in terms of this irreducible set of initial values for the gravitaging "dust" sphere, $a_0(\chi)$ and $\tau_0(\chi)$:

$$\begin{gathered} R(\chi,\tau) = S(\chi)a(\tau,\chi), \quad e^{\frac{\omega}{2}} = a\left(1 + \frac{\partial \ln a}{\partial \ln S}\right), \\ \dot{a}^2 = \frac{a_0}{a} + \frac{\Lambda a^2}{3} + \epsilon, \quad \varkappa\rho = \frac{3a_0}{a^3} \frac{\left(1 + \frac{d\ln a_0}{d\ln S^3}\right)}{\left(1 + \frac{\partial \ln a}{\partial \ln S}\right)}. \end{gathered} \tag{22}$$

* The velocity of light and the Newtonian constant $c = G = 1$. Einstein's constant $\varkappa = 8\pi$.

Degenerate quasi-Euclidean models with $f = 0$ correspond in (22) to $a_0 = \text{const}$, $S(\chi) = \chi$, $m(\chi) = \frac{a_0}{2}\chi^3$, and they contain only one essentially arbitrary function, $\tau_0(\chi)$:

$$a = \left(\frac{3a_0}{\Lambda}\right)^{\frac{1}{3}} sh^{\frac{2}{3}} \frac{\sqrt{3\Lambda}}{2}[\tau - \tau_0(\chi)], \ \Lambda > 0 ;$$
$$a = \left(\frac{3a_0}{|\Lambda|}\right)^{\frac{1}{3}} \sin^{\frac{2}{3}} \frac{\sqrt{3|\Lambda|}}{2}[\tau - \tau_0(\chi)], \ \Lambda < 0 \qquad (23)$$

The radius of a fixed spherical "dust" layer satisfies a Fridman-type equation, and the basic results of the analysis of the dynamics of Fridman's models for $\Lambda \neq 0$ /18, 24/ and, in particular, their classification according to Robertson /25/ are directly applicable to the case of "dust" motion in inhomogeneous spherical models. These inhomogeneous models also can be classified according to the general features of expansion: oscillatory O_1, monotonic M_1, M_2, and asymptotic A_1, A_2, all of which approach Einstein's static model with $\Lambda = \varkappa\rho/2$ in the course of expansion or, respectively, collapse. The time dependence $a(\tau, \chi)$ precisely coincides with the behavior of the scale factor in the corresponding Fridman models, and for $\Lambda = 0$ it can be expressed in parametric form in terms of Weierstrass's elliptical functions $\wp(z)$, $\zeta(z)$ and $\sigma(z)$ with the invariants $g_2 = 1/12$, $g_3 = 1/216 - \Lambda a_0^2/48$:

$$a = \frac{a_0}{4}\left\{\wp(\eta) - \wp(\eta_0)\right\}^{-1}, \ \tau - \tau_0 = \frac{1}{\wp(\eta_0)}\left[2\eta\zeta(\eta_0) + \log\frac{\sigma(\eta - \eta_0)}{\sigma(\eta + \eta_0)}\right], \qquad (24)$$

where $\wp(\eta_0) = -1/12$, $\dot{\wp} = d\wp/d\eta$.

The TBL solution includes as a particular case the metric of homogeneous isotropic Fridman models

$$ds^2 = d\tau^2 - a^2(\tau)\left\{d\chi^2 + S^2(\chi)\left[d\vartheta^2 + \sin^2\vartheta\, d\varphi^2\right]\right\},$$
$$a^2 = \frac{a_0}{a} + \frac{\Lambda a^2}{3} - k, \quad \varkappa\rho = \frac{3a_0}{a^3} \geq 0, \ k = \pm 1, 0, \qquad (25)$$

which correspond to a special choice of the initial conditions for the "dust" in the general-relativistic sphere:

$$a_0 = \frac{2m}{|f|^{\frac{3}{2}}} = const, \ \tau = const ; \qquad f = 0, \ \tau_0 = const \qquad (26)$$

and, correspondingly,

$$R(\chi, \tau) = a(\tau) S(\chi), \quad m(\chi) = \frac{a_0}{2} S^3(\chi), \ f = \epsilon S^2(\chi) \qquad (27)$$

Here, the function $S(\chi)$ differentiates between an open, a plane, and a closed model with spaces V_3 of constant negative, zero, and positive curvature $K = k/a^2$ according as $\epsilon = \pm 1, 0$. The homogeneous distribution of matter in the TBL models ($\rho = \rho(\tau)$, $m(\chi) = \frac{4\pi}{3}\rho R^3$) automatically ensures separation of variables $R(\chi, \tau) = S(\chi)\, a(\tau)$ and it therefore invariably presupposes isotropy of the Hubble tensor of deformation rates (i.e., constant ratio of the circumferential distance R to the intrinsic radial distance $L(\chi) = \int_0^{\chi} e^{\omega/2} d\chi = \int_0^{R} \frac{dR}{\sqrt{1 - f}}$ in the physical space V_3 of the co-moving frame of reference of the "dust") and also isotropy of the local curvature of V_3, which should be a space of constant curvature, although in general it has a non-Euclidean anisotropic

and inhomogeneous geometry /11/. Thus, in the centrally symmetric case, the spatial inhomogeneity, the isotropy of expansion, and the curvature of V_3 are all interdependent, although certain aspects of the anisotropy of models are nevertheless compatible with their homogeneity /6, 7/.

Einstein's equations in the co-moving frame of reference of the "dust" and their solution for the spherically symmetric case reveal a far-reaching similarity to the Newtonian dynamics of an arbitrary sphere in Lagrangian form /11, 7/, and the TBL models admit of a quasiclassical treatment, provided we modify the interpretation of the constants in the dynamic equation (19), which is regarded as the equivalent of the Newtonian energy integral in the presence of an additional cosmological force $\vec{F} = \frac{1}{3}\Lambda\vec{R}$ with the potential $\frac{\Lambda R^2}{6}$.

The main difference between the relativistic and the Newtonian models of a sphere is associated with the equivalence principle: in the general relativity theory, the active gravitational mass of the sphere $\mathcal{M}(\chi) = 4\pi\int_0^\chi \rho R^2 R' d\chi$ is represented by its total energy, which for $f \neq 0$ is different from the overall rest mass of the "dust" $M(\chi) = 4\pi\int_0^\chi \rho R^2 e^{\omega/2} d\chi$. It may include the intrinsic gravitational binding energy for $f<0$ (a negative mass defect $\mathcal{M}<M$), or a positive excess of the kinetic energy of the "dust" for $f>0$, when $\mathcal{M}>M$. These nonlinear effects — the mass defect and the gravitation of the excess kinetic energy of the "dust" — characteristically emerge through the non-Euclidean character of the co-moving space V_3, since the relativistic specific energy $W^2 = 1 + f$ which characterizes the ratio of the active to the intrinsic mass of the spherical layer ($\mathcal{M}' = WM'$) also determines the geometry of the space sections $\tau = \text{const}$ /11/. In particular, the sign of the quasi-Newtonian energy $f = 2E$, which for $\Lambda = 0$ differentiates between the different types of motion of the layer, is minus the sign of the local scalar curvature of V_3.

In strong gravitation gields, when the potential binding energy or the kinetic energy of the "dust" are comparable with the rest mass, the nonlinearity of the general relativity theory becomes quite significant and leads to fundamental distinctions between the relativistic and the Newtonian model. These differences primarily affect the global properties, since the classical theory is locally applicable. In this respect, an instructive example is provided by the case of "semiclosed" and closed Fridman models /4, 12/,

$$R(\chi, \tau) = \sin\chi\, a(\tau), \quad \mathcal{M}(\chi) = \frac{a_0}{2}\sin^3\chi, \quad W = \cos\chi,$$

where the mass defect of a layer may exceed its rest mass ($\pi/2 < \chi < \pi$), thus leading to a non-Euclidean topology of V_3. Note that in Fridman's open model (25), the contribution from the excess kinetic energy of the outward motion of the "dust" to the active mass $\mathcal{M}(\chi) = \frac{a_0}{2}\mathrm{sh}^3\chi$ for $\chi \gg 1$ is greater than the total rest mass of the observed matter $M(\chi) = \frac{3}{4}a_0(\frac{\mathrm{sh}2\chi}{2} - \chi)$ and accounts for the bulk of the total mass — energy of the sphere:

$$\Delta T(\chi) = \frac{3}{4}a_0\left(\frac{2}{3}\mathrm{sh}^3\chi - \frac{\mathrm{sh}2\chi}{2} + \chi\right). \qquad (28)$$

If we ignore the non-Euclidean geometry of the co-moving space and identify the active mass with the intrinsic mass, the local properties of the relativistic and Newtonian models of the dust sphere completely coincide; moreover, the density and radial velocity distributions of the "dust" in these models coincide even for anisotropic collapse of the TBL models with $\tau_0(\chi) \neq \text{const}$, when because of the non-Euclidean geometry of V_3 all the radial distances go to infinity and all circumferential distances shrink to zero, so that a "sphere" contracts to a line /3/. It should be emphasized, however, that the classical picture of spherical focusing of the particles from individual spherical envelopes at the center of the sphere is not entirely equivalent to the relativistic collapse, when the particles reach the singular state $\rho \to \infty$ on the space-like hypersurface $R(\chi, \tau_0) = 0$, i.e., almost always simultaneously in an appropriate frame of reference. Because of the global asymmetry of the "contracting" and "expanding" T-regions for $R(\chi, \tau) < 2m(\chi)$, where all the causal phenomena propagate in one direction only (i.e., toward the "central" singularity or away from it, in the outward direction), the anticollapse of the sphere cannot be treated as a simple time-reversal of its collapse /4, 21/.

Because of the analogy in the local properties of relativistic and classical models of a sphere, the results of the Newtonian analysis remain valid and are directly generalized to the general relativity theory.* It is readily seen that a special class of TBL solutions (19) – (24) with the particular initial conditions $a_0 = \text{const}, \tau_0(\chi) \neq \text{const}$ corresponds to inhomogeneous models of a sphere which are isotropized in the course of expansion from a singular state with infinite matter density gradients and asymptotically approach in all their observed properties to Fridman's homogeneous isotropic models. For $\Lambda \geqslant 0$, hyperbolic expansions M_1, M_2, and A_2 of arbitrary inhomogeneous models of a sphere ($a_0(\chi) \neq \text{const}, \tau_0(\chi) \neq \text{const}$) also lead to asymptotic isotropy of deformations and curvature of V_3 in the presence of a slight "frozen" inhomogeneity. At the late stages of expansion, when the cosmological repulsion becomes dominant, these models reduce to de Sitter's universe /7/. In our model of the evolution of the Metagalaxy from a centrally symmetric inhomogeneous singular state, this general case has certain advantages, as it is improbable that the distribution of matter established at the end of the pressure-dominated phase ($P \neq 0$) will have the particular form needed for the perfectly isotropizing outward motion of the "dust."

Lifshits's approximate solution /4, 5/ for weakly perturbed Fridman models in the early superdense and "hot" stages with $P = \varepsilon/3$, which displays only one branch of long-wave Jeans density and velocity perturbations slowly growing with expansion ($\delta\varepsilon/\varepsilon \sim a^{4/3} \sim t^{2/3}$) and reveals absolute instability of the isotropic homogeneous collapse under small perturbations in the distribution of matter and the free gravitation field, indicates that for $P \neq 0$ and in the case without spherical symmetry, there should also exist a sufficiently wide class of inhomogeneous and anisotropic models which isotropize in the process of expansion.

The spherically symmetrical models considered this paper are applicable to the expanding Universe with a globally inhomogeneous

* It is shown in /14/ that the TBL solution is not general and in the general relativity theory there is a special class of T-models of a sphere without classical analog.

singular state and also to the Metagalaxy, when treated as a bounded realtivistic object which expands as a result of the "big bang" from a superdense singular state — the "protonucleus" — whose very inhomogeneity in principle allows conversion of the internal energy released by the hypothetical "explosion" into the kinetic energy of expansion. In accordance with the existing general concepts of cosmogonic evolution — both the traditional /4/ and that developed by V.A. Ambartsumyan /26/ — we can propose two schematic models of the "big bang": 1) continuous relativistic outflow of matter, which in the process of overall expansion is homogenized on a large scale while collecting into small condensations (galaxies and clusters of galaxies) as a result of gravitational instability; 2) ejection of D-bodies (mainly), which in the course of their cosmological outward motion become distributed fairly uniformly and provide the basis for the evolution of Metagalactic structure.

In conclusion note that if the hypothesis of the essentially inhomogeneous initial state of the Metagalaxy is applicable and isotropization indeed occurred at fairly late stages with $z \leqslant 10-100$, observations of distant regions with sufficiently large z should reveal large-scale inhomogeneity and anisotropy /27/. The authors are grateful to L.E. Gurevich, A.G. Doroshkevich, and Ya.B. Zel'dovich for the discussion of results and critical comments.

Bibliography

1. Observational Foundations of Cosmology.— Moscow, IL. 1965. [Russian translation.]
2. Davidson, W. and I.V. Narlicar.— Report Progr. Phys., London Phys. Soc., 29:539. 1966.
3. Landau, L.D. and E.M. Lifshits. Teoriya polya (Theory of Fields).— Moskva, Izdatel'stvo "Nauka." 1967.
4. Zel'dovich, Ya.B. and I.D. Novikov. Relyativistskaya astrofizika (Relative Astrophysics).— Moskva, Izdatel'stvo "Nauka." 1967.
5. Lifshits, E.M. and I.M. Khalatnikov.— UFN, 80:391. 1963.
6. Zel'manov, A.L.— Trudy 6-go soveshchaniya po voprosam kosmologii, p.144, Moskva, Izdatel'stvo AN SSSR. 1959.
7. Heckman, O. and E.M. Schüking.— XI Conseil de Physique Solvays, p.149, Bruxelles. 1958; Gravitation, p.438, New York, Acad. Press. 1962.
8. Misner, C.W.— Astrophys. J., 151:431. 1968.
9. Hawking, S.W.— Monthly Not. RAS, 107:129. 1969.
10. Grishchuk, L.P., A.G. Doroshkevich, and I.D. Novikov.— ZhETF, 55:2281. 1968.
11. Bondi, H.— Monthly Not. RAS, 142:410. 1947.
12. Lemaitre, G.— Rev. Mod. Phys., 21:357. 1949.
13. Partridge, R.B. and D.T. Wilkinson.— Phys. Rev. Lett., 18:557. 1967; Conklin, E.K. and R.N. Bracewell.— Phys. Rev. Lett., 18:614. 1967.
14. Ruban, V.A.— ZhETF, 56(6). 1969; ZhETF Letters, 8:669. 1968.

15. McVittie, G.C. General Relativity and Cosmology, 2nd ed. — Univ. of Illinois Press, Urbana, Ill. 1965.
16. Bonnor, W.B.— Monthly Not. RAS, 117:104. 1957.
17. Lin, C.C., L. Mestel, and F. H. Schu.— Astroph. J., 142:1431. 1965; Lynden-Bell, D.— Proc. Cambridge Phil. Soc., 58:709. 1962.
18. Zel'dovich, Ya.B.— UFN, 95:209. 1968.
19. Tolman, R.C.— Proc. Nat. Acad. Sci., 20:169. 1934.
20. Omer, G.C.— Proc. Nat. Acad. Sci., 53(1). 1965.
21. Novikov, I.D.— Astronom. Zh., 41:1075. 1964.
22. Bonnor, W.B.— Zs. F. Astrophys., 35:10. 1954.
23. Peebles, P.— Astrophys. J., 147:859, 1967.
24. Bondi, H. Cosmology.— Cambridge. 1960.
25. Robertson, H.P.— Rev. Mod. Phys., 5:62. 1933.
26. Ambartsumyan, V.A.— In: "Voprosy Kosmogonii," 8:3, Moskva, Izd. AN SSSR. 1962.
27. Wilkinson, D.T. and R.B. Partridge.— Nature, 215:719. 1967; Rees, I. and D.W. Sciama.— Nature, 217:511. 1968; Nature, 213:374. 1967.

FORMATION OF GALAXIES IN AN EXPANDING UNIVERSE

A. G. Doroshkevich

One of the striking features of the observable part of the Universe is the highly isotropic expansion and the homogeneous distribution of matter over large scales. On a small scale, however, the distribution of matter is distinctly inhomogeneous: stars cluster in galaxies (mean density $\rho_g \sim 10^{-24} - 10^{-25}$ g/cm^3, mass $M_g \sim 10^8 - 10^{11} M_\odot$), galaxies in their turn form clusters of galaxies (mean density $\rho_C \sim 10^{-27}$ g/cm^3, mass $M_C \sim 10^{11} - 10^{14} M_\odot$). The existence of the next higher stage in this hierarchy — superclusters with masses $M_S \sim 10^{14} - 10^{17} M_\odot$ — is doubtful, however /1, 2/. Observations show that starting on a scale of 50 — 100 Mpc, the distribution of observable matter in the Universe is roughly homogeneous /3/.

The isotropic expansion and the homogeneous distribution of matter in the Universe are also evidenced by intensity (or temperature) observations of the relict background radiation. Isotropic radiation with temperature T = 2.7°K was discovered in 1965 by Pensias and Wilson /4/. The interaction of this radiation with matter is very weak (the only interaction channels are Compton scattering and gravitation), so that it provides information about the large-scale distribution and motion of matter at distances beyond the range of modern optical astronomy.

The red shift of the light emitted by an object $z = \frac{\lambda - \lambda_0}{\lambda_0}$, where λ is the wavelength of the incoming light and λ_0 is the wavelength of the emitted light, provides an adequate characteristic of the distance to far objects. The value of z is determined directly from observations of spectral lines. Once z has been found, we can determine the distance of the object (within the framework of the accepted cosmological model), the exact time of light emission, the mean density at the time of emission, etc. Thus, for example, $\rho_z = \rho_0 (1+z)^3$ (ρ_0 is the mean density at present). The brightest galaxies are observed up to $z \sim 0.2 - 0.3$; quasars are observed up to z = 2.2 (i.e., up to $\rho \approx 33 \rho_0$). With regard to relict radiation, the Universe is transparent at least up to $z = z^* \geqslant 8$,* i.e., to densities a factor of 730 as great as the present-day mean density!

According to the observations of Partridge and Wilkinson /5/, the temperature anisotropy of the relict radiation is $\frac{\Delta T}{T} \sim \pm(3 \pm 1) \cdot 10^{-3}$ for angular

* z* depends on the mean density of the Universe at present and increases with diminishing density. z* = 8 for the mean present-day density $\bar{\rho}_0 = 2 \cdot 10^{-29}$ g/cm^3, which corresponds to the critical density $\bar{\rho}_c = 3H_0^2/8\pi G$ (H_0 is Hubble's constant).

resolution of about 15°. The observations of the small-scale anisotropy of the relict radiation carried out by Conclin and Brasewell /6/ and by Pariiskii and Petunina /7/ give $\frac{\Delta T}{T} \lesssim 2 \cdot 10^{-3}$. These data point to excellent isotropy of motion and distribution of matter on a large scale in the Universe. A detailed analysis of the experiments intended to detect a possible anisotropy of the cosmological expansion was given in /8/. The estimates of the possible degree of inhomogeneity in the distribution of matter in the Universe according to these results are given in /9, 10/.

The assumption of homogeneous distribution of matter in the Universe and isotropic expansion leads to Fridman's cosmological model. This model, advanced by A.A. Fridman in 1922–1924 /11/, has been developed in greatest detail among the various currently available cosmological models and it reveals adequate consistency with all the known observations. There is one fundamental difficulty, however, and it is how to make Fridman's model consistent with the existence of galaxies and clusters of galaxies.

Fridman's model is a non-steady-state model. Within its framework, the expansion began at a certain point in a state of infinite density (which is used as the zero point on the time scale). Near this singular point, the classical theory of relativity is evidently inapplicable: quantum effects are not ignorable, and there may be other factors which are unknown under the standard present-day conditions. Dimensionality considerations indicate the probable limits of application of the general relativity theory: distance $l=(Gh/c^3)^{1/2} \simeq 10^{-33}$ cm, time $t = l/c \simeq 0.6 \cdot 10^{-43}$ sec, density $\rho = c^5/G^2h \simeq 10^{93}$ g/cm^3. When Fridman's model is extrapolated into the past of the Universe to $t = 0.6 \cdot 10^{-43}$ sec, the isotropic expansion and the homogeneous distribution of matter near the singularity should be retained on a scale comparable with the horizon $l_H = ct$, i.e., on a scale $l \geqslant 10^{-33}$ cm. A natural solution to the problem of formation of galaxies under these conditions is provided by the fluctuation hypothesis, based on the assumption of small deviations of the distribution and expansion of matter from homogeneous and isotropic.

A number of studies have been published recently which treated the problem of formation of galaxies assuming a breakdown of the Fridman theory in the early stages of expansion. These models remove some of the characteristic restrictions of the Fridman model, and open new possibilities for explaining the origin of galaxies and clusters of galaxies. However, the breakdown of the Fridman model in the early stages of expansion involves a number of basic difficulties. The main thing is to ensure that the early models have the Fridman model as their limit and that they lead to a sufficiently low anisotropy of the relict radiation in accordance with observations /5, 6, 7/. This is a significant point, since not any model will go to Fridman's model with time. The second point is that the alternative models should ensure a sufficiently low content of helium (less than 30% by weight) and the heavy elements in the Universe. This requirement also restricts the permissible deviations of the cosmological model from Fridman's model, since according to Thorne /12/ anisotropic models may lead to an entirely different chemical composition of the protostellar matter (with helium accounting for more than 50% by weight). Finally, we should prevent the formation of objects liable to collapse in the early stages of expansion and large-mass

objects with densities much higher than the mean density of galaxies ($\rho_g \sim 10^{-24} - 10^{-25}$ g/cm^3). No such objects are observed at present and their existence (in numbers) would involve considerable difficulties.

These restrictions severely limit the gamut of the permissible cosmological models. At present, very few simple cosmological models differing from Fridman's model are known /8, 13/. These models are based on the assumption of homogeneous distribution of matter and they do not consider the formation of galaxies.

In this paper, the main emphasis is placed on the formation of galaxies in Fridman's model within the framework of the fluctuation hypothesis. Suppose that in the initial phase of expansion (e.g., for $t \sim 10^{-43}$ sec), the distribution of matter slightly deviates from the homogeneous distribution. Tracing the evolution of this perturbed Fridman's model into the future, we can try to account for the formation of galaxies and clusters of galaxies as a result of these small perturbations of Fridman's model. The problem thus falls into three interrelated parts:

1) the origin of the initial perturbations in the early stages of expansion;
2) the evolution of perturbations in the course of expansion;
3) the formation of galaxies and clusters of galaxies.

At this stage, only the solution of the second problem is available. The evolution of perturbations against the background of Fridman's homogeneous model was considered by Lifshits in 1946 /14/. Specific features arising as a result of the application of the general to Fridman's "hot" model were discussed later by various authors /8, 15, 16/.

In Fridman's "hot" model, four types of perturbations are possible:

1. Adiabatic perturbations of density, velocity, and metric.
2. Entropy perturbations of density, velocity, and metric.
3. Rotational perturbations of velocity and metric.
4. Metric perturbations of the type of gravitational waves.

In an expanding Universe, gravitational waves are evanescent. Rotational perturbations also decay during expansion. Perturbations of these types cannot affect the formation of galaxies in Fridman's model. The attempt to use rotational perturbations as the mechanism of formation of galaxies involved rejection of Fridman's model in the early stages of expansion /17/.

Entropy perturbations are associated with perturbations in the distribution of baryons against the homogeneous background of radiation. These perturbations are "frozen" at the stage $\varepsilon_\gamma \gg \varepsilon_m$ (ε_γ is the radiation energy density, ε_m is the matter energy density) and begin developing only after the stage of hydrogen recombination, where the interaction of radiation with matter has become weak.

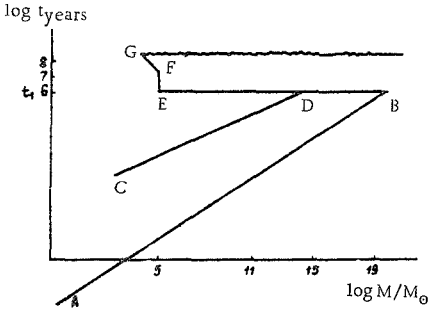

The growth of perturbations in Fridman's "hot" model.

The development of the adiabatic perturbations of density, velocity, and metric in the course of expansion depends on the scale of the perturbation. The evolution of entropy and adiabatic perturbations is illustrated by the figure.

The scale of perturbation is characterized by the combined rest mass of

the baryons encompassed by the perturbation. This is the variable laid off the horizontal axis. The vertical axis gives the time reckoned from the singularity instant. The time $t = t_1$ corresponds to the recombination of hydrogen (the same time approximately corresponds to the condition $\varepsilon_\gamma \sim \varepsilon_m$).

The line ABEFG corresponds to the Jeans wavelength — the boundary separating the instability region (to the right of this line) from the stability region. To the right of the line AB, the adiabatic density perturbations grow in proportion to time $\delta\rho/\rho \sim t$ (on constant scale), whereas to the left of the line AB acoustic oscillations of constant amplitude occur. The line CD limits the range of dissipative processes associated with Compton scattering of photons by electrons. To the right of the line CD, the dissipative processes are insignificant, whereas to the left of this line density perturbations decay exponentially with time.

After recombination, the radiation pressure can be ignored, and the Jeans wavelength therefore falls steeply. For $t > t_1$, there is no obvious difference between entropy and adiabatic perturbations. All density perturbations grow in proportion to $t^{2/3}$ to the right of the line EFG and decay as $t^{-1/6}$ to the left of this line.

In the early stages of expansion, the growth of perturbations was affected by the neutrino viscosity and other processes. These processes, however, were significant on a very small scale, and apparently they could not affect the formation of galaxies in Fridman's model.

Given the laws governing the growth of perturbations in Fridman's model, we can relate the perturbations occurring near the singular point to the third, nonlinear stage of formation of galaxies — the phase when the perturbation becomes comparable with 1 and the perturbation theory does not apply.

However, before proceeding with a discussion of the nonlinear phase of formation of galaxies, let us examine what we know about the origin of perturbations and their amplitudes near the singular point.

One of the possible points of view associates the perturbations with a hypothetical compression phase which possibly preceded the expansion phase. According to this conception, the inhomogeneities arose in the compression phase, remained intact during the transition through the singular point, and subsequently proceeded evolving according to the laws discussed above. The transition through the singular point has been the subject of numerous studies in recent years, but no great success has been achieved so far in this direction. The status of this theory is therefore still highly uncertain.

Another point of view calls for the construction of initial perturbations without resorting to an earlier compression phase. We may assume, for instance, that the homogeneity is only a statistical phenomenon. This will automatically lead to density perturbations $\delta N/N \sim 1\sqrt{N}$, where δN is the perturbation in the number of particles in a volume containing N particles. Lifshits /14/ noted that for a mean density $\bar{\rho} \sim 10^{14}$ g/cm^3 (which corresponds to the nuclear density), these perturbations are insufficient for the formation of galaxies. It is readily seen, however, that if such perturbations are postulated for $t \sim 10^{-43}$ sec, $\bar{\rho} \sim 10^{93}$ g/cm^3, they will be excessively large and will lead to formation of separate objects with masses $M \sim 10^{57} M_\odot$!

There is still another approach possible to the problem of initial perturbations. A perfectly homogeneous distribution of matter can be assumed

to start with, but there are random velocities associated with the temperature. This will naturally lead quite soon to density perturbations, but they will be insufficient for the formation of individualized galaxies. Incidentally, note that all the requirements imposed on the shape and the amplitude of the initial perturbations are borrowed from among the properties of quantum fluctuations of a degenerate Fermi gas, whereas there is no reason whatsoever to assume that such fluctuations indeed arise in Fridman's "hot" model.

There is thus no satisfactory theory of initial fluctuations at this stage. The parameters of the initial perturbations are arbitrary to a considerable extent and they have to be fixed so as to ensure the best fit of the final results of the theory with the current outlook on the Universe.

The third part of the problem of the formation of galaxies and clusters of galaxies in Fridman's model is highly complex, as it involves nonlinear effects. The treatment is generally confined to qualitative analysis of the various phenomena and order of magnitude estimates of the final results /16, 17, 19/. In particular, this is due to the large uncertainty in our information concerning the clusters of galaxies and the intergalactic medium.

The theory of the evolution of perturbations in Fridman's model yields three Jeans wavelengths λ (see figure): λ_1 before recombination corresponds to masses $M \simeq 10^{17} - 10^{19}\ M_\odot$, λ_2 in the dissipation range corresponds to masses $M \simeq 10^{11} - 10^{13}\ M_\odot$, and finally λ_3 after recombination corresponds to $M \simeq 10^5\ M_\odot$. No other wavelengths exist in the hydrodynamic theory for $t > t_1$. Let us relate the masses corresponding to $\lambda_1, \lambda_2, \lambda_3$ with the observed mass distribution of galaxies and clusters of galaxies.

The mass $M \simeq 10^5\ M_\odot$ is significant for entropy perturbations only, since adiabatic perturbations are small on the corresponding scale because of dissipative effects. The origin of galaxies in Fridman's model was prescribed to these perturbations in /16, 19/; a similar attempt was made by Harrison in connection with the theory of charge-symmetrical Universe /20/. These attempts meet with a number of objections in view of the latest estimates of the probable density and temperature of the intergalactic gas /21/. According to Harrison's theory, the perturbations are close to unity at the time of hydrogen recombination /22/, at variance with observations. A further attempt to apply the entropy perturbations was recently made by Peebles, who associated the mass $M \simeq 10^5 M_\odot$ with globular clusters in galaxies. The validity of these attempts is not clear at this stage.

The adiabatic perturbations in Fridman's model are associated with two characteristic masses, $10^{11} - 10^{13}\ M_\odot$ and $10^{17} - 10^{19} M_\odot$. The larger of these masses may be possibly related to the hypothetical superclusters of galaxies. The smaller mass is in good agreement with the estimates of the mass of large galaxies and small clusters of galaxies. It is therefore worthwhile to try and construct a theory of formation of galaxies and clusters of galaxies using this particular mass. The development of this theory meets with certain difficulties. The formation of galaxies and clusters of galaxies from a homogeneous metagalaxy poses a number of questions.

One of the main questions is to determine the exact proportion of matter in the Universe which is observed in the form of galaxies. The observed mean density of matter concentrated in galaxies is close to $\rho_2 \sim 5 \cdot 10^{-31}\ g/cm^3$.

The mean density of the intergalactic field has not been determined so far. The last estimates give an upper limit of $\bar{\rho} \sim (2-6) \cdot 10^{-30}$ g/cm^3 for this density. In other words, the galaxies should contain no less than 10 — 20% of the total mass of the Universe. This is quite a substantial proportion from the point of view of the theory which prescribes the formation of galaxies to small density perturbations. There is a possibility, however, that future observations will yield a lower density estimate for the intergalactic gas.

The second question is how we are to determine the mass distribution of galaxies and clusters of galaxies. The use of the characteristic mass $M \sim 10^{11} - 10^{13}$ $M_\odot$ in the theory gives some hope of finding a successive answer to this question.

The third question of the theory demands that we account for the observed rotation of galaxies and, possibly, clusters of galaxies. In the theory under discussion, no eddy velocities are observed in the early stages of evolution and all the random velocities are potential. This, however, is quite consistent with the rotation of galaxies and clusters of galaxies. This problem was considered in /23/, where it was shown that the rotation of galaxies may be partly related to the "embryonic" rotation which develops when a cloud condenses from a medium with random potential velocities and partly to the existence of a quadrupole moment in galaxies, which makes the galaxies spin through gravitational interaction with other galaxies. These suggestions should be further explored, but nevertheless they appear quite promising.

Still another problem arises in connection with the magnetic fields of galaxies and clusters of galaxies. So far, there is no theory which could account for the observed magnetic fields as a byproduct of the formation of galaxies. As a result, the existence of an "embryonic" magnetic field in the Universe had to be suggested. Cosmological models with a homogeneous magnetic field were constructed and the compatibility of the cosmological magnetic field with Fridman's model was proved /24/. It is by no means clear, however, that this approach is without alternative. Theoretical predictions are still difficult to compare with observations, because the latter are distorted by secondary effects — various ejection processes, explosions, etc. Powerful explosive processes are observed in the immediate vicinity of quasars and radio galaxies. There is some evidence that the significance of these processes was even greater in the past /25/. These processes may largely be responsible for the observed properties of galaxies and clusters of galaxies /24/. Observations of the distant quasars, for example, point to a vanishingly small density of neutral intergalactic hydrogen $\rho_H \leq 10^{-35}$ g/cm^3. On the other hand, according to the fluctuation theory of the formation of galaxies in Fridman's model, the mean density of intergalactic gas may hardly fall below the mean density of the galaxies, i.e., $\rho \sim 10^{-31}$ g/cm^3. The gas therefore should be very hot (T = 10^6 °K), Powerful energy production processes are needed to achieve this heating of the intergalactic gas.

Secondary explosive processes are probably also responsible for the currently observed expansion of the peripheral regions in clusters of galaxies. The observed velocity variance of the galaxies in clusters is of the order of 1000 km/sec, the clusters measuring 1— 3 Mpc across.

If the clusters are maintained under steady-state conditions, their mass should be several times greater than the observed mass of the constituent galaxies /1, 26/. The expansion of clusters cannot be described as residual cosmological expansion, either, since the clusters expand at a much faster rate than the Universe as a whole. This expansion of clusters is possibly associated with powerful energy release processes at the center of the clusters.

In conclusion we should emphasize that although certain advances have been accomplished in the theory of formation of galaxies in an expanding Universe, there are still many unanswered questions. Further theoretical and observational work is needed.

Bibliography

1. Abell, G.O.— Annual Rev. Astronomy and Astrophysics, 3:1. 1965.
2. Zwicky, F. Morphological Astronomy, p.165.— Berlin, Springer-Verlag. 1957.
3. Zwicky, F. and K. Pudnicki.— Astrophys. J., 137:707. 1963.
4. Pensias, A.A. and R.W. Wilson.— Astrophys. J., 142:419. 1965.
5. Wilkinson, D.T. and R.B. Partridge.— Nature, 215:719. 1967.
6. Conclin, E.K. and R.V. Brasewell.— Phys. Rev. Lett., 18:614. 1967.
7. Pariiskii, Yu.N. and N.V. Petunina.— Konferentsiya po radio-astronomii. Riga. 1968.
8. Zel'dovich, Ya.B. and I.D. Novikov. Relyativistskaya astrofizika (Relativistic Astrophysics).— Moskva, Izdatel'stvo "Nauka." 1967.
9. Zel'dovich, Ya.B. and R.A. Sunyaev.— Astrophys. and Space Science. (In press).
10. Ozernoi, L.M. and Chibisov.— Astronomicheskii Zhurnal. (In press).
11. Fridman, A.M.— UFN, 84:505. 1964.
12. Thorne, K.S.— Astrophys. J., 148:51. 1967.
13. Grishchuk, L.P., A.G. Doroshkevich, and I.D. Novikov.— ZhETF, 54:2281. 1968.
14. Lifshits, E.M.— ZhETF, 16:587. 1946.
15. Silk, J.— Astrophys. J., 151:459. 1968.
16. Doroshkevich, A.G., Ya.B. Zel'dovich, and I.D. Novikov.— Astronom. Zh., 44:295. 1967.
17. Ozernoi, L.M. and A.D. Chernin.— Astronom. Zh., 44:1131. 1967.
18. Zel'dovich, Ya.B.— Astronom. Zh., 1969 (in print); Harrison, E.R.— Preprint, Goddard Space Flight Center, Greenbelt, Md. 1968.
19. Peebles, P.J.E. and R.H. Dicke.— Astrophys. J., 154:898. 1968.
20. Harrison, E.R.— Phys. Rev., 167:1170. 1968.
21. Sunyaev, R.A.— Astrophys. Lett. 1969. (In press).
22. Field, G.B.— Preprint, Princeton University Observatory. 1968.

23. Peebles, P.J.E.— Astrophys. J., 155:393. 1969.
24. Zel'dovich, Ya.B.— Astronomicheskii Zhurnal. 1969. (In press).
25. Longair, M.S.— Monthly Notices RAS, 133:421. 1966.
26. Karachentsev, I.D.— Astrofizika, 1:303. 1965.

THE SEPARATION OF GALAXIES INTO THE HALO AND THE DISK SUBSYSTEM

L. E. Gurevich and A. D. Chernin

As is known, our Galaxy is one of the extensive class of spiral galaxies and it comprises a slowly rotating halo subsystem and a rapidly rotating disk subsystem. Theoretical interpretation of the formation of these subsystems from the original protogalactic cloud meets with serious difficulties. The disk and the halo are of comparable sizes, and this is hardly compatible with the assumption that in view of the different shape and rotation velocity of these subsystems, they originated as a result of different degrees of compression of the original clouds. On the other hand, the assumption that the protogalactic cloud "from the start" contained two components rotating with different velocities is unacceptable because in a gas such differential velocities will rapidly level out. The suggested solution of the problem presented in this paper is based on the concept of elastic and inelastic evolutionary processes in concentrated gravitational systems.

In a gravitational system consisting of numerous particles, collision processes of two types are possible: direct (or, as we say, contact) collisions and gravitational interaction between particles as a result of close encounter.

A system with prevalent gravitational interaction as a result of close encounter will evolve in a characteristic manner which, according to /1—3/, is specified by the following processes.

1. The constituent particles gradually evaporate from the system. The characteristic evaporation time if approximately two orders of magnitude the mean time between encounters.

2. Simultaneously with particle evaporation, the system undergoes compression, so that its dimensions decrease in proportion to the square of the number of particles.

3. If the system rotates, the evaporating particles carry off a certain angular momentum, which exceeds the mean angular momentum of the system particles. As a result, the rotation velocity diminishes, and the system becomes progressively more spherical as a result of evaporation. Evolution of this type will be called elastic (in reference to the relevant particle interactions, which are elastic collisions), or evaporational.

A system in which contact collisions predominate undergoes so-called inelastic evolution. Contact collisions are of necessity inelastic, and the kinetic energy of the colliding particles is expended in irreversible processes, in particular, separation of gas which falls to the center of the system or to the equatorial plane. In this inelastic evolution, no evaporation

is possible, and the total angular momentum is thus conserved. The compression of the system in this case does not produce a more spherical shape.

Evolutionary processes of both types occur in concentrated star systems and also in systems consisting of stars and gas clouds. Note that these processes may have played an important role in the formation of the halo and the disk subsystems of our Galaxy.

We will start our examination of the evolution of a protogalaxy from the stage when it was separated into gas clouds of different masses, ranging in all probability from $10^4 - 10^6$ to 10^{10} solar masses. Suppose that the mass of the protogalaxy in this stage was somewhat higher than the mass of a standard galaxy, and the specific (per unit mass) angular momentum of the protogalaxy was close to the specific angular momentum of the disk subsystem. The density of the protogalaxy was $^1/_{10} - ^1/_{30}$ of the standard present-day density. Further suppose that the combined mass of the small clouds was roughly one half of the mass of the entire protogalaxy, and that the large clouds (with masses of up to $10^{10} M_O$) occupied about 10% of the volume of the protogalaxy.

The origin of the mass spectrum of the gas clouds is an independent problem whose analysis clearly falls beyond the scope of the present paper. We will only point to some factors which could produce this mass spectrum: 1) initial turbulence in the protogalaxy, 2) differences in the differential rotation velocity of the protogalaxy in different parts, 3) unequal rate of gravitational condensation in different parts of the galaxy, possibly due, e.g., to differences in the rate of cooling or to differences in the magnetic field strength.

Small clouds, regardless of their origin, would fairly rapidly develop into star clusters, which would then break up into individual stars. The high rate of star formation in the small clouds may be due, in particular, to their high transparency to radiation and the smaller significance of differential rotation in small-sized objects. At the same time, the large clouds would retain their gaseous structure. Their compression and separation into stars would apparently be a much slower process, since their opacity and differential rotation would interfere with gravitational condensation.

The subsequent evolution of the protogalaxy was governed by two processes: elastic interaction of stars and star clusters with large gas clouds in close encounters and inelastic interaction of colliding gas clouds.

The elastic interaction process predominated in the initial stages of evolution. It led to evaporation of some stars and clusters and produced a certain loss of angular momentum in the star subsystem. This system compressed and became progressively more spherical, as it follows from the general theory /3/.

In the subsystem of gas clouds, contact collisions markedly prevailed over the gravitational interaction in encounters. Since the large gas clouds compressed relatively slowly, the inelastic collisions persisted for a long time and led to the separation of large masses of gas from the clouds. The total angular momentum of the entire gas did not change, however.

The separating gas, in addition to its regular rotational velocity, also had random velocities directed toward the axis. The decay of these random velocities, according to the common point of view /4/, leads to the precipitation of the separating gas onto the equatorial plane of the protogalaxy. In addition to gas separation, the dissipation of the kinetic energy of the clouds led to the compression of the entire gas subsystem. This process took place simultaneously with the previously considered compression of the star subsystem.

As the gas clouds deteriorated, their contribution to the elastic evolution of the star subsystem gradually diminished, and eventually this evolution virtually stopped. In the gas subsystem, a substantial fraction of the total mass precipitated to the plane of symmetry and a disk was thus formed. The fraction of the mass of the gas clouds which managed to condense into stars before falling to the plane of symmetry and which underwent partial evaporational evolution lost some of its angular momentum and formed the intermediate subsystems.

The model of the evolution of a protogalaxy explains its separation into subsystems not only qualitatively, but also quantitatively (to orders of magnitude). In particular, it is seen that the compression of the star subsystem and the star clusters to one half the original diameter will halve the rotational velocity, whereas the compression of the gas subsystem by the same factor will increase its rotation velocity — roughly by a factor of 2. The difference in the rotation velocities in the process of contraction of the protogalaxy should markedly increase, and by the time the system reaches the present-day standard density, the disk would spin at 4 — 5 times the velocity of the halo. These are in fact the differences in rotation velocities observed in our Galaxy.

Elastic and inelastic evolution processes in a system consisting of stars and gas clouds probably played an important role in the formation of galaxies of various morphological types, whose origin is attributable to the variety of conditions (specific angular momentum, particular inhomogeneities, etc.) prevailing in the initial protogalactic clouds. For example, for specific angular momenta substantially less than the angular momentum of our Galaxy, the relevant processes would apparently lead to the formation of an elliptical, and not spiral, galaxy.

Bibliography

1. Ambartsumyan, V.A.— Zapiski LGU, 22:19. 1938.
2. Spitzer, H.— Monthly Not. Roy. Astron. Soc., 100:396. 1940.
3. Gurevich, L.E.— Astronomicheskii Zhurnal. (In press).
4. Kaplan, S.A. and S.B. Pikel'ner. Mezhzvezdnaya sreda (Interplanetary Medium).— Moskva, Fizmatgiz. 1963.

CLUSTERS OF GALAXIES AND THE COSMOLOGICAL EXPANSION

A. D. Chernin

Clusters of galaxies are giant cosmic formations consisting of tens, hundreds, and sometimes thousands of galaxies similar to our Galaxy. A substantial number of such objects are known; they are dispersed at large distances from us and recede with velocities proportional to their distance. Some of these clusters have been studied in some detail, and the observation data permit making definite conclusions regarding their characteristic properties.

A fundamental property of clusters is probably their non-steady-state character. Unlike stars and galaxies, clusters have a positive energy and are in a state of expansion. Ambartsumyan /1/ (and later other authors /2/) reached this conclusion by analyzing the relationship between the virial mass M and the luminosity of the clusters.

The virial mass of a gravitational system is the mass that can be computed from the mean velocity v of the constituent particles and the radius R of the system:

$$M_V = \frac{2v^2R}{G},$$

where G is the gravitational constant.

For steady-state gravitationally bound systems, the virial mass is equal to the true mass. This constitutes the basis of the method for determining the mass of a galaxy from measured velocities of the stars and its size.

Taking the ratio of the virial mass to the luminosity for the individual galaxies in the cluster f_g and for the cluster as a whole $f_c = \frac{M_V}{L}$, we find that f_c is never less than f_g, and in most cases it is actually much higher than f_g. To understand the significance of this rule, consider a simple example. Let a cluster consist of N identical galaxies with the same f_g. Since the total luminosity of the cluster L is N times the luminosity of an individual galaxy, and the true mass of the cluster M is N times the mass of an individual galaxy, f_g is evidently equal to the ratio M/L. Now, since $f_c = \frac{M_V}{L}$ is greater than f_g, M_V clearly does not coincide with the true mass of the cluster, which is evidently less than M_V. Hence it follows that the kinetic energy of the cluster $E_k \simeq Mv^2 \simeq M\frac{GM_V}{R}$ is greater

in absolute magnitude than the gravitational potential energy $E_G \simeq -\frac{GM^2}{R}$. The ratio of the two energy components is $\frac{E_k}{|E_G|} \simeq \frac{M_V}{M} \simeq \frac{f_c}{f_g} > 1$. The same result (with f_g replaced by its mean value) clearly can be obtained if we extend our example to the case of a real cluster consisting of different galaxies.

For the largest clusters, f_c is of the order of 500 or even 700 $M_\odot/L_\odot$ ($M_\odot$ and $L_\odot$ are the mass and the luminosity of the Sun); f_g in its turn is different for galaxies of different morphological types, ranging from a few units to several tens. It would therefore seem that the kinetic energy of the largest clusters is roughly a factor of ten greater than the absolute value of the potential energy: $E_x \sim 10|E_G|$.

The unusually high value of the ratio $f_c = \frac{M_V}{L}$ for clusters thus leads to the conclusion that their total energy $E = E_k + E_G$ is positive. Note that in principle it could be inferred that the clusters of galaxies contain some nonluminous mass. However, its presence in the large quantities required to satisfy the relation $M_V = M$ cannot remain undetected /3, 4/.

A certain correlation is observed between f_c and the number of galaxies in the cluster: f_c steadily increases from small groups, where it is close to f_g, to rich clusters, where it reaches maximum values /5, 6/. According to the above, this signifies that the non-steady-state behavior of the clusters becomes more pronounced (on the average) as their mass increases.

What is the origin of the tremendous kinetic energy of the clusters? This is an obvious question, and without first finding a clear answer to it we will not be able to comprehend other, finer properties of clusters (a detailed review of these properties will be found in /7/).

EXPLOSION OR CONDENSATION?

There are two common approaches to the problem of clusters of galaxies. According to Ambartsumyan /1/, the origin of clusters is attributable to a number of explosions of superdense protostellar objects (D-bodies) which prior to the explosion had remained in a dormant frozen state. Each explosion event leads to a fragmentation of the D-body into a number of fragments, which then scatter, propelled by their initial velocities. Each fragment then develops into a galaxy, undergoing in its turn an active fission process with ejection of smaller fragments. According to this conception, clusters of galaxies are in a state of decay: a strongly bound system — the superdense object — is being converted into a free system.

Another more popular point of view considers the clusters of galaxies to have formed by compression under the gravitational forces of a rarefied cloud of appropriate mass, with a density substantially lower than the observed mean density of the clusters. The compression of the protocluster is accompanied by its breakup, for reasons of thermal or gravitational instability, into individual fragments which gradually develop into galaxies through further compression.

Thus the formation of clusters, according to one model, is associated with outward motions, whereas, according to the other model, it is associated with inward motions. If the evolution indeed proceeds through compression, there are no forces capable of reversing the compression and converting it into expansion. It is moreover clear that initial compression is feasible only if the total energy of the protocluster is negative. There is apparently no evidence suggesting that the sign of the total energy has changed for some reason, e.g., due to nuclear reactions. A cluster which formed by compression of a rarefied gas cloud will either continue shrinking or will develop to steady-state conditions. In the latter case, it should have a regular spherical or elliptical shape.

This picture of evolution is inconsistent with some empirical data about clusters and primarily with two basic facts: the positive energy of the clusters (which has been firmly established by now) and the conspicuously nonspherical shape of most clusters. With regard to these two aspects, the explosion hypothesis has distinct advantages compared to the hypothesis of gravitational condensation. The explosion hypothesis is obviously consistent with the above facts; the only additional assumption required is that the energy of the explosion is sufficiently high to ensure an excess of the kinetic energy of the fragments above the overall potential gravitational energy. In terms of morphology, irregular systems of ejections and jets are more likely in the case of explosion than a regular spherically symmetric motion.

Note that the concept of D-bodies formulated more than ten years ago in connection with the problem of clusters has been extended since to a number of other non-steady-state effects in cosmic systems, such as the activity of galactic nuclei and the outward motion of stars in associations. However, although covering a wider ground than originally, the concept met with a number of serious difficulties in its development in depth. The exact nature of the D-bodies still remains uncertain; we do not know what forces maintain them in a superdense state; what are the factors triggering their fragmentation and what are the sources of the explosion energy. No solution to the difficult problem of the angular momentum has been found. Pikel'ner /8/ has noted that the angular momentum of spiral galaxies is somewhat higher than the angular momentum of a compact fragment of the same mass and momentum which cannot exist as a bound system with a substantially smaller radius (the centrifugal forces would tear it apart in this case).

THE KINETIC ENERGY OF CLUSTERS AND COSMOLOGICAL EXPANSION

The contradictions of the traditional condensation approach, the difficulties encountered in the D-body hypothesis, and the understandable desire to check all the alternative possibilities encouraged the search for new ideas, not necessarily related to explosion and condensation. One of the alternative approaches is suggested by a comparative analysis of three cosmic objects: a galaxy, a cluster of galaxies, and the Metagalaxy — the largest formation in the Universe, which incorporates all the observed galaxies, clusters, and any other matter enclosed in this volume. Galaxies, as we know, are stationary (steady-state) bound

systems. Clusters, on the other hand, are nonbound expanding systems. The Metagalaxy is evidently a non-steady-state object in a state of expansion, as is evidenced by the famous cosmological red shift. This comparison hints at a possible genetic relation between the expansion of the clusters and the expansion of the Metagalaxy. We can trace an apparently meaningful smooth transition from an individual stationary galaxy and an almost stationary group of several galaxies through the markedly non-steady-state clusters of medium scale to the highly non-steady-state large clusters and, finally, the expanding Metagalaxy. Recently, the existence of this smooth transition was further accentuated by the work of I.D. Karachentsev /6, 9/, who analyzed a large volume of observation material. What is the "linkage mechanism" between the clusters and the Metagalaxy? To answer this question, we have to consider, at least in general outline, the evolution of the metagalactic medium from distant past to the present epoch.

It has been firmly established /10/ that the earliest phases of the expansion of the Metagalaxy were characterized by high temperature, high mass density, and high radiation density. Stars and star systems in their present form naturally could not exist under these conditions. All matter was thoroughly intermixed, and this state of affairs persisted apparently until the temperature has dropped sufficiently because of expansion, and the mass density has reached a level corresponding to the present-day density of galaxies ($10^{-23} - 10^{-24}$ g/cm^3). One must not believe, however, that prior to that time the metagalactic medium was completely homogeneous and isotropic, apart from statistical fluctuations. As we know from the classical results of Lifshits /11/, the metagalactic medium must have had a definite structure quite early in its evolution as a result of certain deviations from isotropy and/or homogeneity. This structure changed with the variation in the physical characteristics of the Metagalaxy as a whole and, finally, it reached the present level. The elements of the metagalactic structure in the present epoch are the density inhomogeneities – galaxies, clusters – with their proper motions.

The evolution of metagalactic structure is one of the fundamental and hitherto unsolved problems of theoretical astrophysics /12, 13/. However, even before the construction of a comprehensive theory, we can advance some simple general considerations unrelated to special assumptions and models.

One possible line of reasoning is the following. The development of pregalactic structure could have disengaged at a certain stage those objects destined to evolve into the steady-state galaxies from the overall cosmological expansion. Within these objects, the cosmological expansion would be switched off for some reason or other. We do not know how this could happen, but the mechanism turning off the cosmological expansion need not have been restricted to galactic masses: it could operate on a larger scale, encompassing masses of the order of a cluster mass. On this scale, however, the cosmological expansion is more significant (it increases in proportion to the scale) and the particular mechanism would not be able to extinguish the expansion completely, only reducing the corresponding velocities.

If the formation of clusters is indeed associated with the slowing-down of the overall cosmological expansion on an appropriate scale, the clusters expanding at a slower rate than the Metagalaxy as a whole will grow progressively more isolated and their density should progressively deviate from the density of the Metagalaxy. This implies that the clusters, although expanding, are not in a process of decay and actually continue forming. This hypothesis naturally explains why the clusters of large mass retain a more pronounced non-steady-state character.

The expansion of the clusters thus may be regarded as a residual cosmological expansion. The same conclusion also emerges from a more detailed analysis, assuming the existence of turbulent motion of matter and radiation in the pre-galactic stage /14, 12/. The cosmological velocity is damped down in this model by hydrodynamic instabilities.

According to the above assumption, the kinetic energy of a cluster is essentially identical with the energy of the cosmological expansion. We do not know what the exact reasons are for the expansion of the Metagalaxy, what caused the initial acceleration, and where the energy came from. There is no doubt, however, that the expansion is a significant, real effect which can be observed with our instruments. If we were to establish a relationship between the clusters and the Metagalaxy, observations of the properties of clusters would shed light on the properties of the Metagalaxy as a whole.

The non-steady-state character of the clusters was originally deduced from the fact that the ratio of the virial mass to luminosity for clusters significantly exceeded the ratio expected for a steady-state system. The kinetic energy of a cluster E_k is substantially larger than the absolute value of the potential energy E_G. A system with such kinetic energy is not bound and it inevitably expands. Let us compare this conclusion with the preceding discussion. According to our assumption, the expansion of clusters is associated with cosmological factors and therefore does not require any particular relationship between the kinetic and the potential energy. The main contribution to the kinetic energy derives from the residual cosmological expansion. The relation of these expansion velocities to mass (and hence to potential energy) may be quite different in different non-steady-state cosmological models. For this reason, the excess of the kinetic energy above the absolute value of the potential energy is by no means an automatic consequence of expansion. In principle, there may exist non-steady-state expanding clusters even if $E_k < |E_G|$. (This naturally would be a very elusive effect.) The positive energy of the cluster indicates that the kinetic energy of cosmological expansion of the particular mass from which the cluster formed originally exceeded the absolute value of the gravitational potential energy. This is possible only in an open cosmological model with hyperbolic expansion.

If we adopt this particular model, we can evaluate the mean density of matter ρ in the Metagalaxy. Indeed, in the open model, for any sphere consisting of given particles, the ratio of the kinetic energy to the absolute value of the potential energy is equal to the density ratio ρ_c/ρ, which is independent of the radius of the sphere ($\rho_c = \frac{3H^2}{8\pi G} \simeq 10^{-29}$ g/cm^3 is the critical density, H is Hubble's constant). This ratio should not be less

than the ratio $E_k/|E_G|$ in the rich clusters. For the largest clusters (see above) $E_k \sim 10 |E_G|$, and this gives for the density

$$\rho < \frac{|E_G|}{|E_K|} \rho_c \sim 10^{-30} \text{ g/cm}^3.$$

This estimate is fairly uncertain because of inaccuracies in the determination of the mass/luminosity ratio. Nevertheless, a positive total energy of a cluster — under the above assumptions — definitely supports the open cosmological model with a density close to the density of all luminous matter spread throughout the Universe. This result is consistent with some theoretical arguments /15/ and also with new empirical estimates of the density of the intergalactic medium /16/. It is noteworthy that the cosmological model with this particular density has a number of properties which make it stand out (also for other reasons unrelated to clusters) among the great variety of Fridman models with various values of the parameters /17, 18/.

The above estimate of the mean metagalactic density apparently can be regarded as a positive result of the assumption of the cosmological origin of the expansion of clusters.

This assumption will probably yield answers to a number of other questions relating to the internal structure of clusters. This primarily refers to the correlation between cluster type and morphological constitution: why is it that irregular and spiral galaxies prevail in irregular clusters, and elliptical galaxies in regular clusters? Since the formation of galaxies and clusters is attributable, according to the above, to a common factor — e.g., hydrodynamic instability — this correlation seems to be fairly understandable. Turbulent hydrodynamic motions will preferentially result in systems with considerable inhomogeneities and internal motions, rather than regular formations. This corresponds to the observed prevalence of irregular clusters consisting of irregular and spiral galaxies. The existence of a certain number of regular clusters requires a separate interpretation, which apparently can be devised only within the framework of a more detailed and comprehensive system.

No such theory exists at this stage: there are only general qualitative considerations based either on the explosion hypothesis, or on the gravitational condensation model, or finally on the above assumption of the cosmological origin of the expansion of clusters. Each of the three approaches is essentially concerned with different particular aspects of the real clusters, and therefore they possibly supplement one another, without being mutually exclusive. Indeed, the hypothesis of gravitational acceleration accounts for the existence of systems of galaxies with negative total energies (along with the positive-energy expanding clusters), which could have evolved along the lines described for a condensing gravitationally bound gas cloud. The proportion of these systems is apparently not small among low-population clusters. On the other hand, we are familar with well-known cases of powerful explosions in galaxies, which are accompanied by the ejection of large masses and sometimes even compact blobs of matter, presumably reminiscent of dwarf galaxies. There is no need to prescribe these explosions to hypothetical D-bodies, but these effects show that some expanding clusters containing few galaxies could have

formed in principle as a result of active processes in the nucleus of the parent galaxy. Finally, the dynamics of the largest clusters (and also of superclusters, whose possible existence is supported by observational evidence) are not unlike the dynamics of the Metagalaxy, and the kinetic energy of these systems apparently may be regarded as the residual energy of the cosmological "bang." It would also seem that the mean density of the largest clusters and superclusters is markedly less than the critical cosmological density, as is proper for systems with a positive total energy which expand as a result of cosmological factors.

I would like to acknowledge the help of A. G. Doroshkevich, I. D. Karachentsev, I. D. Novikov, and L. M. Ozernoi, who discussed the problem and offered a number of critical comments.

Bibliography

1. Ambartsumyan, V.A.— Izvestiya Armyanskoi SSR, Seriya Fiziko-Matematicheskikh Nauk, 2:9. 1958; Voprosy Kosmologii, 8:3. 1962.
2. Burbidge, G.R. and E.M. Burbidge.— Astrophys. J., 130:629. 1959.
3. Pskovskii, Yu.P. and G.B. Sholomitskii.— In: "Nablyudatel'nye osnovy kosmologii," p.5, Moskva, Izdatel'stvo AN SSSR. 1965.
4. Karachentsev, I.D.— Astrofizika, 3:89. 1967.
5. Poveda, A.— Astrophys. J., 134:910. 1961.
6. Karachentsev, I.D.— Astrofizika, 2:81. 1966.
7. Abel, J.O.— In: "Nablyudatel'nye osnovy kosmologii," p.153, Moskva, Izdatel'stvo AN SSSR. 1965.
8. Pikel'ner, S.B.— Voprosy Kosmogonii, 9:60. 1963.
9. Karachentsev, I.D.— Thesis. Byurakan. 1967.
10. Zel'dovich, Ya.B. and I.D. Novikov. Relyativistskaya astrofizika (Relativistic Astrophysics).— Moskva, Izdatel'stvo "Nauka." 1967.
11. Lifshits, E.M.— ZhETF, 16:587. 1966.
12. Chernin, A.D.— Trudy V Vsesoyuznoi ezhegodnoi zimnei shkoly po kosmofizike, p.29, Apatity, Izd. Kol'skogo filiala AN SSSR. 1968.
13. Doroshkevich, A.G. Present collection, p. 26.
14. Ozernom, L.M. and A.D. Chernin.— Astronomicheskii Zhurnal, 44:1131. 1967; 45:1137. 1968; ZhETF Letters, 7:436. 1968.
15. Chiu, H.Y.— Ann. Phys., 43:1. 1967.
16. Syunyaev, R.A. Present collection, p. 65.
17. Chernin, A.D.—Nature, 220:250. 1968.
18. Chernin, A.D.— ZhETF Letters, 8:633. 1968.

EXPERIMENTAL VERIFICATION OF THE GRAVITATION THEORY IN COSMOLOGY

A. M. Finkel'shtein

There are currently a number of gravitation theories which predict the four known effects of general relativity. This circumstance discloses still another aspect of cosmology as a suitable tool for the verification of the various competing gravitation theories. For gravitation theories which are conceptually independent of general relativity, cosmology is only one of several checking alternatives, whereas for theories which in a sense constitute a generalization of the general relativity theory, cosmology provides the only ground for detecting possible differences between locally indistinguishable theories. However, the construction of a cosmological scheme which would yield results amenable to experimental verification (primarily in the field of extragalactic astronomy) requires a number of general assumptions regarding the structure of the Universe which extend beyond the framework of the particular gravitation theories. In short, some general cosmological principle is needed.

Robertson and Walker /1/ showed that the metric which admits as the isometry group the six-parametric Lie group of continuous transformations with space-like three-dimensional paths may be written in particular in the form

$$ds^2 = dx^{\circ 2} - \frac{R^2(t)}{\left(1 + \frac{kr^2}{4}\right)^2} d\sigma^2, \qquad (1)$$

where $d\sigma^2 = dr^2 + r^2 (\sin^2\theta\, d\varphi^2 + d\theta^2)$, $R(t)$ and $k = \pm 1, 0$ determine the sign and the scale of the Gaussian curvature of the space-like simultaneity hypersurface $x = \text{const}$, and $x^\circ = ct$ is the world time. A universe (the space-time continuum) described by a linear element (1) has a homogeneous and isotropic spatial part at any instant of the world time x° (the restricted cosmological principle), and the simultaneity hypersurfaces are geodesically parallel. Note that the conception of an isotropic Universe as it is defined by the restricted cosmological principle does not coincide with the conception of a homogeneous and isotropic Metagalaxy as formulated in extragalactic astronomy, since the latter only uses observations covering the section of the surface of the past light cone corresponding to the world line of the Earth-bound observer, i.e., the simultaneity hypersurface. The cosmological postulate thus should be considered as an independent principle, and all the consequences of the postulate may be regarded as potential verifications of the principle.

Robertson and Hoyle and Sandage /2/ proposed a method which made it possible to derive expressions for some observational relations of extragalactic astronomy in the form of expansions in powers of a small parameter, without using any field equations or resorting to any hypotheses concerning the present-day state of matter: the only starting point was the expression for the linear element (1). The same approach, though a much simpler technique, can be used to construct a scheme for the derivation of the observational relations in the form of expansions which are subsequently linked up with various gravitation theories, without integrating the corresponding field equations.

Let L be the bolometric luminosity of a point source at the time of emission. Then the observed bolometric luminosity will be

$$\ell_{bol} = \mathcal{L}\cdot(1+z)^{-2} Sn^{-2}\ell\, R_0^{-2}\,(4\pi)^{-1}, \qquad (2)$$

where $Sn\,l = \sin\sqrt{k}l/\sqrt{k}$, $l = \int_{x}^{x_0} dR/R\dot{R}$ is the world angular distance, $\dot{R} = dR/dx^0$, and the subscript 0 here and in what follows indicates that the corresponding parameters refer to the present epoch. We expand $R_0 Sn\,l$ in powers of the small parameter $R - R_0$, assuming $R(t)$ to be an analytical function near x_0^0. Retaining terms of the order $(R-R_0)^3 \sim z^3$ and introducing as the main parameters to be determined Hubble's constant $H_0 = \dot{R}_0/R_0$, the retardation parameter $q_0 = -\ddot{R}_0 R_0/\dot{R}_0^2$, the factor characterizing the sign and the scale of curvature of the surface $x^0 = \text{const}$ $-k/R_0^2$, and the parameter $\tau_0 = \dddot{R}_0/R_0$, we obtain

$$R_0 Sn\,\ell = H_0^{-1} z\left[1 - \tfrac{1}{2}(1+q_0)z - \tfrac{1}{6} z^2 (k R_0^{-2} H_0^{-2} + \tau_0 H_0^{-3} - 3q_0^2 - 4q_0 - 2)\right]. \qquad (3)$$

Inserting (3) in (2), changing over to stellar magnitudes, and writing out the appropriate expansions, we obtain an expression for the observed dependence of the apparent stellar magnitude on the red shift (designated $[m_{bol}, z]$):

$$m_{bol} = M + 5\log_{10} H_0^{-1} z + 1.086\left[(1-q_0)z + \tfrac{z^2}{4}(3q_0^2 + \tfrac{10}{3}q_0 - \tfrac{7}{3} - \tfrac{4}{3} k R_0^{-2} H_0^{-2} - \tfrac{4}{3}\tau_0 H_0^{-3})\right], \qquad (4)$$

where $M = -2.5\log_{10} 4\pi L$ is the absolute stellar magnitude.

The terms in (4) proportional to z and z^2 constitute small corrections to Hubble's linear law $z = H_0 D = \bar{D}$, where $D = 10^{0.2(m_{bol} - M)}$. Hubble's law, regarded as a representation of the red shift phenomenon, is a direct consequence of the form of the linear element, being independent of any other factor. To terms of the order of z, relation (4) coincides with Robertson's formula /2/. The latter formula is independent of the sign of the curvature of the space part of the model and, like Hubble's law, it is of pure kinematic origin, being independent of and unrelated to any field equations. The term in (4) which is proportional to z^2 and contains the parameters k/R_0^2 and τ_0 determines the corrections to Hubble's law may be fixed by choosing a particular gravitation theory and a particular hypothesis regarding the equation of state of matter in the present epoch. It is this term which will probably enable us in some cases to distinguish between the competing gravitation theories.

A similar procedure leads to "kinematic" expressions for other famous relations of extragalactic astronomy: 1) the dependence of the number of sources vs. the red shift, [N, z]

$$N = \frac{4\pi}{3}\frac{\rho_{eff}}{Q} H_0^{-3} z^3 \left[1 - \frac{3}{2}(1+q_0)z + z^2\left(\frac{5}{2} + 5q_0 + 3q_0^2 - \frac{1}{2}kR_0^{-2}H_0^{-2} - \frac{1}{2}\tau_0 H_0^{-3}\right)\right] \qquad (5)$$

where ρ_{eff} is the number of sources per unit volume, and Q is the number of degrees squares on the observation sphere, and 2) the dependence of the apparent angular parameter vs. the red shift $[\theta_0, z]$,

$$\theta_0 = \zeta H_0 z^{-1}\left[1 + \frac{3+q_0}{2}z + \frac{1}{6}\left(kH_0^{-2}R_0^{-2} + \tau_0 H_0^{-3} + \frac{5}{2} + 2q_0 - \frac{3}{2}q_0^2\right)z^2\right], \qquad (6)$$

where ζ is the linear size of the sources in the local system of coordinates.

Since galaxies are still observed when the red shift is no longer measurable, it is advisable to replace the z in (5) and (6) with the bolometric distance. Since $D = \frac{R_0^2}{R}$ Snl and

$$D = H_0^{-1} z\left[1 + \frac{1-q_0}{2}z - \frac{1}{6}z^2\left(kH_0^{-2}R_0^{-2} + \tau_0 H_0^{-3} - 3q_0^2 - q_0 + 1\right)\right], \qquad (7)$$

we can invert (7) and eliminate z between (5) and (6) to obtain an expression for the observed number of sources vs. bolometric distance dependence [N, D]:

$$N = \frac{4\pi}{3}\frac{\rho_{eff}}{Q} H_0^{-3}\bar{D}^3 \left[1 - \frac{3}{2}(1+q_0)\bar{D} + \left(\frac{13}{4} + 5q_0^2 + \frac{9}{4}q_0^2 - \frac{1}{2}kR_0^{-2}H_0^{-2} - \frac{1}{2}\tau_0 H_0^{-3}\right)\bar{D}^2\right] \qquad (8)$$

and for the angular source diameter vs. bolometric distance dependence $[\theta_0, D]$,

$$\theta_0 = \zeta H_0 \bar{D}^{-1}\left[1 + \frac{3+q_0}{2}\bar{D} + \frac{1}{6}\left(kH_0^{-2}R_0^{-2} + \tau_0 H_0^{-3} - 2 + 5q_0\right)\bar{D}^2\right]. \qquad (9)$$

Before proceeding with particular theories of gravitation, or more specifically with those of Einstein and Hoyle, we have to make one basic remark. The region of small z, where the approximate relations apply, evidently does not cover all the possibilities of observational cosmology. Moreover, for objects with large z, the cosmological effects are the most pronounced. In this case, however, the "kinematic scheme" for the derivation of the observational relations is no longer applicable and rigorous integration of the field equations is needed, which in most cases constitutes a highly complex problem. The simple approximate expressions, which can be derived without integration of the field equation, may nevertheless be used for choosing between the different conceptions of gravitation. For Einstein's field equations with a cosmological term and a hydrodynamic energy—momentum tensor, the equation of state of matter + radiation has the form

$$\tau_0 H_0^{-3} = 4q_0 - 1 + 2\Lambda H_0^{-2} - kR_0^{-2}H_0^{-2}. \qquad (10)$$

Using (10) to eliminate the parameter $\tau_0 H_0^{-3}$ from (4)—(6), we obtain $[m_{bol}, z]$:

$$m_{bol} = M + 5\log_{10} H_0^{-1} z + 1.086\left[(1-q_0)z + \left(3q_0^2 - 2q_0 - 1 - \frac{8}{3}\Lambda H_0^{-2}\right)\frac{z^2}{4}\right]; \qquad (11)$$

$[N, z]$:

$$N = \frac{4\pi}{3}\frac{\rho_{eff}}{Q} H_0^{-3} z^3 \left[1 - \frac{3}{2}(1+q_0)z + z^2\left(3 + 3q_0^2 + 3q_0 - \Lambda H_0^{-2}\right)\right]; \qquad (12)$$

$[\theta_0, z]$:

$$\theta_0 = c H_0 z^{-1}\left[1 + \frac{3+q_0}{2} z + \left(\frac{1}{2} + 2q_0 - \frac{1}{2}q_0^2 + \frac{2}{3}\Lambda H_0^{-2}\right)\frac{z^2}{2}\right] \qquad (13)$$

A similar procedure can be applied to relations using the bolometric distance.

We wish to emphasize two points regarding these relations (including the relations expressed in terms of D). First, these relations do not contain the parameter k/R_0^2 and, second, these relations contain only two parameters (in addition to Λ) which have to be determined, whereas the known exact relations obtained for $\Lambda = 0$ contain three fundamental parameters /3/ and the resulting accuracy of estimates is much lower.

For the two limiting cases $W^* = 0$ (a model with matter without pressure) and $M^* = 0$ (a model with radiation) we have

$$\frac{k}{R_0^2} = \begin{cases} 2q_0 H_0^2 - H_0^2 + \Lambda \\ q_0 H_0^2 - H_0^2 + \frac{2}{3}\Lambda \end{cases}, \quad \frac{\tau_0}{H_0^3} = \begin{cases} 1 + \frac{k}{R_0^2} H_0^{-2} \text{ for } W^* = 0 \\ 3q_0 + \frac{4}{3}\Lambda H_0^{-2} \text{ for } M^* = 0 \end{cases} \qquad (14)$$

which leads to expressions for the observational relations which are entirely analogous to (11)—(13). The latter point signifies that observations associated with these relations cannot indicate which of the two components — matter or radiation (or both) — plays the leading role in the Universe in the present epoch. Clearly this conclusion is exactly applicable only to observations related to relatively near sources. Relations (11)—(13) are thus valuable because in principle they enable us to find the values of q_0 and Λ without imposing particularly restrictive assumptions on the equation of state of matter in the present epoch.

Hoyle /4/ proposed gravitation equations which in a sense constitute a generalization of Einstein's field equations (they were supplemented with a creative tensor, defined by the field of unit vectors orthogonal to the congruence characteristic of geodesics). We know that for the case $k = 0$ and $p = 0$ Hoyle's equations have a particular integral $R = \exp\left\{\frac{Btc}{3}\right\}$, where $B = 3H_0$, which defines the metric of the Bondi—Gold steady-state Universe /5/. Since for a steady-state Universe $q_0 = -1$, this conception hardly fits the observations (especially if selection effects are ignorable). However, this possibility nevertheless exists in more general models corresponding to the solutions of Hoyle's equations for $k \neq 0$. Indeed, in this case for $p = 0$

$$k R_0^{-2} H_0^{-2} = 2 + 2q_0, \quad \tau_0 H_0^{-3} = \frac{3}{2} + \frac{1}{2}q_0 \qquad (15)$$

we may also have a solution with $q_0 > 0$ ($\inf q_0 = -3/2$). Inserting (15) in (4), we obtain, in particular, an expression for the observational relation $[m_{bol}, z]$:

$$m_{bol} = M + 5 \log_{10} H_0^{-1} z + 1.086 \left[(1 - q_0) z + (3 q_0^2 - 7) \frac{z^2}{4} \right]. \qquad (16)$$

For $q_0 = 1.0 - 1.5$, there is a definite possibility of making the brightness data (at least for the nearest sources) consistent with Hoyle's theory. The term $m_c^x - m_c^x = (q_0 - 3 + \frac{4}{3} \Lambda H_0^{-2})$ which characterizes the difference between the relations $[m_{bol}, z]$ in Hoyle's and Fridman's theories may prove to be relatively large for certain q_0 and Λ, so that starting with $z > 0.2 - 0.3$ the detailed differences between the two theories may be detected with the 200-in. telescope /6/.

A similar method can be applied to determine the observational relations for Hoyle's theory containing a generalizing Λ-term and expressed in a general covariant form. This procedure also can be applied to the theories of Dicke and Jordan /7/. The general conclusions regarding the possibilities of observational verification of these theories remain unaffected.

Bibliography

1. Robertson, H.— Astrophys. J., 82:284. 1935; Walker, A.G.— Proc. Lond. Math. Soc., 42:90, part 2. 1936.
2. Robertson, H.— PASP, 67:82. 1955; Hoyle, F. and A.Sandage.— PASP, 68:301. 1956.
3. Sapar, A.A.— Publ. TAO AN EstSSR, 34:223. 1966; 35:368. 1966; McIntosh, C.— Monthly Notices Roy. Astron. Soc., 138:423. 1968; Finkel'shtein, A.M.— Astronomicheskii Zhurnal. 1969. (In press).
4. Hoyle, F.— Monthly Notices Roy. Astron. Soc., 108:372. 1948; 109:365. 1949.
5. Bondi, H. and T. Gold.— Monthly Notices Roy. Astron. Soc., 108:252. 1948.
6. Sandage, A.— Astrophys. J., 133:353. 1961.
7. Finkel'shtein, A.M.— Byulleten' ITA AN SSSR, 12(6). 1969.

EJECTION OF GAS FROM STARS IN THE LATE STAGES OF EVOLUTION

G. S. Bisnovatyi-Kogan

Stars lose some of their mass apparently in all stages of evolution. Observations reveal an efflux of mass from the Sun (the solar wind) /1/, from hot O and B stars /2/, from red and yellow giants and supergiants /3/, i.e., mass is ejected both from young stars (the first two categories) and from stars in the late stages of evolution (the red giants). An example of objects which lose mass at a high rate is provided by planetary nebulae, which are currently regarded as stars far advanced in their evolution, and destined to evolve into white dwarfs.

The importance of mass ejection in stellar evolution depends on whether or not the star loses a significant portion of its mass during its lifetime. Observations yield certain estimates for the rates of mass loss. The rate of mass loss for the solar wind is $10^{11}-10^{12}$ g/sec /1/, which is equal to $10^{-15}-10^{-14}$ $M_\odot$/years (where $M_\odot$ is the solar mass). Since the evolutionary scale of the Sun is of the order of 10^9 years, solar-wind ejection is evidently of no importance in its evolution. The hot stars, according to Morton /2/, lose up to $10^{-8}-10^{-6}$ $M_\odot$/year, which is more significant; the lifetime of these stars, which have masses of about 30 $M_\odot$, generally does not exceed 10^6-10^7 years. Of the greatest evolutionary importance in this category is the loss of mass by the red giants, which may reach, according to /4/, $10^{-5}-10^{-3}$ $M_\odot$/year, and by the planetary nebulae.

In addition to direct observations, there are indirect theoretical considerations which establish the great evolutionary impact of mass ejection. It seems that after the nuclear fuel has burnt up, the star will quietly cool down and terminate its evolution as a cold star. We know from the modern theory of cold stars /5/ that their mass does not exceed $1.2\,M_\odot$ (for white dwarfs) and $1.6\,M_\odot$ (for neutron stars). Large-mass stars collapse into frozen stars with a radius close to the gravitational radius for the corresponding mass. The evolution into a neutron or a frozen star is accompanied by an eminently nonstationary process of the type of supernova explosion. The masses of observable stars reach up to $100\,M_\odot$, and the frequency of supernova explosions is therefore expected to be such as to account for the last stages in the evolution of the sufficiently massive stars. And yet the statistics of supernova explosions reveals a distinct shortage of these phenomena: their frequency is approximately $1/30-1/300$ of the number predicted from evolutionary considerations /3/. This discrepancy can be eliminated either by assuming a "silent" nonstationary process, which does not produce any immediately observable

effects, which is not very likely, or assuming that the loss of mass in the course of evolution is effective to such an extent that most massive stars eventually evolve into white dwarfs.

GENERAL PROPERTIES OF HYDRODYNAMIC EJECTION

We will only consider the loss of mass during the quasi-stationary stage of evolution, without dealing with explosive mass loss processes.

Mass ejection during the quiet stage of evolution is caused by processes which occur in the outer envelopes of stars. Whereas the bulk of the stellar mass (some 97 — 99%) is in a state of static equilibrium, the outer envelope is in a state of outward hydrodynamic flow. The solar corona, for example, is produced by this hydrodynamic outflow of solar matter; the coronal mass, however, is so negligible that it can be ignored in terms of evolution. In a red giant, on the other hand, up to 3% of its mass may be tied up in hydrodynamic ejection processes. The mass losses in this case are highly significant for evolution, which should be considered in terms of a model with a static core and a hydrodynamic envelope /6, 7/. In this, as in the totally static case, an unambiguous model can be constructed. The general equations describing the outflow of stellar matter are the equations of hydrodynamics. They are valid since in all the known cases the particle path length l is less than the system dimensions L. The ejected matter escapes to infinity. The process of ejection may be regarded as steady-state, since the ratio of the partial derivative $\partial/\partial t$ to the convective derivative $u\,\partial/\partial r$ is equal to the inverse of the ratio of the evolution time t_{ev} to the time it takes the flowing matter to cover the characteristic size of the star R/u, which is clearly much less than unity /8/. The density and the temperature of the ejected matter monotonically decrease with the distance from the star and vanish at infinity. Steady-state flow with monotonic variation of the parameters is feasible only if the solution of the equations of hydrodynamics passes through a singular point where the flow velocity is equal to the adiabatic velocity of sound $u_a^2 = (\partial p/\partial \rho)_S$ /1/. Near the singular point (Figure 1) the solution behaves in such a manner that a saddle point is obtained. A physical solution is that with a monotonically increasing velocity, ab. Note that in this case the solution is necessarily passed through the point where the flow velocity is equal to the isothermal velocity of sound $u_T^2 = (\partial p/\partial \rho)_T$. In fact, the following situation is obtained: if we consider hydrodynamics without transport processes, the singular point is that where $u^2 = (\partial p/\partial \rho)_S$ is equal to the adiabatic velocity of sound. If heat conduction is taken into consideration, the properties of the

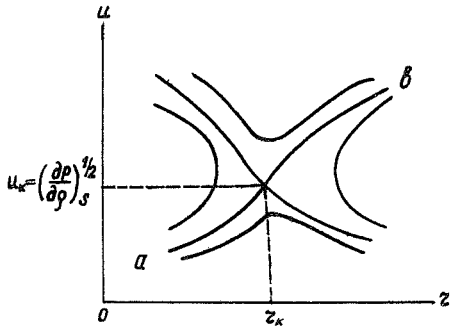

FIGURE 1. The integral curves of the equations of hydrodynamics describing gas outflow.

equations change discontinuously, and two singular points are obtained, one where $u^2 = (\partial P/\partial \rho)_T$ is equal to the isothermal velocity of sound and the other for r = ∞, T = 0, $\rho = 0$. If we further allow for viscosity, we are naturally left with a single singular point, the one at infinity. Although the properties of the equations change markedly when dissipative processes are introduced, the solution passing through the singular point and satisfying the boundary conditions is a continuous function of the parameter /9/. Ejection from stars of various types is characterized by different processes of interaction with radiation and different ejection mechanisms.

EJECTION FROM STARS NEAR THE MAIN SEQUENCE

The mean optical density τ of the solar wind and of the ejection from early-type stars is close to zero, although in individual lines it may approach unity. In this case, the equations of hydrodynamics are used with transport terms — viscosity and heat conduction. In a completely ionized gas. the contribution from viscosity is small compared to the contribution from heat conduction. Radiation is not in thermodynamic equilibrium with matter. It leads to local cooling of the ejected gas, thus accelerating the supersonic flow and decelerating the subsonic flow /3, 10/. Radiation also produces a certain acceleration of the gas flow due to pressure in spectra lines /11/. The factor responsible for the outflow of matter is the non-thermodynamic heating of the base of the corona.

MASS LOSSES OF STARS IN LATE STAGES OF EVOLUTION

The matter ejected from red giants and planetary nebulae is in equilibrium with radiation ($\tau \gg 1$) throughout the main ejection region, the critical point included. Therefore the properties of ejection and its very existence are significantly dependent on the opacity of matter. In this case, matter is in thermodynamic equilibrium with radiation, and an important contribution is due to the radiant heat conduction, whereas the effect of viscosity is negligible /7, 9/.

A star may be in a state of static equilibrium only if its luminosity /5/ is less than some critical luminosity (Eddington's condition) $L < L_c = \frac{4\pi cGM}{\varkappa}$, where $\varkappa$ is the opacity. If we draw a qualitative plot of opacity as a function of the star's radius, we obtain for stars with $M \approx 30\ M_\odot$ the curve shown in Figure 2 /1, 2/.

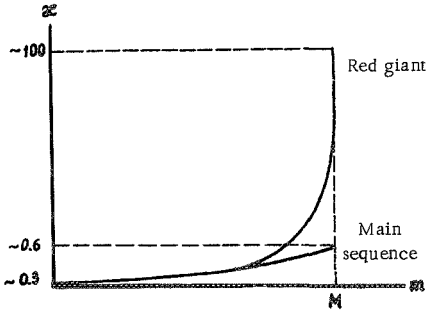

FIGURE 2. A qualitative curve of the opacity of a star in the late stages of evolution.

It is clear from Figure 2 that while on the main sequence $\varkappa$ is always relatively small, so that $L < L_c$, the opacity in the red giant stage steeply increases because of the significant cooling of the star's envelope, which produces a zone of incompletely ionized hydrogen. Moreover, the luminosity also increases by a considerable factor, and hydrodynamic ejection begins /7/. Note that convection effectively lowers the transparency and suppresses ejection, but in the outer layers the convection is highly nonadiabatic and may transport only a small fraction of the heat flux /7/. The larger the mass, the smaller is the density of the surface layers and the less effective is the convection. For $M \simeq 30\,M_\odot$, it does not prevent ejection after helium has begun burning. For $M \simeq 9\,M_\odot$, the convection does prevent ejection at this stage and the static evolution continues. The larger the mass, the less important is the external convection.

We see from the expression for L_c that the onset of ejection, in addition to $\varkappa$, also depends on the ratio L/M. It follows from the theory that on the main sequence $L \sim M^3$ or even $\sim M^4$ for small masses, and therefore the ratio L/M increases with increasing mass in this range. On the main sequence it is equal to $\sim 5 \cdot 10^{-5} \varkappa$ for $1\,M_\odot$ and reaches $0.3\varkappa$ for $30\,M_\odot$ /7, 13/. Thus, the larger the mass, the smaller is the increase in opacity and luminosity needed to initiate ejection. For small masses, on the other hand, the hydrodynamic ejection of the relevant type will begin at substantially later stages of evolution.

Computations of the static evolution of stars also lead to ejection. If the velocity is formally ignored in the equations and the envelope is considered as static even for $L > L_c$, we arrive at glaring contradictions: a strong inverse density gradient develops in the envelope, the expansion velocity obtained from a comparison of two static models increases and approaches the velocity of sound, and finally the solution with a static envelope breaks down completely. This occurs at the following stages of stellar evolution: for stars with $M > \sim 15\,M_\odot$ /12, 14/, when helium begins burning; for $\sim 5\,M_\odot < M < 15\,M_\odot$ /15 – 17/ when carbon begins burning; and for low-mass stars $\sim 1.3\,M_\odot$ /18/, ejection of this type occurs in the planetary nebula stage, when the star is evolving into a white dwarf. This ejection is evolutionarily significant: estimates for $30\,M_\odot$ give /7/ a mass loss of the order of $3 \cdot 10^{28}$ g/year, or about $10^{-5}\,M_\odot$/year.

To find the exact rates of mass loss, the evolution should be computed using instantaneous self-consistent models with a static nucleus and a hydrodynamic envelope. Such models can be constructed unambiguously /6, 7/ using the same techniques as for models with a static envelope. The static envelope is fully characterized by two parameters, e.g., L and the radius R. The conditions of matching with the nucleus lead to a unique model in each case. Although a hydrodynamic model contains one further variable – the velocity – and one more parameter – the rate of mass loss μ – the solution is constrained to pass through a singular point and to satisfy certain conditions at infinity, so that the hydrodynamic envelope is completely described by only two variables, e.g., L and the critical density ρ_k, which is also uniquely determined from the matching conditions. The rate of mass loss is a function of the state of the star.

Bibliography

1. Parker, E.N. Interplanetary Dynamic Processes. — New York, Wiley. 1963.
2. Morton, D.— Astrophys. J., 147:1017. 1967; 150:535. 1967.
3. Weyman, R.— Ann. Rev. Astron. and Astrophys., 1:97. 1963.
4. Rublev, S.V.— Kosmogonii, 10:119. 1964.
5. Zel'dovich, Ya.B. and I.D. Novikov. Relyativistskaya astrofizika (Relativistic Astrophysics).— Moskva, Izdatel'stvo "Nauka." 1968.
6. Bisnovatyi-Kogan, G.S. and D.I. Nadezhdin.— Nauchnye Informatsii Astronomicheskogo Soveta AN SSSR, 2:28. 1969.
7. Bisnovatyi-Kogan, G.S. and Ya.B. Zel'dovich.— Astronomicheskii Zhurnal, 45:241. 1968.
8. Bisnovatyi-Kogan, G.S. and Ya.B. Zel'dovich.— Astronomicheskii Zhurnal, 43:1200. 1966.
9. Bisnovatyi-Kogan, G.S.— Prikladnye Metody Mekhaniki, 31:762. 1967.
10. Bisnovatyi-Kogan, G.S.— Mekhanika Zhidkosti i Gaza, 4:182. 1968.
11. Lucy, L. and P. Solomon.— Astron. J., 72:310. 1967.
12. Nadezhdin, D.K.— Nauchnye Informatsii Astronomicheskogo Soveta AN SSSR, 4:37. 1966.
13. Haselgrove, C. and F. Hoyle.— Monthly Notices Roy. Astron. Soc., 119:112. 1959.
14. Kotok, E.V.— Astronomicheskii Zhurnal, 43:316. 1966.
15. Hofmeister, E., R. Kippenhahn, and A. Weigert. Stellar Evolution, p.263.— New York, Plenum Press. 1966.
16. Hofmeister, E.— Zeitschrift Astrophys., 65:164. 1967.
17. Weigert, A.— Colloq. Late-Type Stars, Proc., p.388. Trieste. 1966.
18. Savedoff, M., et al.— Astrophys. and Space Sci., No.1. 1969.

LOW-FREQUENCY OSCILLATIONS OF A MAGNETIC ROTATING NEUTRON STAR

Yu. V. Vandakurov

A neutron star with an internal magnetic field may undergo unstable nonradial low-frequency oscillations of convective character if the field falls off sufficiently fast away from the center /1/. In the present paper, we intend to analyze the equations of oscillations for an ideally conducting rotating configuration with a toroidal field. The rotation and the field are treated as small perturbations, and general relativity effects are ignored. The results bear out the possible existence of instability, although the self-sustained oscillations asymmetric relative to the spin axis are in no way related to convective oscillations (in particular, the instability region is much wider).

Introductory remarks

The instability of low-frequency nonradial oscillations of a star leads to convection. In a normal star the instability develops when the temperature gradient exceeds a certain limit value. In the presence of a magnetic field, a different instability criterion applies to the adiabatic nonradial oscillations, but when the ratio of the magnetic to gravitational force is low the corrections are not large.

Consider a superdense cold object in which the pressure p is a function of density ρ alone; the form of the function $p(\rho)$ is assumed to be independent of whether the object oscillates or not. This condition is observed for the case of a neutron star or a structurally homogeneous white dwarf. The case when the rate of nuclear reactions plays a significant role in the process of oscillation was discussed in /2/.

If $p = p(\rho)$, the Lagrangian components of the pressure and density perturbations (δp and $\delta\rho$) in the oscillating state are related by the equality

$$\frac{\rho\delta p}{p\delta\rho} = \frac{\rho dp}{pd\rho}. \qquad (1)$$

For adiabatic motions, the left-hand side of (1) is equal to the adiabatic index γ. Inserting (1) into the Schwartzschild criterion, we find that the neutron star is neutrally stable relative to convective perturbations. This result was derived in /1/.

A neutron star with a magnetic field may be convectively unstable /1/. The stability criterion is considered below in some detail. We should

stress, however, that because of the neutral stability of an unperturbed neutron star, the smallest field may cause instability. This situation is cardinally different from what we observe in normal stars. Because of the definite damping produced by the emission of gravitational waves and other processes, the field strength causing instability has a finite, and not infinitesimal, magnitude.

The equilibrium state

The equilibrium equations of an ideally conducting gas sphere with a general magnetic field distribution $\vec{H}(r,\vartheta)$ and a general angular rotation velocity $\Omega(r,\vartheta)$ were analyzed in /3/. Expressing the field $\vec{H}$ in terms of two scalar functions U and W, we find

$$\varepsilon \vec{H} = \sqrt{4\pi}\,(-\vec{e}_\varphi \times \nabla U + \vec{e}_\varphi W), \quad \vec{v} = \vec{e}_\varphi \Omega \xi, \quad |\vec{e}_\varphi| = 1, \tag{2}$$

$$\frac{\nabla p}{\rho} + \nabla \Phi = \frac{1}{2}\Omega^2 \nabla \xi^2 - \frac{1}{2\rho\xi^2}\left\{\nabla W^2 + 2\xi(\vec{e}_\varphi \cot[\tfrac{1}{\xi}\vec{e}_\varphi \times \nabla U])\nabla U\right\}, \quad \xi = r\sin\vartheta. \tag{3}$$

Here r, ϑ, φ are the spherical coordinates.

In a neutron star, $p = p(\rho)$ and the rotor [curl] of the right-hand side of (3) should vanish. Since the rotation and the magnetic field are treated as perturbations, the right-hand side of (3) is a small quantity and we may therefore replace ρ with $\rho_0 = (\rho)_{\Omega=0, H=0}$.

Without a poloidal field (U = 0), we have a solution $\Omega = \Omega(\xi)$, $W = W(\rho\xi^2)$. Let us further consider a solution in which the expansion in Legendre polynomials $P_n(\cos\vartheta)$ of the difference $\rho - \rho_0$ contains terms with P_0 and P_2 only. Then

$$\Omega = \Omega(r) \text{ and } U = 0, \quad W = \xi f(r), \quad (\Omega^2) = \rho_0 (f^2/\rho_0^2)', \tag{4}$$

where prime denotes differentiation. Choosing some $f(r)$, we obtain a certain law of differential rotation. On the stellar surface, ff'/ρ_0 should be bounded.

In the presence of a poloidal field, the condition of frozen fields and the absence of rotational forces impose more exacting restrictions on the field and rotation velocity distribution. In this case $\Omega = \Omega(U)$ (or Ω = const), $W = W(U)$. Suppose that the series for $\rho - \rho_0$ contains the polynomials P_0 and P_2 only. Then Ω = const,

$$\begin{cases} U = \varepsilon^2 q(r), \quad W = EU, \quad E = \text{const} \\ rq'' + 4q' + \varepsilon^2 rq = -Dr\rho, \quad D = \text{const} \end{cases} \tag{5}$$

The solution differs from (4) in that the field at the center is of the same order of magnitude as on the surface. For example, taking $\rho = \rho_c(1 - r^2/R^2)$, E = 0, ρ_c = const, we find $q = q_c - \frac{D\rho_c r^2}{10}\left(1 - \frac{5r^2}{14R^2}\right)$.

The equations of low-frequency oscillations

Let a small perturbation be applied to the equilibrium state, which is described by equations (2), (3) together with the equation of state and the

Poisson equation. Because of the perturbation, the field, the density, and other variables take on the perturbed values $\rho+\rho^*, \vec{H}+\vec{H}^*$, etc. The dependence of the perturbations $\rho^*, \vec{H}^*, \ldots$ on φ and t is taken in the form $\exp i(m\varphi+\omega t)$.

We will only consider low-frequency oscillations, when ω is either of the order of Ω or of the order of $H/\sqrt{4\pi\rho_c R^2}$, where $\rho_c = (\rho)_{r=0}$, R is the radius of the star. This means that $|\omega| \ll \sqrt{\pi G \rho_c}$. Corrections of the order $\omega^2/\pi G\rho_c$ are dropped. Note that in this approximation the difference $\rho - \rho_0 = \rho - (\rho)_{\Omega=0,\vec{H}=0}$ is small.

Equation (1) remains valid if the Lagrange variables $\delta p, \delta\rho$ are replaced by Euler variables p^*, ρ^*. The linearized equation of motion may be written in the form

$$i\omega\vec{v}^* + (\vec{v}\cdot\nabla)\vec{v}^* + (\vec{v}^*\cdot\nabla)\vec{v} + \nabla\Pi - \frac{1}{4\pi\rho_0}\{(\vec{H}\cdot\nabla)\vec{H}^* + (\vec{H}^*\cdot\nabla)\vec{H}\} + \frac{\nabla\rho_0}{4\pi\rho_0^2}\vec{H}\cdot\vec{H}^* = 0, \tag{6}$$

where

$$i\omega\vec{H}^* = rot(\vec{v}\times\vec{H}^* + \vec{v}^*\times\vec{H}). \tag{7}$$

$\Pi = \Phi^* + p^*/\rho + \vec{H}\cdot\vec{H}^*/4\pi\rho$. In equation (6), the terms $\rho^*(\vec{H}\times rot\vec{H})/4\pi\rho^2$, $(\rho-\rho_0)(\vec{H}^*\times rot\vec{H})/4\pi\rho^2$, etc., have been dropped, since they constitute small corrections to the term $\nabla(p^*/\rho)$. The order of magnitude estimate for ρ^* which follows from (6) and (1) has the form $\rho^* \sim R\omega\rho_c^2 v^*/p_c$, and the equation of continuity in our approximation therefore takes the form

$$div\,\rho_0\vec{v}^* = 0. \tag{8}$$

Equations (6) through (8) constitute a complete system for the unknowns $\vec{v}^*$ and $\vec{H}^*$. Note that the coefficients of this system depend only on the unperturbed density distribution $\rho_0(r)$.

Low-frequency oscillations of an infinite gravitating cylinder

A convenient model for investigating the general spectrum of frequencies of oscillating gravitating objects is provided by the cylindrical configuration. For a homogeneous density distribution, the analogy between the oscillations of a cylinder (in a plane perpendicular to its axis) and the oscillations of a sphere was emphasized in /4/.

Let the cylindrical coordinates be ξ, φ, z ($\xi = r\sin\vartheta$). Suppose that in the equilibrium state the cylinder rotates with a uniform angular velocity Ω, and the magnetic field is $\vec{H} = \sqrt{4\pi}[\vec{e}_\varphi \xi f(\xi) + \vec{e}_z h(\xi)]$ inside the cylinder and $\vec{H} = 0$ outside the cylinder (for $r > R$). For perturbations which are independent of z, we find from equations (7), (6) (the factor $\exp i(m\varphi+\omega t)$ and the index 0 of ρ_0 are omitted)

$$\omega_* \vec{H}^* = \sqrt{4\pi}\left\{mf\vec{v}^* + i\rho v_\xi^*\left[\xi\left(\frac{f}{\rho}\right)'\vec{e}_\varphi + \left(\frac{h}{\rho}\right)'\vec{e}_z\right]\right\},$$
$$\omega_*\Pi' + i(a+d)v_\xi^* - cv_\varphi^* = 0, \quad m\omega_*\Pi = \xi(icv_\xi^* - av_\varphi^*); \tag{9}$$

$$a = \omega_*^2 - \frac{m^2 f^2}{\rho}, \quad c = 2\omega_* \Omega - \frac{m f^2}{\xi \rho^2}(\xi^2 \rho)', \quad \omega_* = \omega + m\Omega,$$
$$g = \frac{1}{2}(\xi^2 \rho)'\left(\frac{f^2}{\rho^2}\right)' + \frac{1}{2}\rho'\left(\frac{h^2}{\rho^2}\right)' - \frac{1}{a}\left(\frac{mfh\rho'}{\rho^2}\right)^2. \tag{10}$$

Using equation (8), we replace the initial system with a single equation for $X = \xi v_\xi^*$:

$$\xi \frac{d}{d\xi}\left(\frac{a\xi}{\rho}\frac{d\rho X}{d\xi}\right) - \left\{\xi\rho\left(\frac{c}{\rho}\right)' + m(a+g)\right\} mX = 0. \tag{11}$$

Without a field ($f = 0$, $h = 0$), taking $\rho = \rho_c (1-y)^w$, $y = (r/R)^\nu$, w, ν = const, we can express the solution of (11) in terms of the hypergeometric function $X = (1-y)\, F(\alpha, \beta, \alpha+\beta-1-w, y)$, $\alpha + \beta = 2 + w + 2m/\nu$, $\alpha\beta = 1 + w + \frac{m}{\nu}\left(2 + w + \frac{2\Omega w}{\omega_*}\right)$. The condition of boundedness of X for $\xi = R$, $y = 1$ gives $\alpha = -\kappa$, where $\kappa = 0, 1, 2, \ldots$ Thus

$$\frac{\omega}{m\Omega} + 1 = -\frac{2w}{\nu\left\{\kappa(\kappa + 2 + w + 2m/\nu) + 1 + w + \frac{m}{\nu}(2+w)\right\}}. \tag{12}$$

For a rotating cylinder with longitudinal magnetic field only ($f = 0$, $h \neq 0$), a and c are constant and there are always solutions of equation (11) with small ω_* (ω_* is the frequency in the coordinate system rotating with the cylinder). For these frequencies, using the method of /5/, we obtain the following asymptotic expression:

$$\omega + m\Omega = \pm \frac{2i}{\pi(2j + d)} \int \frac{\sqrt{m^2 g}}{r}\, dr, \tag{13}$$

where j is a large positive number, d is some constant ($|d| \ll j$), and integration is carried out over the regions where $g > 0$ (it was assumed in the derivation that such regions exist).

A convective instability arises if in some regions the field falls off faster than the density. The reason for the development of instability is clearly understood from simple qualitative considerations /1/. Consider interchangeability of individual magnetic force tubes, together with the particles enclosed in these tubes. If there are regions with a rapidly diminishing field, the outward displacement of such a tube substitutes hydrostatic pressure for field pressure in the interior regions while substituting field pressure for hydrostatic pressure in the outer layers. This process produces an instability of the same type that is observed in a high-density liquid supported from below by a low-density liquid.

A more interesting model is the one with a toroidal field ($h = 0$, $f \neq 0$), since the oscillations of such a system constitute to a certain extent a two-dimensional analog of the oscillations of a sphere. This model was analyzed by means of numerical integration of equation (11). In the equilibrium state, we took

$$p = p_c \theta^{n+1}, \quad \rho = \rho_c \theta^n, \quad f = f_c \theta^{n\beta}, \quad n = 1.5, \tag{14}$$
$$\frac{d^2\theta}{d\xi^2} + \frac{1}{\xi}\frac{d\theta}{d\xi} + \theta^n = 0, \quad \xi = \frac{\xi}{R_\xi}, \quad R_\xi^2 = \frac{(n+1)p_c}{4\pi G \rho_c^2},$$

where $\beta = \text{const} > \frac{5}{6}$. The radius and the mass per unit cylinder length are $2.6\, R_\xi$ and $6.5 \rho_c R_\xi^2$.

The calculations were carried out as follows. For some complex ω_*, the solution of (11) was obtained first by integration from the center $\xi=0$ and then by integration from the surface $\xi=R$. The condition of matching of the two solutions at an intermediate point ξ_f requires that the complex determinant Δ be equal to zero. If for the particular ω_* chosen $\Delta \neq 0$, a new ξ_f is chosen from the condition that $|\Delta|$ should decrease at the fastest rate. No provision was made in the program, however, for encircling the regular singular point $\alpha = 0$, and therefore for $f_c \neq 0$ the roots ω_* with a very small imaginary part could not be computed.

For $f_c = 0$, by analogy with (12), there are numerous solutions ω_*. For example, if $m = 2$, the largest root is $\omega_* = -0.62\,\Omega$.

For $m = 2$, $\beta = 1.5$, $f_c^2 \rho_c = 200\,\Omega^2$, we obtained the root $\omega_* = (-0.066 \pm i\,0.12)\Omega$, but all attempts to determine the second root failed. Irrespective of the initial ω_*, the computations yielded the same root. All the other solutions are apparently real. The root is highly sensitive to changes in m: if $m = 1$ we have $\omega_* = (-0.18 \pm i\,1.4)\,\Omega$, and there are again apparently no other complex roots. No complex roots could be found for $m = 3$ and the same β and $f_c^2 \rho_c$.

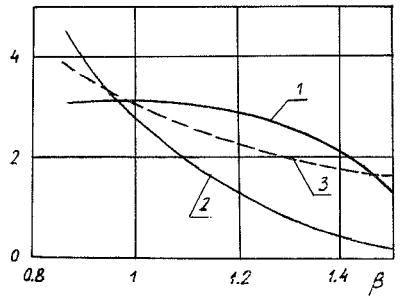

Oscillation frequency ω vs. β characterizing the rate of field decrease:

1) $\left[-\frac{Re(\omega + m\Omega)}{\Omega} \cdot 20\right]$; 2) $\left[\frac{|Im(\omega + m\Omega)|}{\Omega}\right]$;

3) approximate ratio of magnetic energy to rotational energy divided by 25.

For $\beta = 1$ and $f_c^2/\rho_c = 10\,\Omega^2$ (the ratio of the magnetic energy to rotational energy $\varkappa$ is around 4), the following roots were obtained:

$$m=1 \quad \omega_* = (-0.147 \pm i\,0.54)\,\Omega,$$
$$m=2 \quad \omega_* = (-0.153 \pm i\,0.63)\,\Omega.$$

In this case, the dependence on m is different from that observed for $\beta = 1.5$. The figure plots the real and the imaginary parts $\mathrm{Re}\,\omega_*$ and $[\mathrm{Im}\,\omega_*]$ as a function of the parameter β. The curve $\varkappa(\beta)$ is also drawn approximately.

The existence of instability for $\beta \leq 1$ is an unexpected result, since an analysis of the interchangeability of individual force tubes leads to the conclusion that for the distribution corresponding to the stability limit, f is proportional to ρ or $\beta = 1$. It is clear, however, that this remark is valid only for axisymmetric perturbations $m = 0$. Indeed, if we assume that the dependence of the perturbation on φ and z is expressed by $\exp i\kappa z$, we find for $h = 0$, $f \neq 0$ instead of (11)

$$\xi \frac{d}{d\xi}\left(\frac{1}{\xi \rho} \frac{d\rho X}{d\xi}\right) - \left(1 + \frac{g}{\omega^2}\right)\kappa^2 X = 0, \qquad (15)$$

where g is expressed by (10) with $h = 0$. We thus see that instability develops if there exist regions with $g > 0$.

The stability of a star with a toroidal field

Let the equilibrium state of a rotating neutron star with a toroidal magnetic field be described by equations (2), (4). From the equations

of oscillations (7) and (6) we have

$$\begin{aligned}
&\omega_* \vec{H}^* = \sqrt{4\pi}\left\{mf\vec{v}^* + i\xi\vec{e}_\varphi\left[f\,\mathrm{div}\,\vec{v}^* + \omega_*\vec{v}^*\cdot\nabla\left(\frac{f}{\omega_*}\right)\right]\right\}\\
&ia\vec{v}^* + \omega_*\nabla\Pi - 2\Omega\omega_* v_\varphi^*\nabla\xi + \frac{f\nabla(\xi^2\rho)}{\xi\rho^2}\left[mfv_\varphi^* + \right.\\
&\left. + i\xi\rho\omega_*\vec{v}^*\cdot\nabla\left(\frac{f}{\omega_*\rho}\right)\right] + \frac{\omega_*}{\xi}\vec{e}_\varphi\left\{\vec{v}^*\nabla(\xi^2\Omega) - \frac{mf^2}{\omega_*\rho^2}\vec{v}^*\cdot\nabla(\rho\omega_*\xi^2)\right\} = 0,
\end{aligned} \tag{16}$$

where ω_* and a represent the same combinations as in (10). Since m only enters as $m\Omega$ and m^2, we may take $m \geq 0$.

We seek a solution in the form of a series in associate Legendre polynomials $P_\kappa^m(\cos\vartheta)$:

$$\begin{cases}
v_z^* = i\omega_*\sum_\kappa X_\kappa P_\kappa^m, \quad \Pi = z\sum_\kappa W_\kappa P_\kappa^m, \quad b = \omega_*\Omega - \frac{mf^2}{\rho},\\
v_\vartheta^* = \frac{\omega_*}{\sin\vartheta}\sum_\kappa\left[\mathcal{Z}_\kappa - \frac{z\omega_* f\sin^2\vartheta}{b}\left(\frac{f}{\rho\omega_*}\right)'X_\kappa\right]P_\kappa^m.
\end{cases} \tag{17}$$

The additional term in the expression for v_φ^* is chosen so that (16) gives the simplest possible expression for v_ϑ^*:

$$v_\vartheta^* = \frac{i\omega_*}{a}\sum_\kappa\left(W_\kappa\frac{\partial P_\kappa^m}{\partial\vartheta} - \frac{2b\cos\vartheta}{\sin\vartheta}\mathcal{Z}_\kappa P_\kappa^m\right).$$

Multiplying equation (8) by $\sin^3\vartheta\,P_\ell^m$ and the first and the third components of (16) by $\sin\vartheta P_\ell^m$ and $\sin^2\vartheta P_\ell^m$, respectively, we obtain after integration over ϑ from 0 to π

$$\begin{cases}
\sum_\kappa\left\{\left(ma\mathcal{Z}_\kappa + m^2W_\kappa\right)\delta_{\kappa\ell} + \left[\frac{a(z^2\rho X_\kappa)'}{z\rho} + 2b\mathcal{Z}_\kappa - \kappa(\kappa+1)W_\kappa\right]\mathcal{J}_{\kappa\ell}^\circ - \right.\\
\left. - 2b\mathcal{Z}_\kappa\mathcal{J}_{\kappa\ell}'\right\} = 0,\\
\sum_\kappa\left\{\left[aX_\kappa + c\mathcal{Z}_\kappa - (zW_\kappa)'\right]\delta_{\kappa\ell} + \frac{z^2f\rho'}{\rho}\left(\frac{f}{\rho}\right)'X_\kappa\mathcal{J}_{\kappa\ell}^\circ\right\} = 0,\\
\sum_\kappa\left\{\left[\left(a - \frac{4b^2}{a}\right)\mathcal{Z}_\kappa + mW_\kappa\right]\delta_{\kappa\ell} + \left(cX_\kappa + \frac{4b^2}{a}\mathcal{Z}_\kappa\right)\mathcal{J}_{\kappa\ell}^\circ + \frac{2b}{a}W_\kappa\mathcal{J}_{\kappa\ell}'\right\} = 0,\\
c = 2\omega_*\Omega - \frac{mf^2(z^2\rho)'}{z\rho^2}
\end{cases} \tag{18}$$

Here

$$\begin{aligned}
&\mathcal{J}_{\kappa\ell}^\circ = \frac{1}{I_\ell}\int_0^\pi P_\kappa^m P_\ell^m\sin^3\vartheta\,d\vartheta = -\mathcal{K}_\ell^{(-)}\delta_{\kappa+2,\ell} + \mathcal{K}_\ell\delta_{\kappa\ell} - \mathcal{K}_\ell^{(+)}\delta_{\kappa-2,\ell};\\
&\mathcal{J}_{\kappa\ell}' = \frac{1}{I_\ell}\int_0^\pi\frac{\partial P_\kappa^m}{\partial\vartheta}P_\ell^m\sin^2\vartheta\cos\vartheta\,d\vartheta = (\ell-2)\mathcal{K}_\ell^{(-)}\delta_{\kappa+2,\ell} + \left(\tfrac{3}{2}\mathcal{K}_\ell - 1\right)\delta_{\kappa\ell} - (\ell+3)\mathcal{K}_\ell^{(+)}\delta_{\kappa-2,\ell};\\
&I_\ell = \frac{2}{2\ell+1}\frac{(\ell+m)!}{(\ell-m)!};\quad \mathcal{K}_\ell = \frac{2[\ell(\ell+1)+m^2-1]}{(2\ell-1)(2\ell+3)};\quad \mathcal{K}_\ell^{(\pm)} = \frac{(\ell\pm m\pm1)(\ell+1\pm m\pm1)}{(2\ell\pm3)(2\ell+2\pm3)}.
\end{aligned}$$

$\delta_{\kappa\ell} = 1$ for $k = \ell$, $\delta_{\kappa\ell} = 0$ for $k \neq \ell$.

The integrals are readily evaluated if $\sin^2\vartheta P_\kappa^m$, etc., are expressed with the aid of known recursive relations /6/ in terms of the three polynomials P_κ^m and $P_{\kappa\pm2}^m$. The problem of oscillations thus reduces to finding the eigenvalues ω of a system of coupled equations (18).

Consider an approximate method of solution of this system. Let ℓ be equal either to m or to $m+1$, when $\mathcal{K}_\ell^{(-)} = 0$. If we omit the terms containing $\mathcal{K}_\ell^{(+)}$, we obtain a system of two first-order differential equations for X_ℓ and W_ℓ. We will refer to this as the first approximation. In the second approximation, we obtain a system $X_\ell, X_{\ell+2}, W_\ell, W_{\ell+2}$, etc.

The convergence of this process for a system similar to (18) is considered for one particular numerical example in /8/, where the nonradial oscillations of a nonmagnetic rotating normal star are investigated to a certain approximation. The first approximation ensures an accuracy of about 4%, and the second approximation 0.2%.

If we restrict the analysis to the first approximation only, we obtain a system which has some features in common with equations (8)—(9) for a cylinder. The principal properties of the unstable oscillations of a sphere are in all probability qualitatively similar to the unstable oscillations investigated in the previous example. Numerical integration of equations (18) will be carried out in the nearest future.

The above analysis leads to the conclusion that two types of instabilities are apparently possible in a neutron star with a toroidal magnetic field. The first type is symmetrical about the spin axis ($m = 0, \ell \neq 0$). This is a convective instability, and a criterion of its existence can be derived by simple qualitative considerations based on considerations of interchangeability of magnetic force tubes. For the distribution corresponding to the stability limit, the field H_φ is proportional to $\rho r \sin\vartheta$.

By analogy with the oscillations of a cylinder, we can expect that the conditions of the excitation of the second type of instability ($m \neq 0, \ell \geq |m|$) are much more favorable. In this case, the self-sustained oscillation modes are isolated and their number increases with the increase in the ratio of the magnetic energy to the rotational energy. If, moreover, the field falls off sufficiently fast away from the center, the effect of the field on oscillation modes which have numerous nodes along the radius or in the azimuthal direction is markedly suppressed. It therefore seems that there exist configurations with only one unstable harmonic $\ell = 1$, $m = 1$.

For both types of instability, the density, the pressure, and the gravitational potential experience characteristically small perturbations during the oscillations. On the surface of the star, the particles are displaced almost horizontally (to orders of magnitude, the vertical component is less than the horizontal component by a factor of $H_\varphi^2/G\rho_c^2 R^2$). For $m \neq 0$, the instability is oscillatory with a frequency $\mathrm{Re}\,\omega$ which mainly depends on the rotation velocity and with an increment $|\mathrm{Im}\,\omega|$ which is mainly determined by the magnetic field strength.

Let us now consider the hypothesis /1/ according to which the recently discovered pulsating radio sources /8/ are in fact magnetic rotating neutron stars with instabilities of the type described above.

If a star of the Sun's mass with an internal magnetic field of the order of 10^3 Oe is converted into a neutron star with a radius $R \sim 10^6$ cm, the field on the average increases to 10^{13} Oe, and the magnetic energy in the final state will be $E_m \sim 10^{43} - 10^{44}$ erg. The strength of the poloidal field of the neutron star near the surface will markedly increase, since this field has the same order of magnitude in the outer and the inner layers of the star. In all probability, it will be ejected from the star in the earlier stage of gravitational collapse.

The magnetic energy in the form of a toroidal field may have any degree of concentration toward the center. Both types of instabilities will probably be excited in such a star ($m = 0$ and $m \neq 0$). Convection will intermix the various layers until a convectionally stable state is formed. The amplitude of the unstable oscillation modes with $m \neq 0$ (or of one such mode) will be

determined by nonlinear effects and probably by processes involving ejection of lumps of matter with frozen-in field. The latter instability apparently may exist until the field is reduced below some limit value which depends on the oscillation damping factors. An estimate of the instability lifetime τ is obtained if we divide the magnetic energy E_m by the luminosity L. For $E_m \sim 10^{44}$ erg and $L \sim 10^{30}$ erg/sec, we find $\tau \sim 3 \cdot 10^6$ years.

The recurrence frequency of the pulses will be comparable with the angular rotation velocity, since $\omega + m\Omega$ is generally small. Rotation periods from 0.03 to a few seconds are quite likely for neutron stars. A more detailed comparison with experimental data requires further development of the theory.

Bibliography

1. Vandakurov, Yu.B.— ZhETF Letters, 9:133. 1969.
2. Meltzer, D.W. and K.S. Thorne.— Astrophys. J., 145:514. 1966.
3. Vandakurov, Yu. V. —Astronomicheskii Zhurnal, 45:103. 1968.
4. Vandakurov, Yu.V. and E.N. Kolesnikova.— Astronomicheskii Zhurnal, 43:99. 1966.
5. Vandakurov, Yu.V. —Astronomicheskii Zhurnal, 44:786. 1967.
6. Lebedev, N.N. Spetsial'nye funktsii i ikh prilozheniya (Special Functions and Applications).— Moskva, Fizmatgiz. 1963.
7. Durney, B. and A. Skumanich.— Astrophys. J., 152:255. 1968.
8. Hewish, A., S.J. Bell, J.D.H. Pilkington, P.F. Scott, and R.A. Collins.— Nature, 217:709. 1968.

FIELD GENERATION IN MAGNETIC STARS

E. M. Drobyshevskii

There are about a hundred stars with magnetic fields /1/. These are mainly peculiar stars of F2 – B8 types. Their magnetic fields reach a few thousand oersteds. The magnitude and even the direction of the field vary with periods of ~4 – 10 days. These stars possess a thin convective envelope, which disappears for stars of later types /2/. The degree of ionization in the convective zone is high enough to treat the gas as completely ionized.

Plasma acceleration almost invariably involves the development of a certain inertial emf /3/:

$$\vec{E}^{i} = \frac{m_e - f_{ei} m_i}{1 + f_{ei}} \frac{1}{e} \frac{d\vec{V}}{dt}. \qquad (1)$$

Here $f_{ei} = \frac{F_e}{F_i}$, where $\vec{F}_{e,i}$ are forces of an arbitrary nature, except electric and friction forces between plasma components, which act on the average on every particle of the particular component (we take $\vec{F}_i \parallel \vec{F}_e$); m_e and m_i are the particle masses.

In the convective zone of stars, the gas is accelerated in various directions. However, only the Coriolis acceleration in the longitudinal direction in rotating stars is capable of producing large-scale effects: because of the temperature difference of the gas in the ascending and descending convective fluxes, the inertial emf's do not fully cancel one another. A certain resultant eddy emf remains.

Convection in stars is characterized by zero total mass flow through a surface of any radius:

$$\xi \rho_1 V_1 + (1 - \xi) \rho_2 V_2 = 0. \qquad (2)$$

Here the subscript 1 refers to ascending gas streams (with relative volume ξ), and 2 to descending gas streams ($p_1 = p_2 = p$, $T_1 - T_2 \ll T_1 + T_2$). The energy flux transferred by convective streams is

$$\pi F_\kappa = \xi c_p \rho_1 T_1 V_1 + (1 - \xi) c_p \rho_2 T_2 V_2 = c_p \xi \rho_1 V_1 (T_1 - T_2), \qquad (3)$$

where ρ is the gas density, c_p is the heat capacity of the gas.

The current density in a binary mixture of components with different conductivities σ, in the presence of oppositely directed emf's in the two components, falls between the two extreme cases of differently oriented (relative to emf) layer models with the same volume content of the components /4/. The current densities in the layer models are

$$j_{equator} = \xi \sigma_1 E_1 + (1 - \xi) \sigma_2 E_2, \qquad (4)$$

$$j_{\text{merid}} = [\varepsilon E_1 + (1-\varepsilon) E_2] \frac{\sigma_1 \sigma_2}{\sigma_1 + \sigma_2}. \quad (5)$$

Assuming a constant rotation velocity Ω within the convective zone ($dV/dt = 2\Omega V \cos\vartheta$, ϑ is the latitude), and using (1), (2), and (3), we find

$$j_{\text{equator}} = -2\Omega\pi F_\kappa \frac{m_i}{e} \frac{1}{l_0} \frac{a}{dT} \left(\frac{\sigma}{\rho}\right)_p \cos\vartheta. \quad (6)$$

We assumed $1 \leq f_{ei} < \infty$, which corresponds to the case of gas-magnetic or electromagnetic interaction of convective elements with one another. If $\sigma \sim T^{3/2}$, we have $j_{\text{equator}} = 2.5 j_{\text{merid}}$. Integration for the case of spherical symmetry gives for the poloidal magnetic field $H \sim \Omega R \pi F_\kappa$.

The data of /2, 5/ were applied to compute the polar magnetic field H_p for the main-sequence stars (see figure).

An adequate fit is observed. Indeed, 1) the computed fields are of the same order of magnitude as the observed fields, 2) the field gradually increases from F0 to A0 stars, 3) the field markedly diminishes from A0 to B9 stars, this being due to the immersion of the outer boundary of the convective zone in the region of the second ionization of helium.

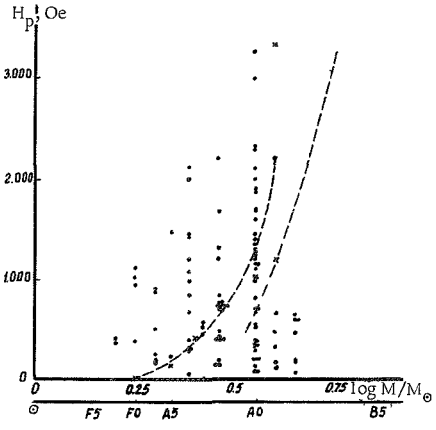

Computed magnetic fields H_p for the pole of main-sequence stars (crosses, dashed lines) and the magnetic fields measured by Babcock /6/ (dots).

Our previous analysis ignored the transient time of the magnetic field. It is generally assumed /7/ that the transient time is comparable to or greater than the lifetime of the star. This is true for stars without mixing. In our case, the main part of the field-generating current is confined to a very thin ($l \sim 10^7 - 10^8$ cm) surface skin layer. The time to establish a nearly steady-state current distribution in this thin layer is small ($\tau \approx \frac{\sigma l^2}{c^2}$), and most of the time is required to allow the magnetic field to penetrate through the remaining volume of the star. If the stellar matter is in a state of vigorous mixing, the magnetic field is transported together with the mixed matter into the stellar interior. A particularly favorable case in this respect is observed when the convective envelope occupies a large part of the star volume (late-type stars, including the Sun). In double stars (the peculiar stars are probably double stars /8/) vigorous mixing occurs, so that despite the small thickness of the convective envelope in F0 — B8 stars, the magnetic field reaches steady-state conditions in a fairly short time. Finally, mixing may be excited in stars by the magnetic field itself if its configuration is far removed from the configuration corresponding to the steady-state current distribution /9/.

Bibliography

1. Severnyi, A.B.— UFN, 88:3. 1966.
2. Gorbatskii, V.G. and A.K. Kolesov.— Astrofizika, 2:273. 1966.
3. Drobyshevskii, E.M.— ZhTF, 38:1609. 1968.
4. Bursian, V.R. Teoriya elektromagnitnykh polei, primenyaemykh v elektrorazvedke (Theory of Electromagnetic Field in Electrical Prospecting), Part 1.— GTTI, Moskva-Leningrad. 1933.
5. Allen, C.W. Astrophysical Quantities, 2nd edition. London. 1963.
6. Babcock, H.W.— In: "Stellar Atmospheres," ed. J.L. Greenstein, Univ. of Chicago Press. 1960.
7. Cowling, T.G.— M.N., 105:166. 1945.
8. Heuvel, E.P.J. van den.— B. A. N., 19:326. 1968.
9. Kipper, A.Ya.— Trudy IV soveshchaniya po voprosam kosmogonii, p.1425. Moskva, Izd. AN SSSR. 1955.

THE SPECTRUM OF THE EXTRAGALACTIC BACKGROUND RADIATION

R. A. Syunyaev

The observations of optical sources through giant telescopes at the beginning of this century led to the discovery of the red shift in the spectral lines of the distant galaxies and provided a proof of the expansion of the Universe. The next fundamental result which shed some light on the properties of the Universe as a whole was only obtained in 1965: this was the discovery of the relict radiation in the radio spectrum — the remnant radiation of the primeval fireball, carrying information about the early stages of evolution of the Universe. The relict radiation is not associated with individually resolvable sources — this is background radiation. In this paper, we will describe the entire spectrum of the background electromagnetic radiation of the Universe — from radio frequencies to gamma rays (Figure 1), discussing its sources and properties.

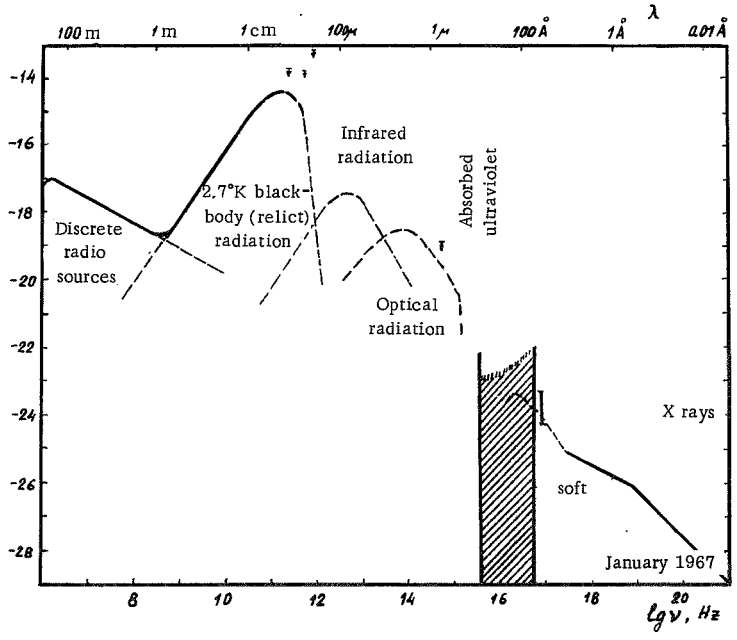

FIGURE 1. The spectrum of the background radiation of the Universe.

The comprehensive description became possible only following the tremendous advances in experimental astrophysics (both in radio astronomy and in the so-called extra-atmospheric — namely ultraviolet, X-ray, gamma-ray, and partly infrared and optical — astronomy).

RADIO FREQUENCIES

The radio spectrum is generally divided into two regions, the long-wave region associated with the total emission of low-power discrete radio sources, and the short-wave region, where relict radiation predominates.

50 cm $< \lambda <$ 300 m, $10^6 < \nu < 6 \cdot 10^8$ Hz

The metagalactic background radiation is very difficult to isolate in this region, since the radio telescopes receive both the true background radiation and the synchrotron radiation of the relativistic electrons in our Galaxy, which apparently accounts for between 60 to almost 100 percent (depending on direction) of the total signal at 1.7 m wavelength. The separation of the extragalactic component was facilitated by the discovery that its spectrum $I_\nu \sim \nu^{-\alpha}$ differs from the radio spectrum of the Galaxy at meter wavelengths. The British radio astronomers /1/ carried out careful measurements at various wavelengths in several directions close to the galactic pole, where the radiation of the Galaxy is minimum. As a result, they succeeded in determining both the spectrum and the intensity of the background radio emission, which at 1.7 m corresponds to a brightness temperature of $T_e = \frac{I_\nu \lambda^2}{2k} = 30 \pm 7°K$. The background is readily accounted for by the radiation from distant discrete radio sources, especially as its spectral index α is 0.75, being equal to the spectral index of most radio galaxies and quasars at these wavelengths. However, the spatial density of galaxies and radio galaxies and their power proved insufficient to ensure the observed background intensity. The situation clarified only after a careful computation of the number of weak (and apparently distant) radio sources carried out by the British radio astronomers. They obtained a curve plotting the number of radio sources with a flux greater than a given value N(s) as a function of the incoming flux s. This curve provided evidence of evolution of the number or the power of radio sources in the past. The density of the powerful radio sources in unit moving volume (moving together with the expanding Universe) or their mean power should be much higher than the present-day figures /2/. At present, we can count weak sources with received fluxes exceeding $s = 10^{-28}$ W/m$^2 \cdot$Hz at 1.7 m; these counts require radio telescopes of tremendous sensitivity, and the number of these sources over the entire sky is over a million, while each (a radio galaxy or a quasar) has an enormous power output. The shape of the curve N(s) is such that the main contribution to the background radiation comes from the weakest sources. This is due to the rapid increase in the number of sources with the decrease in their flux. A dependence of this kind is a clear sign of

evolution. The growth of the N(s) is somewhat slowed down at very low s. This feature is also predicted by the background intensity, which is only slightly higher than the total flux from all the known radio sources.

We have mentioned above that the spectrum of our Galaxy ($\alpha \sim 0.4$) at meter wavelengths differs from the background spectrum ($\alpha \sim 0.75$), so that at longer wavelengths the contribution of the extragalactic component received by the Earth radio telescopes is larger. Measurements at 150 m revealed a surprisingly low intensity, which apparently could not be related to strong absorption in the Galaxy /3/. This effect is probably due to self-absorption in the sources. We can apply it to our purposes to compute the spatial density of radio quanta in the Universe: such a computation would have been unfeasible had the number of quanta continued increasing with wavelength. The density of radio quanta and the energy density of the background radio emission are listed in the table for comparison with other spectral regions.

Density of quanta and energy density of background radiation in various frequency ranges

Frequency range	Energy density, eV/cm^3	Density of quanta, cm^{-3}
Discrete radio source	10^{-7}	1
Relict radiation	0.25	400
Infrared sources	10^{-2}	1
Optical spectrum	$3 \cdot 10^{-3}$	10^{-3}
Soft X-ray spectrum	10^{-4}—10^{-5}	$3 \cdot (10^{-7}$—$10^{-8})$
Hard X-ray spectrum	10^{-4}	$3 \cdot 10^{-9}$

$3 \cdot 10^{-2}$ cm $< \lambda <$ 50 cm, $6 \cdot 10^{8} < \nu < 10^{12}$ Hz

The main contribution to the observed background comes from the relict radiation, whose discovery in 1965 confirmed the validity of the hot model of the Universe /4, 5/. The temperature of the relict radiation is currently known with a 5% accuracy. According to Princeton measurements at wavelengths of 0.86, 1.58, and 3.2 cm, $T = 2.68^{+0.09}_{-0.14}$ °K /6/. Measurements carried out by the same group at 0.33 cm /7/ and indirect determination of the temperature of the relict radiation from the population of the levels of the interstellar CN molecules ($\lambda = 0.264$ cm) /8/ show that the background spectrum at these wavelengths deviates from the straight line and develops a Planckian shoulder. The sensational report /9/ of the discovery of a tremendous radiation flux between $4 \cdot 10^{-2}$ cm and 0.13 cm — almost double the expected flux for the Planckian spectrum (brightness temperature $T_b \sim 8$°K) — was disproved by observations of the level populations of the interstellar molecules CN, CH, CH^+ ($\lambda = 0.132$, 0.0559, 0.0359 cm) /8/. The true intensity and the true spectrum in the Wien region have not been established so far. And yet these measurements are of the highest importance. The spectrum of the relict radiation in the Wien region should be distorted by the interaction of this radiation component with hot intergalactic gas: Compton scattering of the relict

quanta by thermal electrons with temperatures $T_e >> T_r$ increases the mean energy of the quantum and alters the radiation spectrum /10, 11/. The amount of distortion provides an indication of the time when the secondary, nonequilibrium ($T_e >> T_r$) heating of the metagalactic plasma occurred. Modern experimental data confirm that the recombination of hydrogen in the Universe ($t \sim 10^{13}$ sec, red shift $z \sim 1500$) was followed by a period of neutral hydrogen and that the metagalactic gas was not always ionized.

Relict radiation also carries information about the earlier stages of the evolution of the Universe ($t << 10^{13}$ sec). The point is that even before the recombination of hydrogen in the Universe, the primary plasma and radiation were not maintained in a perfect thermodynamic equilibrium: radiation and matter had the same temperature, the electrons showed a Maxwellian velocity distribution, but the characteristic time of the slowing-down process exceeded the cosmological time for the relevant period. Therefore, if a large quantity of energy were to be released for some reason at that time, the radiation spectrum would be distorted. The radiation energy would increase in such a case, whereas the number of quanta would remain the same because of the slow slowing-down processes. In other words, no Planckian distribution would be obtained. Compton scattering of quanta by electrons establishes a Bose-Einstein distribution $I_{B-E} \sim x^3/(e^{x+\mu}-1)$ rather than the Planckian distribution $I_P \sim x^3/(e^x-1)$, where $x = h\nu/kT$. For $x < \mu < kT$, these distortions become significant, $I_{P-E} \sim x^3$, whereas the Rayleigh–Jeans law gives $I_P \sim x^2$. The absence of pronounced distortions of the relict radiation spectrum in the Rayleigh–Jeans region imposes definite restrictions on the velocities of turbulent motion in the Universe, precludes the existence of antimatter regions in the Universe, and provides a powerful argument in favor of charge asymmetry of the Universe /12/. Possible deviations from the Planckian curve are shown in Figure 2.

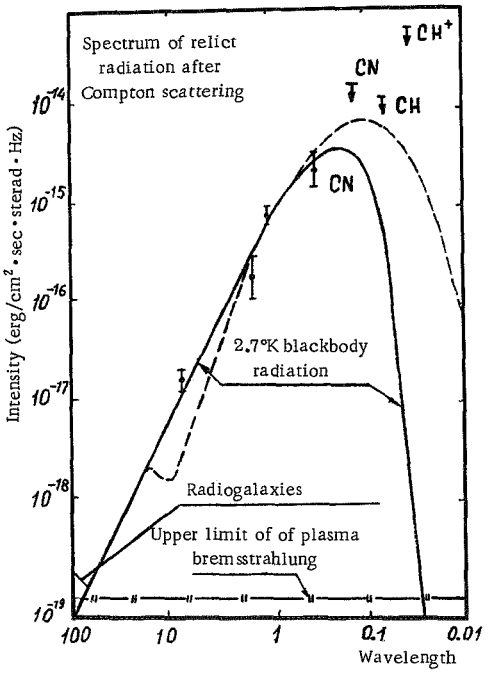

FIGURE 2. Possible distortions of the relict radiation spectrum (dashed curve).

INFRARED RADIATION

In this region ($3\mu < \lambda < 300\mu$, $10^{12} < \nu < 10^{14}$ Hz), no direct measurements of the background radiation are available, but a wide class of objects

are known with a maximum at the infrared. These are both galactic sources, such as the Crab Nebula and the galactic center region, and extragalactic sources, including normal galaxies, Soifert galaxies, and N-galaxies, as well as quasars. No accurate estimate of the background from these sources can be obtained at present, since neither the number nor the luminosity function is known. Order of magnitude estimates were made by Low and Tucker /13/; their results are shown in Figure 1 and in the table.

OPTICAL RADIATION

For this region ($3000\,\text{Å} < \lambda < 3 \cdot 10^4\,\text{Å}$, $10^{14} < \nu < 10^{15}$ Hz), observers only give the upper limit of the background radiation intensity $I_\nu < 1.3 \cdot 10^{-19}$ erg/cm^2 · sec · sterad · Hz at 5560 Å /14/. The extragalactic component is very difficult to isolate against the background of the Earth's atmospheric radiation, zodiacal light (solar light scattered by interplanetary dust), and the light of the stars in our Galaxy, which produce a flux 100 times as high as the expected luminous flux from the normal galaxies and almost one order of magnitude higher than the above upper limit figure. The upper limit was derived by eliminating the atmospheric contribution, which is a function of the angle and the time of observation, and making measurements at wavelengths corresponding to Fraunhofer absorption lines in the solar spectrum and in the spectrum of the zodiacal light, so as to reduce the interplanetary intensity. The main contribution to the background radiation of the Universe in the optical spectrum is apparently due to the normal galaxies. The expected spectrum /14/ is shown in Figure 1. Improved data for the background radiation at these wavelengths would enable us to fix significant constraints for the evolution of galaxies and their luminosities in the past.

ULTRAVIOLET RADIATION

This spectral region can be divided into two parts: the right-hand part is accessible only to observations from satellites and rockets outside the atmosphere, and the left-hand part which cannot be observed from inside the solar system.

$912\,\text{Å} < \lambda < 3000\,\text{Å}$, $10^{15} < \nu < 3.3 \cdot 10^{15}$ Hz

The only experimental measurements are the data of Kurt /15/ based on the material collected by the VENUS spacecraft:

$$I_\nu < 10^{-21} \text{ erg/cm}^2 \cdot \text{sec} \cdot \text{sterad} \cdot \text{Hz at } \lambda = 1300\,\text{Å}.$$

These measurements also provide an estimate of the integrated luminosity of stars in our Galaxy, $L \sim 10^{40}$ erg/sec for $1225\,\text{Å} < \lambda < 1340\,\text{Å}$ /16/ and establish an upper limit for the energy density ($W < 10^{-3}$ eV/cm^3) of subcosmic particles with energies of the order of 100 keV in the interstellar medium.*

Only the hot stars emit in this region, and the expected background from the normal galaxies is therefore several orders of magnitude lower than the above upper limit. The main contribution is apparently from the emission of the hot intergalactic gas.

$50\,\text{Å} < \lambda < 912\,\text{Å}$, $3.3 \cdot 10^{15} < \nu < 6 \cdot 10^{16}$ Hz

This region of the background radiation spectrum of the Universe is fundamentally inaccessible to direct observations from inside the solar system because of the absorption of the ultraviolet quanta by the interstellar neutral hydrogen. When absorbed, the background radiation creates ionization zones around galaxies, not unlike the Stromgren zones near hot stars. The available observations of galaxies at 21 cm reveal the presence of neutral hydrogen far beyond the optical limits of galaxies. The density of hydrogen and the number of atoms along the line of sight in the peripheral regions of galaxies are exceedingly low, and this hydrogen is fully ionized for background radiation intensities exceeding $I_\nu = 10^{-23}$ erg/cm^2 sec · sterad near 912 Å (this corresponds to 10,000 ionizing quanta for each cm^2 of the surface of galaxies each second) /18/. An estimate of the density of the intergalactic gas based on this result is given below.

X-RAY RADIATION

The observed spectrum of the hard X-ray background radiation may be fitted with two power functions, $I_\nu \sim \nu^{-\alpha}$, with $\alpha = 0.7$ between 1.5 and 40 keV and with $\alpha = 1.2$ for $E > 40$ keV. The latter slope does not change up to around 1 MeV. For $E < 1.5$ keV, only measurements at 40 — 70 Å are available /19, 20/ (the effective energy corresponding to these wavelengths is $E_{ef} \sim 270$ eV). The exact flux value in this region is not known because of the uncertainty in the absorption corrections in the Galaxy. However, even without correcting for absorption, the soft X-ray flux is seen to be higher than the value expected on the basis of extrapolation from the hard region.

Measurements of the X-ray background provided fundamentally new information about the properties of the hot intergalactic gas (observations at 21 cm and the conspicuous absence of the absorption band corresponding to the L_α line in the spectra of distant quasars show that the intergalactic gas should be highly ionized and have a high temperature).

* Nonresonant charge exchange between a subcosmic proton and the atoms of neutral hydrogen in the interstellar medium produces a fast excited atom, which emits L_α quanta of Doppler-shifted frequency. The estimates of /17/ impose certain restrictions on the intensity of this radiation, and there is thus a way to determine the upper limit of the density of subcosmic particles.

The transparency of the intergalactic gas for 270 eV quanta indicates that the helium in this gas (the content of helium in the primordial matter in the "hot" model of the Universe is fixed at 30 wt.%) is completely ionized, which is possible only at temperatures $T > 10^5$ °K. At the same time, if the density of the intergalactic gas is of the order of the critical density $\rho_{crit} = \frac{3H_0^2}{8\pi G} = 2 \cdot 10^{-29}$ g/cm^3, its temperature may not exceed 10^6 °K, since otherwise the emission of the intergalactic gas in the X-ray region would exceed the observed background radiation. This is quite clear, since the bremsstrahlung intensity of an optically thin gas layer is proportional to $T^{-1/2} e^{-h\nu/kT} \rho^2$ rapidly decreasing with the increase in the ratio $h\nu/kT$. A gas heated to 10^5—10^6 °K will mainly lose energy in the form of quanta with $h\nu \sim kT$, i.e., in the ultraviolet range. The above restriction on the intensity of the ultraviolet background radiation in the Universe sets an upper limit on the emission of the intergalactic gas, and as it is proportional to the square of the gas density, we obtain an upper limit value for the density of the intergalactic gas $\rho < 1/3 \rho_{crit}$ /18/. It follows in particular, that the intergalactic gas is definitely not the source of the observed soft X-ray background radiation.

Since the hard X-ray radiation is described by a power spectrum, the radiation is generally assumed to originate in extragalactic objects or in the intergalactic space as a result of energy redistribution between low-energy quanta and relativistic electrons with a power spectrum formed by Compton scattering. Radio galaxies hardly can be regarded as the main source of relativistic electrons. If this were so, only one thousandth of the energy released by radio galaxies would fall in the radio spectrum. As we see from the table, the energy density of the X-ray background quanta is 1000 times the energy density in the long-wave part of the radio spectrum, associated with radio sources. Moreover, this mechanism would not produce the observed break in the X-ray spectrum.

Longair and the author proposed a model which explains the principal features of the X-ray background radiation in the soft and the hard region. This model associates the sources of relativistic electrons with the nuclei of extragalactic objects, which are sources of infrared radiation. Compton scattering of the infrared radiation by relativistic electrons is responsible for the generation of the hard part of the X-ray background spectrum. The break in the spectrum occurs when the high-energy electrons lose their entire energy on being scattered by the infrared quanta (in this process $\frac{dE_e}{dt} \sim E_e^2$) and change their spectrum, whereas the lower-energy electrons escape into the intergalactic space having lost only part of their energy and without changing the spectrum. Then these electrons scatter quanta of the relict radiation, whose mean energy is one order of magnitude lower than the energy of the infrared quanta, and soft X-ray quanta are produced in this way. We see from the table that to ensure the observed intensity of the X-ray background, only 1% of the energy converted in the nuclei of galaxies into infrared radiation should be released in the form of relativistic electrons. So far, no reliable measurements have been made of the background radiation in the gamma-ray spectrum ($E \gg 1$ MeV). This range probably carries valuable information about metagalactic cosmic rays.

Bibliography

1. Bridle, A.N.— Monthly Notices Roy. Astron. Soc., 136:219. 1967.
2. Longair, M.S.— Monthly Notices Roy. Astron. Soc., 133:421. 1966.
3. Bridle, A.N.— Nature, 219:136. 1968.
4. Zel'dovich, Ya.B.— UFN, 89:647. 1966.
5. Zel'dovich, Ya.B. and I.D. Novikov. Relyativistskaya astrofizika (Relativistic Astrophysics).— Moskva, Izdatel'stvo "Nauka." 1967.
6. Wilkinson, D.T.— Phys. Rev. Lett., 19:1195. 1967.
7. Broynton, P.E., R.A. Stokes, and D.T. Wilkinson.— Phys. Rev. Lett., 21:462. 1968.
8. Bortolot, V., J.F. Clauser, and P. Thaddeus.— Preprint. 1968.
9. Shivanandan, K., J.R. Houck, and M.O. Harvit.— Phys. Rev. Lett., 21:1460. 1968.
10. Weymann, R.— Astrophys. J., 145:560. 1966.
11. Zel'dovich, Ya.B. and R.A. Syunyaev.— Preprint, IMP. 1968.
12. Zel'dovich, Ya.B. and R.A. Syunyaev.— Preprint, IMP. 1969.
13. Low, S.J. and W.N. Tucker.— Phys. Rev. Lett., 21:1538. 1960.
14. Peebles, P.J.E. and R.B. Partridge.— Astrophys. J., 148:713. 1967.
15. Kurt, V.G. and R.A. Syunyaev.— Kosmicheskie Issledovaniya, 5:573. 1967.
16. Kurt, V.G. and R.A. Syunyaev.— Astronomicheskii Zhurnal, 44:1157. 1967.
17. Kurt, V.G. and R.A. Syunyaev.— ZhETF Letters. 1968.
18. Syunyaev, R.A.— Astronomicheskii Zhurnal. (In press); Astrophys. Lett., 3:33. 1969.
19. Bowyer, C.S., G.B. Field, and J.E. Mack.— Nature, 217:32. 1968.
20. Henry, R.C., G. Fritz, J.E. Meekins, H. Friedman, and E.T. Byram.— Astrophys. J., 153:L11. 1968.

COMPUTATION OF THE OPACITY OF STARS WITH ALLOWANCE FOR LINE ABSORPTION

A. F. Nikiforov and B. V. Uvarov

The opacity of stellar matter has a significant effect on the structure of stars, since the main mechanism of energy transfer in stars is in the form of radiant energy. In the stellar interior, where the diffusive approximation is applicable to the equation of radiative transfer, the radiant energy flux is expressed in terms of the Rosseland photon mean free path.

At a given temperature and density, the Rosseland free path is obtained by averaging, with a certain weight, the free paths $l(\omega)$ computed for fixed photon frequencies ω. The free path $l(\omega)$ is determined by the effective scattering and absorption cross sections of electrons for the respective photons. The most significant factors are Compton scattering, line absorption, photoionization, and bremsstrahlung absorption. Until recently, stellar opacity computations were made using photoionization and bremsstrahlung absorption only. Keller and Meyerott's tables computed in this approximation for a number of mixtures in a wide range of temperatures and densities have found extensive uses in astrophysics. Although the frequency-integrated absorption cross sections of lines are comparable with the photoionization cross sections, the discrete-discrete transitions were ignored. However, the very first computations of opacity with allowance for line absorption indicated that in the astrophysically relevant range of temperatures and densities, the Rosseland mean free path may decrease to $1/3 - 1/5$ of the earlier value as a result of line absorption. These computations were carried out in the USA by A. Cox and co-workers /1 – 2/ and very recently by T. Carson et al. in England /3 – 4/.

The effect of discrete-discrete transitions on the opacity of stellar matter is attributable to the presence of relatively heavy elements in stars, whose atoms at high temperatures have a large number of states with various degrees of ionization and excitation. As a result, the spectrum shows thousands of lines at different frequencies. Moreover, ions with a given electron occupancy of the levels have different systems of lines depending on the position of the nearby ions and the resulting Stark splitting. Other factors may also cause line broadening. They include various processes which reduce the lifetime of an ion in a given state of excitation: collisions of the ion with free electrons, interaction of the ion with the electromagnetic radiation field, Auger effect. Frequency shift associated with the thermal motion of ions leads to Doppler broadening.

Since the results obtained by Cox and Carson for the Rosseland mean free path are markedly divergent (by a factor of 2 – 3), we will try to analyze in some detail each of the computation methods. The physical approach to the problem and the allowance for the various effects influencing the stellar opacity are nearly the same in the work of Cox and that of

Carson. The main difference is in the particular methods used for the determination of the electron wave functions of the continuous and the discrete spectrum, the electron energy levels, and the chemical potential of the electrons.

Cox used a model with constant density of free electrons, and the wave functions were those of the hydrogen-like atom, determined with the aid of Slater's semiempirical screening constants. One of the principal shortcomings of Cox's procedure is that the occupancies of the electron shells are highly sensitive to the choice of the screening constant, which on the other hand cannot be determined with sufficient reliability. Moreover, in computing the electron energies, Cox ignored external screening created by bound electrons, which in some cases may be quite significant.

Carson's recent study /3/ using the Thomas–Fermi self-consistent potential /5/ is free from these shortcomings. Carson /4/ therefore considers his results as the first serious attempt to overcome the shortcomings of the hydrogen-like model in opacity computations. Carson's results, however, are adversely affected by a number of significant errors in the physical formulation of the problem, which are associated with improper application of the Thomas–Fermi model. One of the basic errors is the clearly wrong choice of the conditions of thermodynamic equilibrium for the various mixture components in the computation of the Thomas–Fermi potential of each atom in the stellar mixture. In thermodynamic equilibrium, the chemical potentials of the electrons for each component should be constant, and at the boundaries of atomic cells /5/, where the electrons are not affected by Coulomb forces, the free electron density in case of equal chemical potentials will be the same for each mixture component, as is physically proper. Carson, on the other hand, described thermodynamic equilibrium in terms of equal total pressures of electrons and atoms of each element at the boundaries of the atomic cell. As a result of this definition, the free electron density is discontinuous at the atomic cell boundaries in Carson's model. Another reason why the total pressure at the cell boundaries may not be equal is that thermodynamic equilibrium of electrons, because of their high velocities compared to the velocities of the nuclei, is established over a length of time during which the nuclei remain virtually stationary, so that in fact we may speak of the thermodynamic equilibrium of electrons for fixed nuclei.

We carried out some opacity computations illustrating the importance of this effect. Even without line absorption, our results sometimes differ from Carson's figures by as much as a factor of 2, and on the whole are closer to the results of Cox, although in individual instances there is a difference of about 50% between the two sets of data. The computations were carried out for a mixture of the following composition (mixture 1 in /3/):

Element	z	m_i
H	1	0.7440
He	2	0.2360
C	6	0.0007
N	7	0.0029
O	8	0.0057
Ne	10	0.0070
Al	13	0.0015
Si	14	0.0013
Fe	26	0.0009

(m_i is the weight fraction of the element).

The following results were obtained:

T	ρ	k	k_1	k_2
0.1	0.2017	63	106	54
0.3162	0.0627	1.37	2.66	1.54
0.3162	0.629	6.44	8.00	6.43

Here T is the temperature of the mixture, keV; ρ is the density, g/cm^3; k, k_1, k_2 are the opacities, in cm^2/g, computed by the present authors, by Carson /3/, and by Cox /1/, respectively. Note that /3—4/ also contain a number of other errors. For example, the Fermi—Dirac statistics is improperly used in the case of strong degeneracy of matter.

Let us briefly describe the procedure used in our computations. To compute the effective photon absorption and scattering cross sections, we require 1) the electron wave functions of the continuous and the discrete spectrum and the energy levels of the bound electrons; 2) the mean occupancies of the electron states and the mean degree of ionization of matter; 3) the probability distribution of various occupancies of the electron states; 4) the probability distribution for various electric field strengths set up by the ions; 5) the shape and the position of the spectral lines.

Since the Thomas—Fermi statistical model for given temperature and density is sufficiently accurate and convenient at high temperatures, we computed the electron wave functions in the first approximation using the Schroedinger equation with the Thomas—Fermi potential. The Thomas—Fermi potential was found using the procedure described in /6/. The electron states within an atomic cell can be classified, depending on the electron energy, into the states of the discrete and the continuous spectrum or intermediate states. An analysis has shown that the electrons of the intermediate group are relatively few under the relevant conditions, and they may be lumped with the electrons of the continuous spectrum. An approximate method, which may be called the test potential method, has been proposed for the determination of the discrete energy levels and the corresponding wave functions $R_{nl}(r)$ /7/. Using this method, we analyzed the applicability of the hydrogen-like wave function. The method was tested on a large number of problems and the results proved to be inadequate agreement with those obtained by a direct solution of the Schroedinger equation by the phase method /8/. The wave functions of the continuous spectrum were also found without numerical integration of the Schroedinger equation. An improved WKB approximation /9/ was found to ensure adequate accuracy, the vicinity of turning points included. The Coulomb wave functions proved to be a poor approximation for the continuous spectrum.

The mean occupancies for the discrete-spectrum electrons were determined according to the Fermi—Dirac statistics. Note that the application of the Fermi—Dirac statistics to the atomic electrons is by no means trivial, since we are dealing with a system of interacting particles, and not with an ideal gas in an external field. It can be shown that the Fermi—Dirac statistics is applicable to the atomic electrons.

A binomial distribution was used for the occupancies /3/. This distribution is derived from the Gibbs distribution for subsystems with a

variable number of particles when the deviations of the occupancies from the mean values are small.

The position of the spectral lines was determined with allowance for relativistic effects and line shift due to fluctuations of the electron occupancies. Effects associated with deviations of the self-consistent field from central symmetry were ignored, as in /1—4/.

The effective photon absorption cross sections were computed in the nonrelativistic dipole approximation. Since the photoionization formulas can be obtained in the limit from expressions for the line absorption cross sections, discrete-discrete transitions were effectively taken into consideration for overlapping lines using the corresponding expressions for the photoionization cross sections. Therefore, in some cases, the discrete-discrete transitions could be taken into consideration for small values of the principal quantum number n only. Since the Stark splitting markedly diminishes with the decrease in n, the Stark effect could be ignored in some cases. Since the effect of line shape on opacity is not very pronounced, Lorenzian line contours were used, as in /1—4/. The line widths were computed using the electron wave functions.

In conclusion, we would like to acknowledge the help of A.A. Samarskii, who actively participated in discussions, and Yu.N. Babaev and E.S. Fradkin, who suggested the original problem.

Bibliography

1. Cox, A.N. Stellar Structure (ed. G. Kuiper), p. 195. Chicago, London. 1965.
2. Cox, A.N., J.N. Stewart, and D.D. Eilers.— Astrophys. J., Suppl., 11(94):1. 1965.
3. Carson, T.R., D.F. Mayers, and D.W.N. Stibbs.— Monthly Notices, Roy. Astron. Soc., 140:483. 1968.
4. Carson, T.R. and H.M. Hollingsworth.— Monthly Notices, Roy. Astron. Soc., 141:77. 1968.
5. Feyman, R., N. Metropolis, and E. Teller.— Phys. Rev., 75:1561. 1949.
6. Nikiforov, A.F. and V.B. Uvarov.— ZhVM i MF, 9. 1969. (In press).
7. Nikiforov, A.F. and V.B. Uvarov.—ZhVM i MF, 1:177. 1959.
8. Uvarov, V.B. and V.I. Aldonyasov.— ZhVM i MF, 7:436. 1967.
9. Schiff, L. Quantum Mechanics. — New York, McGraw-Hill. 1955.

CHARGE SYMMETRY OF THE UNIVERSE

N. A. Vlasov

Dirac's theory and the discovery of antiparticles established the existence of charge symmetry in nature. A universe consisting of protons and electrons is definitely asymmetric, since the positive charge is associated with a heavy particle, whereas the negative charge is associated with a light particle. The discovery of the positron and the antiproton proved the existence of charge-conjugate antiparticles: both the positive and the negative charges are associated with particles of equal mass. Every charged particle has an oppositely charged antiparticle. The charge conjugation operation, moving a particle into its antiparticle, is universal, and the fundamental laws of nature governing the transformations of elementary particles are therefore charge independent, or in other words they possess charge symmetry.

Particles and antiparticles are created and annihilated in pairs, and matter consisting of particles of a finite rest mass could be created some time in the past by the process of pair production. As a result charge symmetry may be characteristic of the Universe as a whole. Charge symmetry of the Universe would indicate that on the whole it is neutral: the total charge of particles and antiparticles in the Universe is zero. This charge neutrality of the Universe does not follow from the charge symmetry of the elementary reactions: it should be proved separately, or adopted as an independent starting hypothesis.

Neutrality of electric charge is essential in a homogeneous and isotropic Universe. If the total electric charge of matter were different from zero, an electric field would result which would violate the isotropy of space. The exact equality of the proton and the electron charge (in absolute value) was considered in connection with the problem of the electric neutrality of the Universe. If the proton charge e_p is not quite equal to the electron charge e_e, i.e.,

$$e_p = -(1+y)\,e_e, \text{ for } y \neq 0,$$

the resultant charge of a system containing protons and electrons in equal number is no longer zero and Coulomb repulsion arises between the individual elements. For $y = 0.9 \cdot 10^{-18}$, the gravitational attraction of the hydrogen atoms will be fully compensated by the Coulomb repulsion. The value of y can be estimated from certain astrophysical observations, e.g., from the magnetic moments of rotating celestial bodies. The magnetic moment of the Earth gives $y \leqslant 2 \cdot 10^{-19}$. Laboratory measurements of y in experiments

passing beams of neutral atoms and molecules through strong transverse electric fields yielded even lower upper limits. The neutron charge, which should be $|ye|$ if the charge conservation in the reaction $n \to p + e$ is exact, was found to be $|e_n| < 3 \cdot 10^{-20} e$ /2/. The non-deflection of a beam of SF_6 molecules yields $y < 2 \cdot 10^{-22}$. Thus, if we assume that the Universe is isotropic and homogeneous and the electric charge is conserved, we are inevitably led to the conclusion that the Universe is electrically neutral.

No such conclusion can be reached regarding the baryon charge, however. No long-range forces with a potential of the form $u \sim 1/r$ are known for the baryon charge. Therefore, neutrality with regard to the baryon charge does not clash with the isotropy of the Universe. If the hot model is valid, the Universe in a state of high density and temperature ($kT \simeq M_p c^2$) was very close to neutrality or was simply neutral with regard to the baryon charge. In this state, the bulk of matter was represented by baryon — antibaryon pairs in a state of thermodynamic equilibrium with radiation. As the Universe expanded, these pairs annihilated. The residual matter in the present-day Universe comprises $10^{-8} - 10^{-9}$ of the annihilated matter in the hot Universe. Even if the residual matter displays baryon charge asymmetry, i.e., there is no antimatter in the present-day Universe, the asymmetry of the hot Universe, for $kT \simeq M_p c^2$, was truly negligible, the relative excess of baryons over antibaryons having been of the order of $10^{-8} - 10^{-9}$. The assumption of perfect symmetry under the hot Universe conditions is naturally more attractive, although it is not indispensible. Thus Zel'dovich and Novikov /3/ assume that there is in fact an excess of baryons over antibaryons in the hot state, so that further evolution gives a Universe with distinct matter asymmetry.

The assumption of charge neutrality in the hot Universe admits of different evolutionary alternatives in the course of expansion. Sakharov covered this topic in his paper at the GAISh* seminar in January 1969 in Moscow and in /4/. To derive the present-day asymmetric Universe from the charge-neutral hot state, Sakharov postulates that at the stage of quark-to-baryon conversion, there occur certain reactions which are asymmetric with regard to the baryon charge, in the same sense that the following decays are asymmetric:

$$K_2^0 \begin{cases} \nearrow \pi^- \mu^+ \nu \\ \searrow \pi^+ \mu^- \bar{\nu} \end{cases} \quad \text{and} \quad K_2^0 \begin{cases} \nearrow \pi^- e^+ \nu \\ \searrow \pi^+ e^- \bar{\nu} \end{cases}.$$

Both decay modes are relatively unlikely compared to the fundamental decay $K_2^0 \to 3\pi$. The two branches of each of these decay modes are charge-conjugate and should have the same probability if the combined CP parity is conserved. In fact, however, the first branches (with μ^+ and e^+) are about 0.5% more probable than the second branches (with μ^- and e^-) /5, 6/.

The asymmetry of these decays incidentally points to a fundamental difference between matter and antimatter. If radio astronomers were to establish communication with a distant civilization, this asymmetry would enable them to identify whether the planet of our counterparts consists of matter or antimatter. To this end, it suffices to inquire what electrons are more numerous in their atoms — those which are more numerous in K_2^0 decay or those which are fewer in this decay.

* [GAISh — The Shternberg State Astrophysical Institute.]

If the answer is that the former is true, our counterparts exist in an antimatter world.

The above examples of CP-asymmetric decays, however, have no bearing on the subject of the baryon charge: for all the particles taking part in these decays, the baryon charge is zero. Therefore, the nonconservation of CP-parity in K_2^0 decay is not sufficient to indicate the existence of reactions which are asymmetric relative to the baryon charge. This evidence only spurs us to examine this possibility. There is always a possibility that the interaction is CP-noninvariant in K_2^0 decays or that another similar interaction is responsible for the asymmetry of quark-to-baryon conversions. Assuming a certain type of such asymmetric reactions, Sakharov derived in the final state a Universe in which all the visible matter carried positive baryon charge, whereas the negative baryon charge was confined to the invisible electrically neutral antiquarks. The total baryon charge was zero. In the first version, Sakharov assumed compensation of the baryon charge of matter by the muon charge of the muonic neutrino, but this variant proved to be inconsistent with baryon charge conservation, which had been established with very high accuracy. It is a known fact that nucleon decays forbidden for reasons of baryon charge conservation are characterized by times greater than 10^{28} years /7/. The second version of Sakharov's hypothesis does not contradict the baryon charge conservation, but it leads to a mass of unobservable antiquarks which is markedly greater than the mass of visible matter (approximately by a factor of 40). There are three antiquarks for each nucleon, and their mass is approximately one order of magnitude higher than the nucleon mass. It is hard to visualize how this tremendous invisible mass can be fitted into the Universe.

Sakharov's hypotheses constitute an interesting exercise the purpose of which is to reconcile the charge neutrality of the hot Universe with the present state in which antimatter (in the form of aggregations of antinucleons) is assumed to be absent. Both Sakharov's hypothesis of the asymmetry of quark-to-baryon conversions and Zel'dovich's hypothesis of the aboriginal charge asymmetry of the Universe are motivated by the assumption that the present-day Universe contains no antimatter objects (antigalaxies, antistars, etc.).

If we assume charge symmetry of the present-day Universe, its total charge will be zero, so that matter and antimatter objects on the average will be equiprobable, though definitely separated in space. We will then have, first, to find suitable mechanisms for separation of matter from antimatter and, second, to explain the total lack of observational evidence pointing to the existence of antimatter.

The separation of matter and antimatter constitutes an unsolved problem within the framework of the hot model and should be further investigated. Some separation mechanisms, however, have been proposed already. Konstantinov /8/ suggests that the existence of magnetic fields in the symmetric plasma is a basic premise for separation of matter and antimatter. In an inhomogeneous magnetic field, charged particles wind onto the magnetic lines of force and also "drift" in the transversal direction. This drift occurs in opposite directions for particles and antiparticles, as it is determined by the electric charge sign.

Separation in combined gravitational and electromagnetic fields was discussed by Alfvén /9/. The gravitational field exerts a different force on the heavy (protons and antiprotons) and the light (electrons and positrons) components of the symmetrical plasma. If the plasma is in thermodynamic equilibrium, a homogeneous gravitational field produces an exponential variation of density "with altitude." The exponential argument for the heavy component is a factor of 1836 higher than for the light component, as it is proportional to the particle mass. The heavy component is therefore concentrated "at the bottom," and in a certain region of space a transition is observed from a predominantly heavy plasma to a predominantly light plasma. If there is moreover an electrical field with a component normal to the interface of the two regions, it will displace the electrons and protons (or the positrons and antiprotons, depending on the field direction) one toward the other. The electrical field may be generated by a nonstationary magnetic field. Thus an excess of matter or antimatter will arise near the interface; in other words, separation of a symmetrical plasma has occurred.

Neither of these separation mechanisms can be immediately related to the conditions of the very dense plasma in the hot Universe. In this ultra-dense plasma, however, it suffices to ensure separation of a very small fraction ($\sim 10^{-8} - 10^{-9}$) of matter and antimatter in order to form the present-day Universe with equal numbers of galaxies and antigalaxies, or stars and antistars. If there is a mechanism capable of achieving this separation, the present-day Universe need not be regarded as asymmetric, and our task is to establish the exact manifestation of symmetry: are there galaxies and antigalaxies, or are the galaxies themselves symmetric and there are stars and antistars in equal numbers.

With regard to observations which are interpreted as evidence against the existence of antimatter, we would like to call attention to a common inconsistency which probably leads to the excessively pessimistic outlook. For example, the intensity of gamma rays accompanying particle-antiparticle annihilation may give the averaged product of proton and antiproton densities $\overline{p^+ p^-}$ along the line of sight. The result obtained for this product is divided by the known value of p^+, and the quotient is regarded as the average density of p^-. This approach ignores the space separation. If the separation of matter and antimatter is complete, we have $\overline{p^+ p^-} = 0$ for all p^+ and p^-. Despite the prevailing opinion, there are actually no firm data which prove the absence of antimatter even in our Galaxy, let alone in other galaxies. Among observations which are consistent with the possible existence of antimatter in the Galaxy, we should mention the observation of Clark et al. /10/ who discovered a gamma-ray flux with energies greater than 100 MeV from the plane of the Galaxy, and especially from its center. If the Galaxy has charge symmetry, matter—antimatter collisions leading to annihilation and emission of gamma quanta in pion decay are most probable in its center!

Bibliography

1. Hughes, V. W.—In: "Gravitation and Relativity", H.-Y. Chiu and W. F. Hoffman, editors.—N. Y., W. Benjamin. 1964.

2. Shull, C.G., K.W. Biliman, and F.A. Wedgwood.— Phys. Rev., 153:1415. 1967.
3. Zel'dovich, Ya.B. and I.D. Novikov. Relyativistskaya astrofizika (Relativistic Astrophysics).— Moskva, Izdatel'stvo "Nauka." 1967.
4. Sakharov, A.D.— ZhETF Letters. 1969. (In press).
5. Dorfan, D., J. Enstrom, D. Raymond, M. Schwartz, S. Wojcicki, D.N. Miller, and M. Paciotti.— Phys. Rev. Lett., 19:987. 1967.
6. Bennet, S., D. Nygren, H. Saal, J. Stenberger, and J. Sunderland.— Phys. Rev. Lett., 19:993. 1967.
7. Gurr, H.S., W.R. Kropp, F. Reines, and B. Meyer.— Phys. Rev., 158:1321. 1967.
8. Konstantinov, B.P., M.M. Bredov, A.I. Belyaevskii, and I.A. Sokolov.— *Kosmicheskie Issledovaniya*, 4:66. 1966.
9. Alfven, H.— Arkiv Fys., 23:187. 1963.
10. Clark, G.W., G. Garmier, and W.L. Kraushaar.— Astrophys. J., 153:L203. 1968.

GAMMA-RAY MEASUREMENTS FROM KOSMOS-135 SATELLITE WITH A VIEW TO POSSIBLE DETECTION OF ANTIMATTER METEOR STREAMS

B. P. Konstantinov, R. L. Aptekar', M. M. Bredov, S. V. Golenetskii, Yu. A. Gur'yan, V. N. Il'inskii, E. P. Mazets, and V. N. Panov

The possible existence of antimatter in the Universe has been repeatedly discussed in the literature in various forms over a number of years. A hypothesis of the antimatter constitution of comets and the associated meteor streams was advanced, among other things. Experiments intended to check this hypothesis were described in /1, 2/. These experiments measured the correlation between the intensity of the hard gamma quanta and neutrons at altitudes of 12 — 18 km in conjunction with the entry of individual meteors into the atmosphere. The results obtained seem to point in favor of the antimatter hypothesis.

To substantiate the hypothesis, we naturally need more than one independent piece of evidence. One of the possible ways of verifying the antimatter hypothesis is by observing the integrated fluxes of annihilation radiation which may arise in the upper atmosphere under the impact of antimeteors. Measurements of the intensity of the electron-positron annihilation radiation in the epochs of the Geminids, Ursids, and Quadrantids were carried out from KOSMOS-135 as part of the general study of the gamma-ray spectra and intensities in the Earth space.

EQUIPMENT AND MEASUREMENT TECHNIQUE

The KOSMOS-135 satellite was launched on 12 December 1966 into an orbit with the following parameters: apogee height 662 km, perigee height 259 km, orbit inclination 48.5°, orbital period 93.5 min. The satellite was equipped with a scintillation gamma spectrometer (Figure 1) and a 64-channel pulse amplitude analyzer which measured the spectra of gamma quanta between 0.3 and 2.5 MeV. The spectrometer also carried out integrated measurements of the gamma-ray counting rates at 0.4 — 0.6 MeV and 0.6 — 2.5 MeV and measured the counting rate of charged particles (electrons with $E_e \geqslant 1.5$ MeV and protons with $E_p \geqslant 27$ MeV).

The "phoswich" scintillation detector of the spectrometer consisted of a 40×40 mm NaI(Tl) crystal surrounded by a shielding plastic scintillator. The spectrometer also incorporated a pulse shape discriminator

circuit, which separated between gamma quanta and charged particles, a 64-channel pulse amplitude analyzer, a two-channel differential analyzer for measuring the counting rates of gamma quanta in a wide energy interval, and other electronic devices essential for automatic functioning of the equipment /3/. Detector shielding does not exceed 0.8 g/cm^2 Al in a solid angle equal to 80% of 4π. The spectrometer resolution is 13% for the 661 keV line.

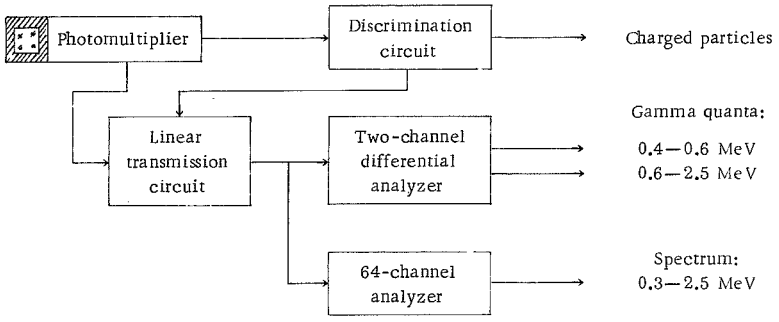

FIGURE 1. Block diagram of the gamma spectrometer.

Gamma spectrum measurements with the multichannel analyzer were carried out at fixed intervals of 10 min; the duration of each measurement was 2 min. The gamma quanta in wide energy intervals and the charged particles were counted every 2 min.

Figure 2 gives a specimen recording to the counting rate of charged particles (top) and 0.6 – 2.5 MeV gamma quanta (bottom) for successive orbital circuits of the satellite. The intensities of both charged particles and gamma rays depend on the geomagnetic latitude. The minimum counting rates correspond to the geomagnetic equator.

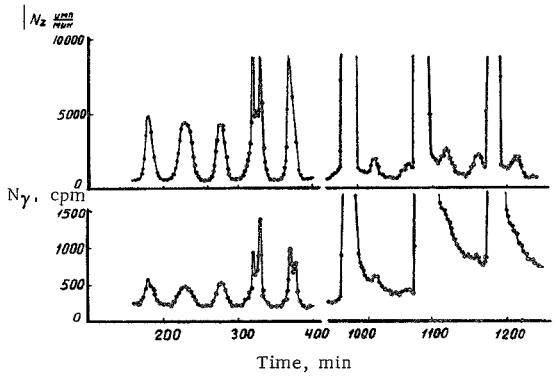

FIGURE 2. Variation of the counting rate of gamma quanta and charged particles with the satellite moving in the geomagnetic field.

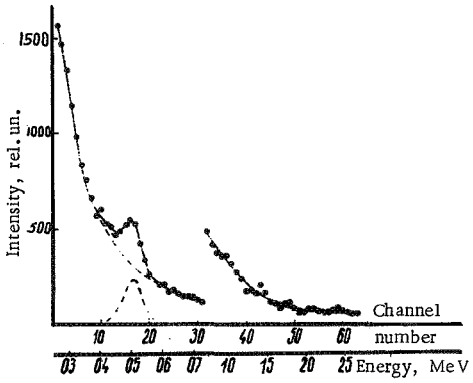

FIGURE 3. The total gamma spectrum from measurements of 13 Dec. 1966.

The counting rate increases at higher geomagnetic latitudes. Electron bremsstrahlung is picked up at latitudes where the satellite touches the radiation belts (320 and 350 min). At 1000, 1100, and 1200 min the satellite passed over the radiation zone in the area of the South Brazilian Anomaly. The detector and the satellite were then exposed to a high-intensity flux of protons.

The total spectrum of gamma quanta from measurements during the first day in orbit is shown in Figure 3. The strong line in the spectrum corresponding to channels 16 — 17 represents positron annihilation radiation.

BACKGROUND EFFECTS

The recording of weak gamma-ray fluxes in orbit is difficult because of the considerable secondary radiation background produced in the detector and satellite material by cosmic rays and protons from the radiation belts. Analysis of the experimental data shows that in low orbits, the main source of background radiation is provided by the activation of the scintillation detector material by the protons of the South Brazilian Anomaly. The nuclear reactions with the participation of the principal components of the NaI crystal (mainly iodine) produce a number of radioactive isotopes with half-lives ranging from a few minutes to several days. It is highly significant that, as these isotopes are produced in the detector, their radiation cannot be recorded in the form of discrete lines: the beta spectrum is inherently continuous. The results of measurements of the residual counting rate for 0.6 — 2.5 MeV gamma quanta after the emergence from the radiation zone are given in Figure 4. This is a typical decay curve of induced radioactivity and it may be used to derive the necessary corrections.

The experimental data (Figure 5) also show — and this is further confirmed by an analysis of the possible nuclear reactions with the material surrounding the detector — that the source of the background radiation comprises exclusively the short-lived components. These are the β^+-active isotopes C^{11} and F^{18} with half-lives of 21 and 110 min, respectively. The isotope C^{11} is produced by the (p, pn) reaction with the carbon of the plastic scintillator. F^{18} may be produced by the (p, pn) reaction from F^{19}, which is present in small quantities in the detector, and also by the reaction (p, 5p5n) from aluminum.

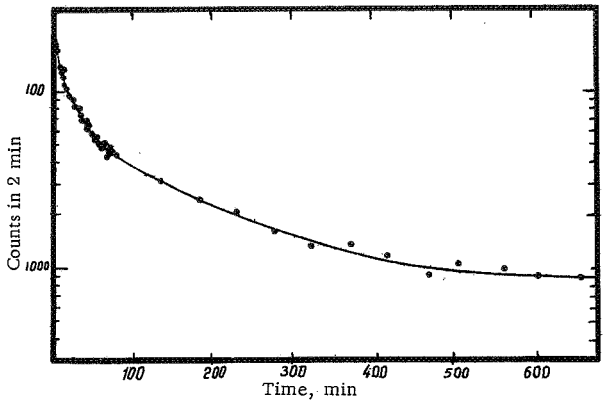

FIGURE 4. The excess counting rate of gamma quanta, associated with induced radioactivity.

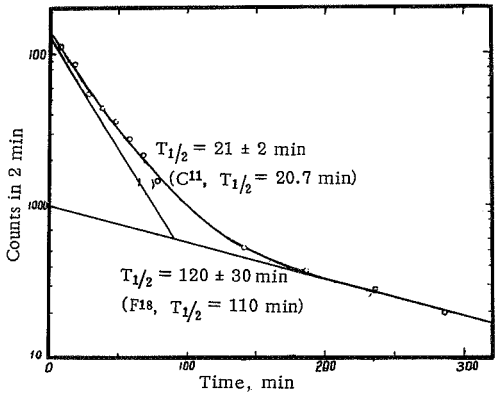

FIGURE 5. The decay of the induced β^+ activity.

The detailed data on the induced radioactivity may be applied to determine the background correction. In practice, however, in order to reduce the various errors in studying the intensity variations of the annihilation line, the measurements used for processing are those made 4 — 5 hrs after re-emergence from the radiation zone. The corrections for the short-lived background components to the line and to the entire spectrum are then quite negligible. The corrections for the long-lived background components to the integrated gamma-ray fluxes were determined daily from the observed variation of the counting rate near the geomagnetic equator. The corresponding curve for December 1966, January and February 1967 is shown in Figure 6 (curve 1). The variation of the correction in the initial period is associated with the buildup of the long-lived component, whereas its variation in the subsequent period is due to changes in the conditions of exposure in the anomaly zone because of a change in the flight altitude of the satellite in this area. Curve 2 gives in relative units the integrated

proton fluxes in the area of the anomaly, determined from the intensity of the short-lived components of the induced radioactivity. On the average, the corrections for the background of the long-lived gamma activity between 0.4 and 2.5 MeV reached about 50% near the geomagnetic equator and about 20% at high latitudes.

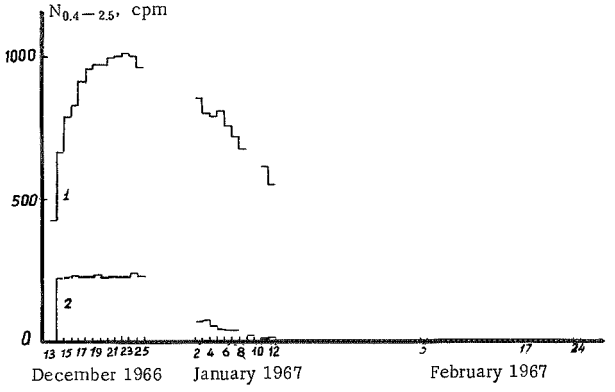

FIGURE 6. Gamma-ray counting rate near the geomagnetic equator (1) and the relative variation of the proton flux in the anomaly zone (2).

INTEGRATED MEASUREMENTS OF GAMMA QUANTA AND CHARGED PARTICLES

The flux measurements of charged particles and gamma quanta are shown in Figure 7. Curve 1 plots the charge-particle flux as a function of the threshold rigidity at altitudes of 250 — 350 km. Since the intensity of the primary cosmic-ray component is reliably known in the entire rigidity range, we can estimate the intensity of the Earth's albedo particles at the altitudes of the satellite orbit.

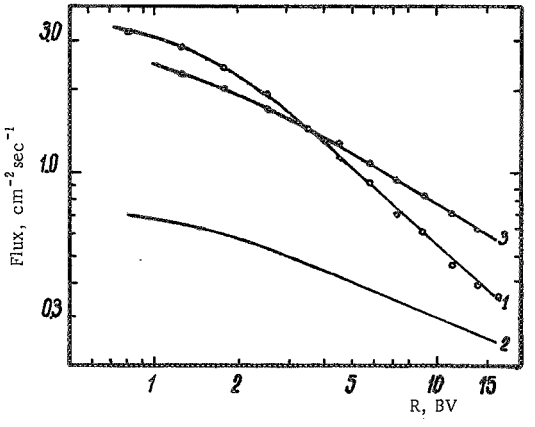

FIGURE 7. Fluxes of the charged component (1), albedo (2), and gamma quanta (3).

Curve 2 gives the albedo at the same altitudes as a function of rigidity. These particles include electrons with energies over 1.5 MeV and protons with energies over 27 MeV. Curve 3 plots the averaged dependence of the flux of 0.4 — 2.5 MeV gamma quanta (minus the flux of annihilation gamma quanta) on rigidity. Figure 8 shows the averaged dependence of the gamma-ray flux on the geomagnetic threshold rigidity on a linear scale for the observation period from 13 to 18 December 1966. The experimental points closely fit a smooth curve. The errors marked on the graph include statistical scatter, the scatter of measurements in the rigidity range over which averaging is performed, and the scatter of data over altitude. The subsequent gamma-ray measurements in December, January, and February are consistent with this dependence within the margin of error shown (3 — 7%).

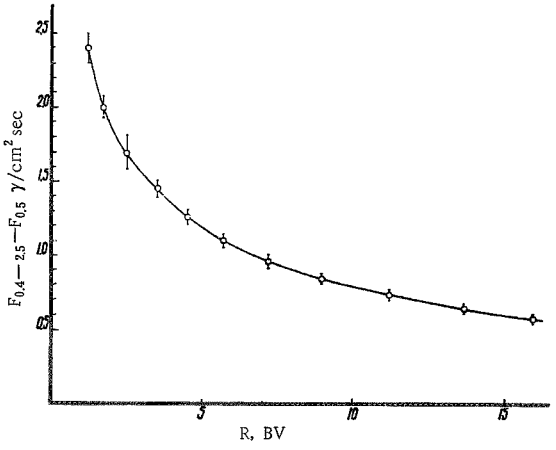

FIGURE 8. Gamma-ray flux between 0.4 and 2.5 MeV.

Using similar data on charged-particle intensities, we conclude that no statistically significant time variations were observed between 13 December 1966 and 25 February 1967 in the intensity of charged particles and 0.4 — 2.5 MeV gamma rays forming continuous spectra.

MEASUREMENTS OF THE FLUXES OF 0.511 MeV ANNIHILATION GAMMA RAYS

The experimental values of the flux of the 0.511 MeV annihilation gamma quanta also may be plotted as a function of the rigidity R. Figure 9 shows the measured results for 13 — 22 December 1966. On the average, the intensity of the annihilation radiation increases with decreasing rigidity. The scatter of points on the whole is consistent with the accuracy of

individual measurements, but in some measurements the deviations are markedly larger than the permissible statistical fluctuations.

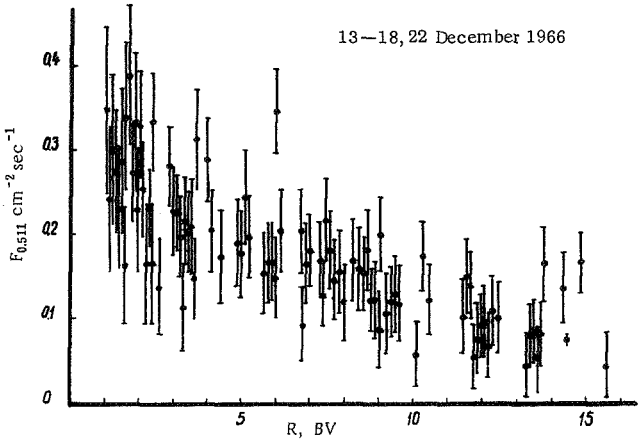

FIGURE 9. Gamma-ray fluxes at 0.511 MeV.

Balloon measurements of the gamma-ray intensity in the upper atmosphere were carried out in /4, 5/. The gamma-ray fluxes extrapolated to the boundary of the atmosphere are on the whole consistent with our data for the corresponding threshold rigidities R.

The statistical accuracy of the individual measurements of the annihilation radiation fluxes is on the average 20 — 30%. In principle, the error should be reduced by summing the spectra over a sufficient length of time. As we have noted, the spectra were measured at fixed intervals of 10 min. The observation conditions in the course of the orbital motion of the satellite are continuously variable, and close rigidities therefore occur seldom, even during long spans of time.

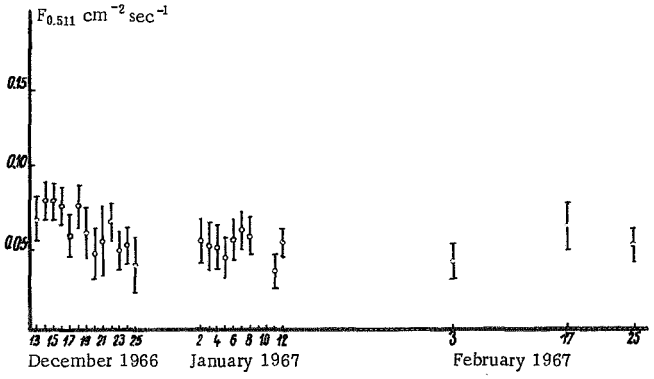

FIGURE 10. Daily average fluxes of 0.511 MeV gamma rays in the equatorial region.

The averaging is best carried out for the geomagnetic equator, where the cosmic-ray intensity and hence the intensity of the resulting secondary radiation varies relatively slowly. Figure 10 gives the daily average equatorial fluxes of the 0.511 MeV annihilation radiation for mean rigidity of about 14 GV. In each case, the averaging was carried out over 5 — 15 spectra.

The plot shows that the intensity of the annihilation gamma rays near the geomagnetic equator is apparently subjected to time variations which is a characteristic — from the standpoint of our hypothesis — trend. A more detailed analysis of the space and time distribution of the gamma-ray fluxes is indicated, using the data obtained for higher geomagnetic latitudes.

STATISTICAL ANALYSIS OF MEASUREMENT RESULTS

The discrete measurements of the gamma-ray spectra do not provide sufficient data for the straight-line approach, which calls for a comparison of spectra successively taken in the same parts of the geomagnetic fields. The total number of the individual spectra taken in the region of space free from strong fluxes of trapped radiation is about 600 for the period of December through February. These measurements are fairly uniformly distributed over the various geomagnetic coordinates and on the average they correspond to points with a considerable separation in space. Moreover, the statistical accuracy of the individual measurements is not high (20 — 30%). On the other hand, the dependence of the radiation intensity of the geomagnetic coordinates is fairly steep. Therefore methods employing integrated distributions and average values had to be used.

The above data show that the intensity of the annihilation radiation, like the intensity of gamma rays in a wide energy range, increases at higher geomagnetic latitudes. The relative variation of these intensities was compared for every day of observations. Figure 11 plots the intensity of the annihilation line as a function of the total gamma-ray intensity between 0.4 and 2.5 MeV on 14 December 1966. $N_{\gamma 0.511}$ on the plot is the counting rate of the 0.511 MeV gamma quanta, and $N_{\gamma\ 0.4-2.5}$ is the counting rate of the gamma quanta between 0.4 and 2.5 MeV. The lines were drawn by the least squares method. In view of the given statistical accuracy of the individual measurements and their volume, the regression curve contains two terms. This is a straight line passing very near the origin. Figure 11 shows the exact characteristics of the distribution of errors for the coefficients of the regression line and the small (40%) and the large (85%) confidence regions for the sought correlation.

A similar analysis was carried out for every day of observation, and the $N_{\gamma 0.511} = f(N_{\gamma 0.4-2.5})$ lines were found to fall into two groups: 1) the observations in the second ten-day period in December (13 — 18 and 22 December) and 2) the observations in the third ten-day period in December (19 — 21 and 23 — 25 December) and in January and February.

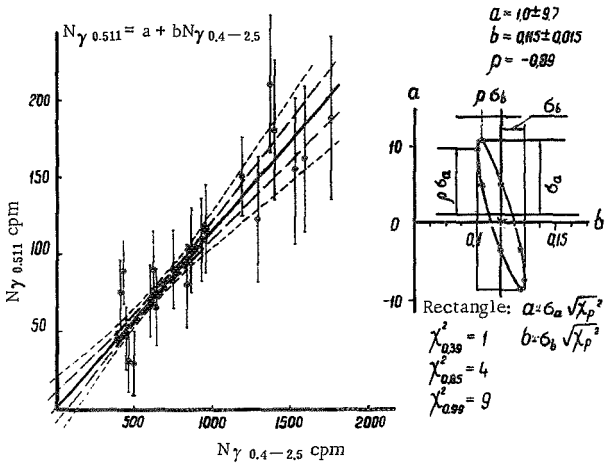

FIGURE 11. The dependence of the intensity of the annihilation line on the total intensity of the gamma spectrum between 0.2 and 2.5 MeV (measurements of 14 December 1966).

The averaged lines for the first and the second period of observation are shown in Figure 12. The dashed lines are the 99% confidence limits for the corresponding solid lines. Application of statistical tests to the comparison of regression lines shows that the observed difference between the two groups has virtually a 100% significance.

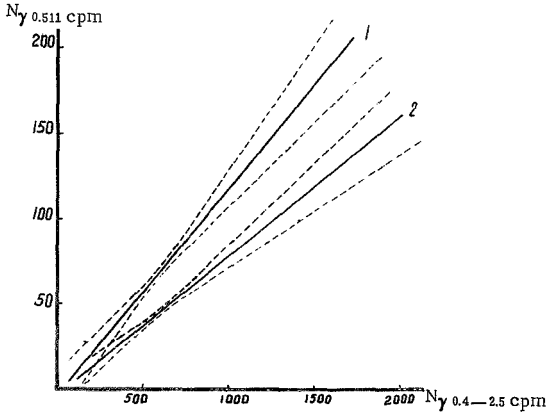

FIGURE 12. The dependence of the 0.511 MeV line on the total intensity of the gamma spectrum for two observation periods:

1) 13—18 and 21 December 1966; 2) 19—21, 23—25 December 1966, January and February 1967.

Let us now consider the distribution of the variable y, which corresponds to the ratio of the annihilation radiation in the entire gamma spectrum, $y = N_{\gamma 0\,511}/N_{\gamma 0\,4-2\,5}$. These distributions for the two observation periods are shown in Figure 13. Statistical samples containing approximately the same number of individual spectra n were used. Each group contains about 85 readings. Figure 13 gives the mean values and the errors for the two groups. We see that the mean fraction of the annihilation radiation in the gamma spectrum reaches 0.130 for the firts group and 0.083 for the second group. In the second group, there are four spectra which markedly deviate from the general distribution. These cases were mentioned before, when we noted that in isolated cases anomalously large annihilation fluxes are observed (see Figure 9).

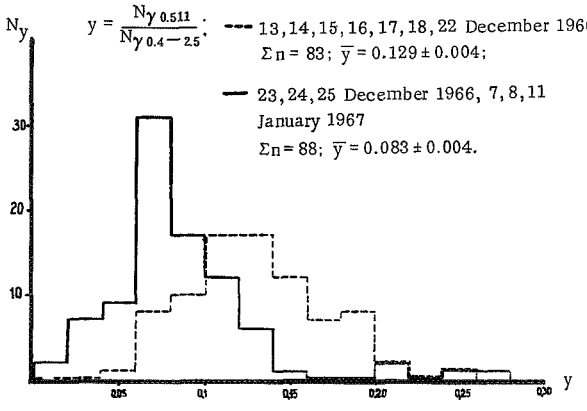

FIGURE 13. Distribution of the relative contribution of the annihilation gamma rays.

The distribution of y was investigated. Figure 14 shows the distribution of the experimental cumulative frequency in coordinates corresponding to the normal distribution of the probability P. For the first group, the experimental points closely follow a straight line, which implies that the distribution is indeed normal. For the second group, in the region of large y, the experimental dependence markedly deviates from a straight line. This deviation is traceable to the four anomalous spectra mentioned above. When they are eliminated from the sample, all the experimental points are seen to follow closely a straight line. This fact signifies that the observation of anomalously large fluxes of 0.511 MeV gamma rays at intervals of less than 10 min is by no means a result of statistical fluctuations.

Figure 14 shows some estimates of the distribution parameters. The observed frequency of occurrence of spectra with $y \geqslant 0.24$, equal to $^2/_{88}$, is a factor of 10^3 higher than the corresponding probability. We conclude that in the Earth space there are cases when the intensity of the annihilation radiation exceeds for a brief time the normal level by as much as a factor of 3—4, whereas the intensity in other spectral regions remains unaffected.

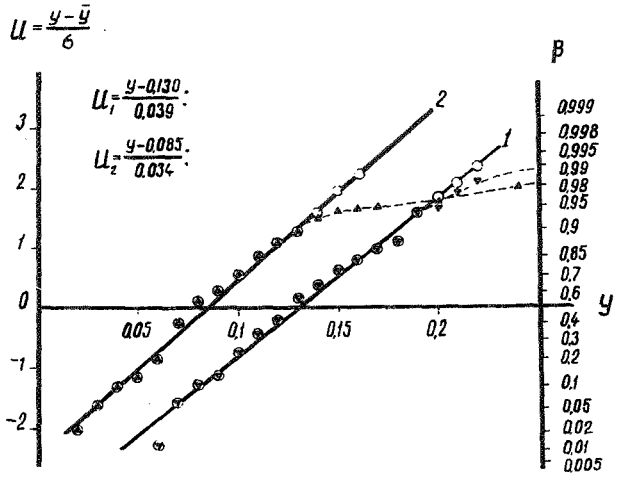

FIGURE 14. A check of the normal distribution.

More accurate estimates of the distribution parameters — the mean, the error of a single measurement, and the error of the mean — are given below:

	n	$\bar{y}$	σ	$\sigma/\sqrt{n}$
Group I	83	0.129	0.038	0.004
Group II	88	0.083	0.040	0.004

Comparison of these figures shows that the intensity of the annihilation radiation fluxes for the first group of observations if a factor of 1.5 higher than for the second group of observations, and the difference between the two groups is greater than 7.5 standard errors. Application of Student's test shows that the observed difference is virtually 100% significant. This conclusion bears out the result obtained from a comparison of the regression lines.

TIME VARIATION OF THE INTENSITY OF THE ANNIHILATION GAMMA RAYS

One day was chosen as the averaging unit for investigating the time variation of the gamma-ray intensity. The intensity of the annihilation line in the overall spectrum summed over one day of observations can be determined with adequate statistical accuracy. However, the relative value $y = \bar{N}_{\gamma\,0.511}/\bar{N}_{\gamma\,0.4-2.5}$ may characterize observations irrespective of geomagnetic coordinates, the number of spectra in the sample, and the duration of measurements. Special analysis has established that the ratio y determined from the overall spectrum is consistent with the figure obtained from the regression line for the corresponding days. This result confirms the validity of our summation and averaging procedure.

The time variation of the daily average fluxes of the annihilation gamma rays is plotted in Figure 15. The figure shows that, in accordance with the preceding analysis, the annihilation fluxes for the first group of observations (13 — 16 and 22 December 1966) are 1.5 times higher than for the other observations. The data reproduced in Figure 15 include the measurements near the geomagnetic equator (see Figure 10). Note that by extending the analysis to higher geomagnetic latitudes, we confirmed and increased the reliability of the observed time dependence of the intensity of the annihilation gamma rays.

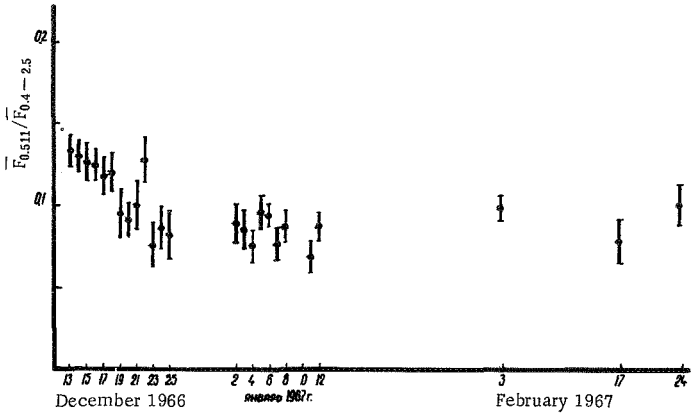

FIGURE 15. The time variation of the relative intensity of the annihilation gamma rays.

We have so far mainly spoken in terms of the relative fraction of the annihilation radiation in the overall gamma-ray spectrum, rather than in terms of the absolute intensities. This approach served a useful intermediate purpose, since the variation of the gamma-ray intensity as a function of the geomagnetic coordinates or as a function of the rigidity R is not linear. In view of the low statistical accuracy of the individual measurements and the limited volume of observations, manipulation of the absolute fluxes would lead to unnecessary complications. However, once the effect has been reliably established in terms of the relative fluxes and the principal features of the time variation have been identified, we may return to the absolute gamma-ray fluxes.

Figure 16 shows the distribution of the annihilation line intensity as a function of the cutoff rigidity R on the Earth's surface for observations in January 1967. The experimental data are based on an analysis of many tens and hundreds of spectra. The relevant rigidity range is divided into 11 intervals. The figure gives the average intensities of the annihilation line for all spectra corresponding to a given interval.

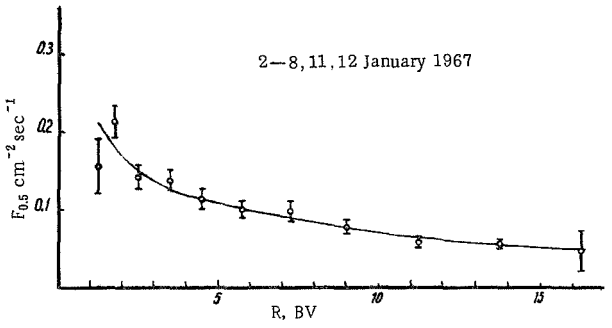

FIGURE 16. The intensity of the 0.511 MeV gamma rays in January 1967.

Similar results for observations from 13 to 18 December 1966 are shown in Figure 17. For comparison, the same plot gives the dependence (dashed line) of the intensity on rigidity for measurements in January 1967. We see that the absolute gamma-ray fluxes at 0.511 MeV for 13 — 18 December 1966 are on the average 1.5 — 2 times higher than the values obtained for 2 — 8 and 11 — 12 January 1967. The statistical significance of the observed differences is fairly high. The average dependences obtained in fact represent the 1.2 regression lines for the first and the second observation periods recalculated for new coordinates (see Figure 12).

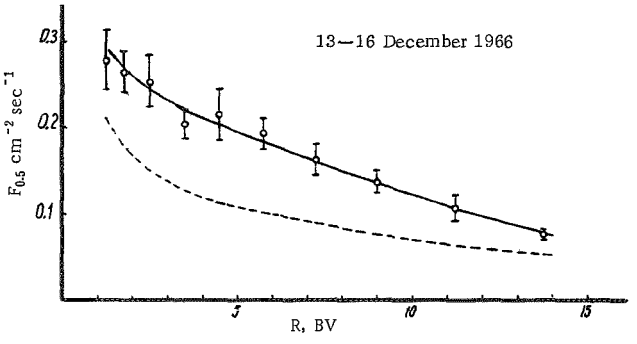

FIGURE 17. The intensity of the 0.511 MeV gamma rays in mid-December 1967.

Unlike the intensity of the gamma-ray line, the intensity of the remaining part of the spectrum from 0.4 to 2.5 MeV does not reveal significant time variation. Figure 18 shows the gamma-ray flux at 0.4 — 2.5 MeV minus the line flux as a function of the threshold geomagnetic rigidity for three observation periods: 13 — 18 December 1966, 19 — 25 December 1966, 2 — 8 and 11 — 12 January 1967.

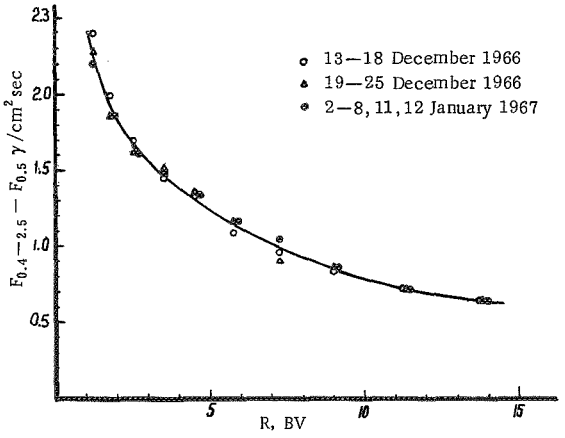

FIGURE 18. The gamma-ray intensity between 0.4 and 2.5 MeV for three observation periods.

The different sets of data closely coincide. No significant time variation in the intensity of charged particles F_Z is observed, either (Figure 19). Note that the scatter of points around the mean curve in the region of low rigidities is a reflection of the variation of the charged-particle intensity with altitude, since the high and the low altitudes are represented in different proportions for different measurement periods. Analogous curves plotted for measurements in smaller altitude ranges reveal a substantially smaller scatter.

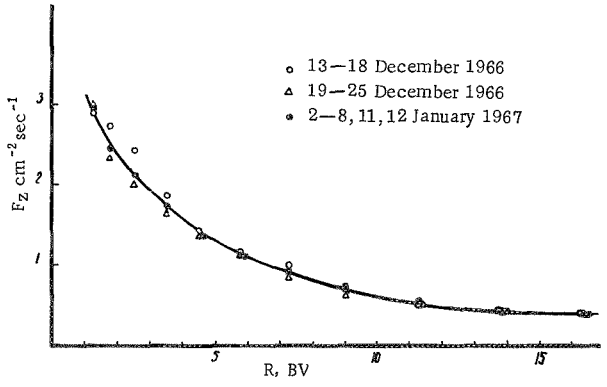

FIGURE 19. Charged-particle intensity for three observation periods.

We have thus established that the intensity of the electron—positron annihilation radiation displays a definite variation in time. The effect reaches about 50—70%. It does not extend to gamma rays of other energies between 0.4 and 2.5 MeV, nor to the fluxes of charged particles

(electrons with $E_e \geqslant 1.5$ MeV and protons with $E_p \geqslant 27$ MeV). The increased line intensity was observed between 13 and 18 December and on 22 December 1966. Figure 15 shows that the intensity of the annihilation radiation according to measurements on various days in February 1967 corresponds to the mean level at the end of December 1966 and in January 1967. Various sources of biased errors were analyzed and all proved to be insignificant.

ANALYSIS OF SOLAR AND METEOR ACTIVITY DURING THE OBSERVATION PERIOD

It is interesting to compare the gamma-ray observation results with observations of solar activity, geomagnetic activity, and cosmic rays in the relevant period. Figure 20 plots the sunspot number R_Z, the planetary geomagnetic index A_p, and the readings of neutron monitors in Apatity and in Moscow for December 1966 and January 1967 /6/. We see from the graphs that the observation period was characterized by moderate solar activity, with numerous active regions moving across the solar disk, geomagnetic field disturbances and geomagnetic storms on individual occasions, and instances of a Forbush effect in cosmic rays. It is clear that the periods between 10 and 20 December 1966 and between 1 and 15 January 1967, which markedly differ with regard to the observed intensity of the 0.511 MeV gamma-ray intensity, are characterized by virtually the same solar and geomagnetic activity. Thus, we can hardly speak of any direct correlation between the observed effect and solar activity. The enhanced intensity of the annihilation radiation is observed at all the geomagnetic latitudes, and yet it is not accompanied by changes in the recorded flux of charged particles and is slowly variable in time. As we have seen, the sudden burst of the annihilation line in individual spectra, its intensity rising to 3—4 times the mean level, is an exceptional event (see Figure 14).

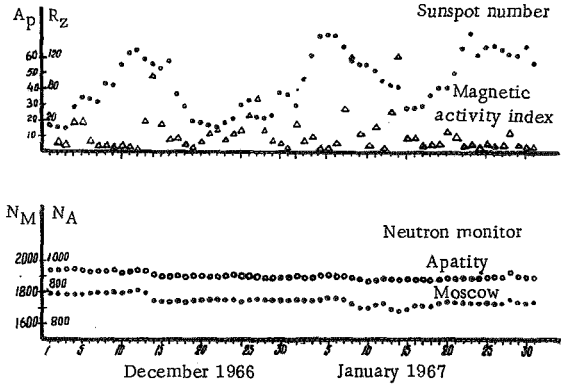

FIGURE 20. Characteristics of solar and geomagnetic activity.

The characteristic features that we have described apparently rule out any possibility of a relation between the observed effect and the injection of trapped radiation into the atmosphere, since the radiation injection is much stronger at high geomagnetic latitudes, and the flux of charged particles varies by several orders of magnitude /7/.

Let us now consider the distribution of meteor activity in the relevant period. In December and January, the Earth crosses the orbits of three annual meteor streams. The maxima according to optical and radar data are observed for Geminids on 13—14 December, for Ursids on 22 December, and for Quadrantids on 2—3 January. The last two streams are active only for a brief period of time. The main Ursid maximum is observed for one day, and that of Quadrantids for a few hours only /8/. The characteristics of these streams in winter 1966/67 did not differ significantly from the many-year averages.

Figures 10 and 15 show that the increase in the intensity of the annihilation radiation coincides with the activity of the Geminids and Ursids, but is not observed for the epoch of the Quadrantids. If we start with the assumption of the antimatter constitution of the meteor streams, the magnitude of the observed effect can be accounted for if 5—10 mg of antimatter are injected into the Earth's atmosphere daily. Note that the data of /1/ also enable us to estimate the range of possible values of the antimatter flux. This estimate gives 100—1 mg of antimatter per day, which is consistent to orders of magnitude with the above figure. In our opinion, the results of the KOSMOS measurements improve the chances of the antimatter hypothesis and require further detailed experimental observations.

Bibliography

1. Konstantinov, B.P., M.M. Bredov, A.I. Belyaevskii, and I.A. Sokolov.— Kosmicheskie Issledovaniya, 4:66. 1966.
2. Konstantinov, B.P., M.M. Bredov, L.P. Pakhomov, V.K. Bocharkin, L.F. Alekseev, N.I. Orlov, and V.I. Chesnokov.— ZhTF, 37:743. 1967.
3. Golenetskii, S.V., V.N. Il'inskii, R.L. Aptekar', Yu.A. Gur'yan, E.P. Mazets, V.N. Panov, T.V.Kharitonova.— PTE. 1969. (In press); Golenetskii, S.V., V.N. Il'inskii, R.L. Aptekar', Yu.A. Gur'yan, E.P. Mazets, V.N. Panov, and T.V. Kharitonova. Present Collection, Part 2, p. 178.
4. Peterson, L.E.— J. Geophys. Res., 68:979. 1963.
5. Chupp, E.L., A.A. Sarkady, and H.P. Gilman.— Planet Space Science, 15:881. 1967.
6. Kosmicheskie Dannye.— Mesyachnye Obzory, No.12(130), December 1966 and No.1(131), January 1967. Moskva, Izdatel'stvo "Nauka." 1967; Lincoln, J. Virginia—J. Geophys. Res., 72:2467. 1967; Lincoln, J. Virginia—J. Geophys. Res., 72:2984. 1967.
7. O'Brien, B. J.—J. Geophys. Res., 69:1964. 1964.
8. Lovell, B.—Meteor Astronomy.—Oxford, Clarendon Press. 1954.

DETERMINATION OF THE ANTIPROTON FLUX IN PRIMARY COSMIC RAYS

E. A. Bogomolov, V. K. Karakad'ko, N. D. Lubyanaya, V. A. Romanov, M. G. Totubalina, and M. A. Yamshchikov

Positively charged particles constitute the main component of the primary cosmic rays. Theoretical estimates made under the assumption that the only source of antiprotons in cosmic rays are nuclear reactions of the cosmic-ray particles with the interstellar gas set an upper limit of $\tilde{p}/p \sim 10^{-3} - 10^{-7}$ for the antiproton-to-proton flux ratio /1 – 5/. Experimental estimates of the fraction of antiprotons in primary cosmic rays were mainly obtained from measurements of east – west asymmetry /6 – 15/. Most of these measurements were carried out in the early 1950s. Recent reports describe results obtained by other methods /16 – 18/.

Apparao /16/ searched for antiproton tracks in emulsions exposed in Churchill, Canada, at residual pressures of 4.2 g/cm^2. For energies between 100 and 150 MeV, Apparao obtained an upper limit of $\tilde{p}/p \sim 3 \cdot 10^{-4}$. Brooke and Wolfendall /17/ obtained $\tilde{p}/p \sim 5 \cdot 10^{-2}$ for particles with energies around 1000 BeV from measurements of the charge composition of particles with energies 30 BeV at sea level. Another estimate of the upper limit of the relative content of antiprotons can be derived from the results of /18/, which give the electron spectrum in the range of 0.50 – 8.4 BV measured from a balloon with a telescope consisting of spark chambers and a deflecting magnet. The angular distribution of particles which passed through the magnet gap and did not interact in the shower spark chamber gives an upper limit of $\tilde{p}/p \sim 4 \cdot 10^{-2}$ for energies between 2 and 5 BeV.

Measurements of the east – west asymmetry between 3 and 20 BeV were carried out from balloons and rockets using Geiger counter telescopes /6 – 13/ and telescopes of directional Cherenkov counters /14, 15/. The experimental asymmetries were compared with the figures computed under the assumption that the primary cosmic rays consist of protons only and the geomagnetic field is a dipole field. The experimental asymmetry was invariably less than the theoretical figure. This divergence, according to the estimates of /1, 19/ may be accounted for by the presence of about 10% of antiprotons in cosmic rays. (The antiproton spectrum is assumed to be similar to the spectrum of protons.) It seems that the sum total of the experimental data does not rule out a substantial content of antiprotons in primary cosmic rays.

We tried to establish a better estimate for the upper limit of the ratio $\tilde{p}/p$ obtained in east – west asymmetry experiments. We planned to measure

with a balloon the differential spectra of singly charged particles in the east and west directions in the region of the geomagnetic thresholds with suitable correction for the albedo and the particles produced in the residual atmosphere. On the other hand, in order to improve the theoretically computed asymmetry, we meant to determine the geomagnetic thresholds with allowance for the non-dipole terms in the geomagnetic field expression.

A telescope consisting of two scintillation counters, a directional Cherenkov counter with a Plexiglas radiator, and a gas Cherenkov counter was built /20, 21/. The directional Cherenkov counter eliminated the albedo particles and isolated the singly charged particles. The gas Cherenkov counters working in the anticoincidence mode generated the particle spectrum at energies between 1.7 and 5 BeV (for protons), i.e., in the region of middle-latitude geomagnetic thresholds. The upper energy threshold of the instrument was adjusted in flight by letting out the gas in portions from the gas counters. The spectrum of the secondary particles between 0.6 and 1.7 BeV was determined by means of pulse amplitude analysis using the directional Cherenkov counter. The measurements were carried out at a zenith angle of 60°. The telescope was alternately pointed east and west. The instrument was oriented relative to the geomagnetic field. The figure shows the spectra of singly charged particles obtained in August 1967 at geomagnetic latitude $\lambda_m = 47°$ and residual pressure of about 10 g/cm^2 (from the results of four flights). The background of secondary particles produced in the residual atmosphere was computed as follows. The background spectrum between 0.6 and 1.9 BeV was determined from the data collected over the flight section with 1.9 BeV gas counter threshold and the analysis of the directional counter pulses. The resulting spectrum was then extrapolated to high energies. Absorption and ionization losses of the primary particles in the residual atmosphere were taken into consideration. These two corrections are significant only for the derivation of the absolute particle fluxes. They are not particularly important for the determination of the relative fluxes $\tilde{p}/p$, since their contribution is virtually identical for protons and antiprotons.

The dashed lines in the figure represent the proton spectra generated by a computer. The penetrability of the region of geomagnetic thresholds was determined by numerical integration of the equations of particle motion in the geomagnetic field /22/. The Earth's magnetic field was represented by six spherical harmonics, and the Gaussian coefficients g_n^m and h_n^m for the epoch 1960 were used /23/. The theoretical spectrum was computed using $\gamma = 2.3$ for the index of the differential energy spectrum of the primary protons /24/.

There are significant differences between the experimental spectra and the spectra computed for protons alone. The computation of penetrability with the coefficients g_n^m and h_n^m for 1967 /25/ has shown that this parameter hardly changed between 1960 and 1967. For energies between 1.9 and 2.6 BeV, the ratio $\tilde{p}/p$ is equal to $N_{east}(1.9 - 2.6\ \text{BeV})/N_{west}(1.9 - 2.6\ \text{BeV})$. The small fraction of protons entering this interval from the east can be subtracted by using its computed value. Averaging over the four flights gives $\tilde{p}/p = 0.24 \pm 0.05$.

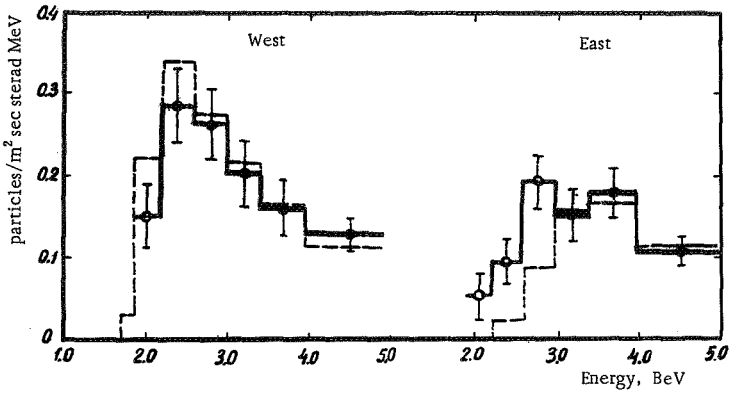

Spectra of singly charged particles in east and west directions at geomagnetic latitude $\lambda_m = 47°$. Zenith angle 60°.

Solid line, experimental; dashed line, computed.

The observed differences in the spectra cannot be attributed to any short-lived magnetospheric disturbances, since the measurements were continued for one month and the ratio $\tilde{p}/p$ was constant for all flights within the margin of error. Moreover, comparison of the proton intensities at E > 30 MeV measured at the same time by VENUS-4 /26/ beyond the limits of the magnetosphere with the data of Earth measurements /27/ reveals a total absence of strong magnetospheric disturbances in the relevant period.

There is a possibility, of course, still undecided, that the differences in spectra are associated with geomagnetic field irregularities (deformation of the magnetosphere by solar wind, ring current, etc.). Further experiments should be carried out in order to establish whether the relative content of antiprotons in the primary cosmic rays actually exceeds the theoretically expected figure. With regard to measurements of the east–west asymmetry, the computation of geomagnetic effects clearly should be based on all the currently available data concerning the Earth's magnetosphere and low-latitude experiments should be performed in the nearest future.

Bibliography

1. Fradkin, M.I.– ZhETF, 29:147. 1955.
2. Milford, S.N. and S. Rosen.– Nature, 205:582. 1965.
3. Rosen, S.– Phys. Rev., 158:1227. 1967.
4. Shen, C.S. and G.B. Berkley.– Phys. Rev., 171:1344. 1968.
5. Wayland, J.R. and T. Bowen.– Phys. Rev., 171:1376. 1968.
6. Johnson, T. and J. Barry.– Phys. Rev., 56:219. 1939.
7. Vernov, S.N., N.L. Grigorov, N.A. Dobrotin, S.I. Sokolov, F.D. Savin, and A.I. Kurakin.– DAN SSSR, 68:253. 1949.
8. Vernov, S.N., A.M. Kulikov, and A.N. Charakhch'yan.– DAN SSSR, 85:525. 1952.

9. Winckler, J.R., T. Stix, K. Dwight, and R. Sabin.— Phys. Rev., 79:656. 1950.
10. Winckler, J.R.— Phys. Rev., 85:1054. 1952.
11. Allen, J.A. van and A.V. Gangnes.— Phys. Rev., 79:51. 1950.
12. Singer, S.F.— Phys. Rev., 80:47. 1950.
13. Shafer, Yu.G., V.D. Sokolov, N.G. Skryabin, S.K. Dergeim, and R.B. Selimzibarov.— Kosmicheskie Issledovaniya, 2:933. 1964.
14. Winckler, J.R. and K. Anderson.— Phys. Rev., 93:596. 1954.
15. Agrawal, P.C., S.V. Damle, G.S. Gokhale, C. Joseph, P.K. Kunte, M.G.K. Menon, and R. Sunderrajam.— Proc. Ninth Intern. Conf. on Cosmic Rays, 1:457. 1965.
16. Apparao, M.V.K.— Nature, 215:727. 1967.
17. Brooke, G. and A.W. Wolfendall.— Nature, 202:480. 1964.
18. Fanselow, I.L.— Astrophys. J., 152:783. 1968.
19. Bhowmic, B.— Phys. Rev., 89:327. 1953.
20. Bogomolov, E.A., V.K. Karakad'ko, N.D. Lubyanaya, V.A. Romanov, M.G. Totubalina, and M.A. Jamshchikov.— In: "Kosmicheskie luchi," No. 10. 1969.
21. Bogomolov, E.A., V.K. Karakadko, N.D. Lubjanaja, V.A. Romanov, M.G. Totubalina, and M.A. Jamshchikov.— Can. J. Phys., 46:S805. 1968.
22. Belous, L.G., E.A. Bogomolov, V.K. Karakad'ko, N.D. Lubyanaya, V.A. Romanov, V.S. Smirnov, M.G. Totubalina, and M.A. Jamshchikov. — Materialy Vsesoyuznoi Konferentsii po fizike Kosmicheskikh luchei v Tashkente. 1968. (In press).
23. Adam, N.V., N.I. Osipov, L.O. Tyurlina, and A.P. Shlyakhtina.— Geomagnetizm i Aeronomiya, 4:1130. 1964.
24. Freier, P.S. and C. J. Waddington. — J. Geophys. Res., 73:4261. 1968.
25. IGRF coefficients adopted by the Third IAGA Committee. Washington. 1968.
26. Vernov, S.N., A.E. Chudakov, P.V. Vakulov, E.V. Gorchakov, N.N. Kontor, S.N. Kuznetsov, Yu.I. Logachev, G.P. Lyubimov, A.G. Nikolaev, N.V. Pereslegina, and B.A. Tverskoi.— Trudy V Vsesoyuznoi ezhegodnoi zimnei shkoly po kosmofizike, Apatity, Izd. Kol'skogo filiala AN SSSR, No. 5. 1968.
27. Kosmicheskie Dannye (Space Data).— Moskva, Izdatel'stvo "Nauka." 1967.

GEOCHEMICAL FEATURES OF THE COMPOSITION OF THE UNIVERSE AND THE ORIGIN OF ATOMIC NUCLEI

V. V. Cherdyntsev

REGULAR FEATURES IN THE ABUNDANCE OF ATOMIC NUCLEI

The principal features in the abundance of isotopes and elements are known for a number of systems (Earth's crust, meteorites, the outer envelope of the Sun and of most main-sequence stars; interstellar matter and cosmic rays have been studied to a lesser extent). These features /1/ correspond to the "standard" composition of matter in the Universe, irrespective of the particular astrophysical characteristics and the age of the various objects.

1. The curve of the nuclide abundance q as a function of the mass number A, in the form log q = f(A), falls off rapidly in the region of light nuclei, dropping by about 10 orders of magnitude from hydrogen (Z = 1) to gallium (Z = 30). As A increases further, the curve levels out, but there is a minimum in the region of medium mass numbers (A = 140 — 160). This minimum is particularly distinct for the isotopes of one element which have the same parity. The heaviest nuclides exceed the minimum level approximately by one order of magnitude.

2. The abundance of even isotopes (q_S) is higher than the abundance of odd isotopes (q_A) — the Oddo — Harkins rule.

3. The ratio q_S/q_A is a function of the mass number. This ratio reaches 500 for oxygen isotopes, is equal on the average to 10 for the light nuclides, and drops approximately to 2 for the heavy nuclides.

4. Among the even isobars, the low-charge isobars (q_{Z-2}) are more abundant than the high-charge isobars (q_Z, q_{Z+2} — the protected isobars). There is a distinct dependence on the position of the energy levels of the isobars, but even for virtually identical energy states the abundance of the low-charge isobars is higher by a certain factor.

5. The ratio q_{Z-2}/q_Z markedly increases with the increase in the atomic number of the even isobars and varies by two orders of magnitude on passing from the light isobars ($Z < 30$) to the last isobars of the stable elements.

6. The abundance of the low-charge odd isobars is also higher than the abundance of the corresponding high-charge isobars, although among the known cases of radioactive transitions between these isobars, it is the low-charge isobar that is invariably unstable.

The above regular features of abundance cannot be explained by the energy properties of the atomic nuclei. The curve log q = f(A) does not fit the binding energy curve. The energy difference between the even and the odd isotopes diminishes for the heavy nuclides, and yet a distinct prevalence of the even isotopes is observed in this range. Even isobars with approximately identical energy levels show a distinct excess of the low-charge states. The ligher states of the odd isobars are more abundant, although many of them are unstable, i.e., occupy higher energy states.

7. The deviation of the curve log q = f(A) from the level trend is in general considerable, but there are regions of particularly high abundance of nuclides, corresponding to filled neutron shells (A − Z = 50, 82, 126). The high-abundance isotopes Sr^{88} and Zr^{90} occur for A − Z = 50, and Ba^{138} and Ce^{140} correspond to A − Z = 82. A distinct iron peak is observed. The cosmic abundance of Fe^{56} and Ni^{58} is approximately the same as that of Ar^{36} and Ca^{40}, whereas the abundance of the intermediate even nuclei is 1 − 2 orders of magnitude lower. A reverse anomaly — a very low abundance of Sc^{45} — is observed in all the known systems in the Universe /1/. Particularly low abundance is characteristic of high-spin nuclides, whether odd (e.g., Sc^{45}, j = 7/2) or particularly even (K^{40}, V^{50}, Lu^{176}, etc.).

8. There are secondary deviations of the nuclide abundance curve, namely the gap in the region of the light metals (Z = 3 − 5) which burn in the thermonuclear reactions in the stellar interior and the gaps beyond the region of isotopes which are not subject to spontaneous decay (Z > 83), where only the regions with the isotopes Z = 90, 92, and probably also Z ≈ 108 stand out as isolated stability islands.

The isotopic ratio of lithium and boron is markedly different from that of other elements at the beginning of the Periodic Table (the odd and the heavy isotopes prevail). This probably points to a different mechanism of formation of the isotopic composition of these elements.

The above features cover the entire range of atomic nuclei, and no significant gaps or discontinuities are observed. This suggests that nucleogenesis took place in a single system and that the conditions of nucleogenesis did not markedly differ between different parts of the Universe. It is also significant that this primary process produced all the atomic nuclei up to the heaviest radioactive nuclides, unlike the secondary processes (thermonuclear reactions, nuclear reactions triggered by cosmic rays) which are known to be highly selective.

THE DEVELOPMENT OF THE CONCEPTS OF NUCLEOGENESIS

Pokrovskii /2/ was the first to show that the common features governing the chemical composition of virtually all the isotopes in nature are of necessity an indication of the fact that all the atomic nuclei were produced in a medium close to the state of thermodynamic equilibrium. The density of such a system, as is readily seen, should be subnuclear, and its temperature should be close to the nuclear temperature (kT = n MeV). The particular isotopic ratio which developed in the system was fixed to perpetuity because the system apparently "froze," i.e., rapidly moved to the conditions

of relatively low densities and energies commonly characteristic of the Universe as a whole. Nucleogenesis, according to Pokrovskii, thus occurred during the explosion of an ultradense star and, according to the modern terminology, it can be classified as an r-process. The main shortcoming of this theory was that a thermodynamic equilibrium of atomic nuclei for any choice of system parameters led to an abundance curve which greatly differed from the real curve: the theoretical abundance of the heavy elements worked out to be much lower than the actual abundance. Other authors (Weizsäcker developed the most detailed model /3/) failed to overcome this "heavy nuclei difficulty." The attempts to describe the nucleogenesis of the light and the heavy isotopes as two separate processes /4/ did not constitute a significant advance. So far no break or seam has been detected on the abundance curve enabling to separate between the groups of nuclei which allegedly formed under different conditions.

The main difficulty encountered in nucleogenesis is the synthesis of the heavy nuclei from A = 209 (Bi) to A = 232 (Th), which have very short half-lives. Following the discovery of the far transuranide with the probable values $Z \approx 108$ and $A \approx 290$, we were faced with the need of bridging over an even wider range of short-lived isotopes.

In the mid-1930s, Baade and Zwicky /5/ discovered the supernovae and advanced the suggestion — not easily accepted by other astrophysicists — that the supernova explosions produced a neutron phase. In the same period, theoretical physicists, and primarily S. Chandrasekhar /6/, L. Landau /7/, and H. Bethe /8/, proved the possible existence of ultradense stars and established the relative enrichment of neutrons in the course of evolution of stellar matter. In 1940, the synthesis of atomic nuclei in a medium consisting almost entirely of neutrons and maintained in thermodynamic equilibrium was described in /9/. These conditions fitted the conditions of supernova eruptions. The neutron fragments undergo beta decay and produce the common atomic nuclei. Among the even isobars, the low-charge isobars are preferably formed. The high-charge even isobars are produced by secondary reactions in the post-explosion stage under conditions far from thermodynamic equilibrium. This conception led to a quantitative description of the various features of the abundance curve and explained the dependence of the abundance on parity. It also provided a qualitative explanation of the observed abundance of the isobars. It was shown that the evolution of stars with masses below some critical value is terminated with the formation of neutron stars — the "vacuum cleaners" of the Universe which actively trap all disperse matter in their ultrastrong gravitational field. These theoretical conceptions have meanwhile received partial experimental corroboration in astrophysics.

The range of pressure-unstable atomic nuclei extends to $A = (1-3) \cdot 10^4$ /9/. The recent computations of Swiatecki /10/ give an upper limit of $A = 1.3 \cdot 10^4$. If such ultraheavy atomic nuclei actually exist in nature, they are probably concentrated in stellar interiors. Their presence in cosmic rays following ejection into space during supernova explosions has not been proved so far.

A more detailed description of nucleogenesis was advanced by G. and E. Burbidge, Fowler, Hoyle, and Christy in 1956–1957 /11, 12/. In

addition to nuclide formation in an exploding neutron system (a fast r-process according to their terminology), they also considered a number of slow processes initiated by neutrons and protons in stars in the late stages of their evolution, and also in the diffuse matter in space.

The bulk of the evidence seems to indicate at this stage that the main process responsible for the formation of the "standard" chemical composition which constitutes the basis of the observed composition of matter in the solar system and in cosmic rays is the extremely fast process of nucleogenesis in a neutron medium. The fine features of the abundance of the atomic nuclei are very difficult to compute, since the energy parameters of the initial neutron fragments cannot be accurately extrapolated. It is clear, however, that the primary nuclei of these neutron fragments are radically different from the stable atomic nuclei of the existing systems. This is obvious from the very ease with which they bridge over the gap at $A = 210 - 230$ or $250 - 290$, where the ordinary atomic nuclei are highly unstable. In addition to "standard"-composition matter, the Universe also contains stars in the late stages of evolution where nuclear processes with the participation of alpha particles and neutrons, as well as protons, actively take place. The character of these slow processes was first discussed in /11, 12/ Stars are known where the proton energy source have been depleted to such an extent that their spectra show no hydrogen lines, and the lines of helium, carbon, and neon predominate. Certain groups of stars are enriched in C^{13}, the C^{12}/C^{13} ratio reaching $3 - 4$, i.e., one magnitude higher than the Earth enrichment of this isotope. Various types of stars in the late stages of evolution reveal a distinct enrichment of the heavy elements of the lanthanide group, zirconium, and lead. Of the greatest interest are the S stars, whose spectrum shows technetium lines. The most long-lived isotope of this element has a half-life of $2.1 \cdot 10^5$ years (Tc^{99}), so that the presence of technetium distinctly points to the presence of active nuclear reactions which encompass the region of the heavy elements /13/.

Further analysis and systematic classification of the relevant material are highly important. These stars, however, hardly inject "non-standard" matter into the Universe. The evolution of the anomalous-composition stars either terminates in a supernova explosion, which restores the "standard" chemical composition of the star, or in the formation of a neutron star.

THE HISTORY OF THE HEAVY ISOTOPES

While the first efforts in the theory of nucleogenesis could not overcome the "heavy nuclei difficulty" – the marked deficit in the computed abundance of the heavy nuclei compared to the actual abundance of these nuclei in the Universe – we are currently faced with an opposite difficulty. The heavy nuclei in the radioactive region are produced in comparable quantities with the neighboring nuclei ($Z < 83$, $Z = 90, 92$), which are either stable or are conserved during nucleogenesis. We will not consider the fate of nuclides with $A > 300$. There is a possibility that the matter of a collapsing star had not become fully converted into a neutron phase before it exploded as a supernova. A certain number of protons in this medium, i.e., a small charge of neutron nuclei, prevents their interaction with

the surrounding matter during the brief explosion phase, so that the conditions of thermodynamic equilibrium are not quite exact. Let us now consider the lighter nuclei.

For nuclei with $A > 250$, spontaneous fission is the predominant mode of decay (except for individual nuclides in the stability region arcund $Z = 108$). The fission products gravitate mainly to regions of filled shells, $A - Z = 50, 82$, and their buildup, as was first noted by Frenkel' and Selinov /14/, may account for the maxima on the abundance curve in these regions. The fision products in meteorites — rare gas isotopes — actually point to two different spontaneously fissile isotopes, U^{238} and some heavy isotope, possibly Pu^{244}. The difference in the fission spectrum of the heavy and the light transuranides may probably account for the buildup of isotopes around $A - Z = 50, 82$. The protected isobars only constitute a minority among the elements corresponding to these maxima. Zirconium has no such isotopes, and their content for Sr, Xe, Ba, and Ce is 10.4, 6.2, 10.4, and 0.4%, respectively. They are definitely not fission products of heavy nuclei, but their abundance does not exceed the normal abundance of the isotopes with given A.

A significant fraction of the atomic nuclei around $A = 236 - 250$ decay into the long-lived isotopes Th^{232}, U^{235}, and U^{238}. U^{236} and Pu^{244}, which are the product isotopes of the Th^{232} decay, possibly existed in the early stage of the solar system. The nuclides of this region with mass number of the form $A = 4n + 1$ rapidly decay to the final stable product Bi^{209}. The atomic nuclei around $A = 210 - 234$ are the decay products of natural radioactive elements formed in nucleogenesis; they apparently decayed rapidly, enriching the isotopes of lead and bismuth. Of these isotopes, U^{234} is probably the only survivor from the pre-solar-system times.

The decay of atomic nuclei with $A \geqslant 210$ thus enriches, on the one hand, the regions of atomic nuclei with filled neutron shells and, on the other hand, results in a buildup of Pb, Bi and also Th and U. The content of the lead isotopes Pb^{206}, Pb^{207}, Pb^{208} may probably increase, although hardly more than by one order of magnitude, compared to the original abundance in the nucleogenesis system. Thsi is evident from the isotopic composition of lead in iron meteorites, which is probably virtually undistorted by radiogenic lead impurities during the entire previous history of the meteorites. The content of the protected isobar Pb^{204} in meteorites is about 2% (compared to the current content of about 1.3% in the lead ores of the Earth's crust).

The quantitative increment of the heavy radioelements due to the decay of the primary transuranides is a big unknown. The enrichment of U^{235} by the decay products of the element $Z \approx 108$ probably reached about 10% of the original content of U^{235} during the last 3.5 billion years of the Earth's history /15/. The lead—bismuth system was probably enriched with decay products of the nucleogenesis alpha emitters to a greater extent that the uranium—thorium system. As a result, the filled shell region at $A = 126$ acquired a maximum on the abundance curve, not unlike the maxima in the region of medium mass number isotopes.